Development of a Liver-Kidney Dual Organ Microphysiological System for Predicting Organ-Organ Interactions in the Toxicity of Xenobiotics: Aristolochic Acid Nephrotoxicity as a proof of Principle

Shih-Yu Chang

A dissertation
submitted in partial fulfillment of the
requirements for the degree of

Doctor of Philosophy

University of Washington
2016

Reading Committee:
David L Eaton, Chair
Terrance J Kavanagh
Edward J Kelly

Program Authorized to Offer Degree:
Environmental and Occupational Health Sciences
Public Health

© Copyright 2016
Shih-Yu Chang

University of Washington

Abstract

Development of a Liver-Kidney Dual Organ Microphysiological System for Predicting Organ-Organ Interactions in the Toxicity of Xenobiotics: Aristolochic Acid Nephrotoxicity as a proof of Principle

Shih-Yu Chang

Chair of the Supervisory Committee:
Professor David L. Eaton
Department of Environmental and Occupational Health Sciences

The liver is the principal organ responsible for drug and xenobiotics metabolism, including inactivation or bioactivation. To improve the predictability of drug safety and efficacy in clinical development, and to facilitate the evaluation of the potential human health effects from exposure to environmental contaminants, there is a critical need to accurately model human organ systems such as the liver *in vitro*. Currently, there are numerous limitations of *in vitro* cell culture models. We developed a microphysiological system (MPS) based on a new commercial microfluidic platform (Nortis Inc., Woodinville, WA) that can utilize primary liver cells from mammals (e.g., rat and human). Compared to conventional monolayer cell culture which typically survives for 5-7 days or less, primary rat or human hepatocytes in MPS exhibited: higher viability, improved hepatic functions, such as albumin production, expression of hepatocyte marker HNF4α and canaliculi structure, up to 14 days and longer. Additionally, induction of cytochrome P450 (CYP) 1A and 3A4 in human hepatocytes was observed in MPS. These results indicate that hepatocytes cultured in MPS provide a promising approach for evaluating chemical toxicity *in vitro*.

Additionally, to test the hypothesis that hepatic clearance of a nephrotoxic chemical might have significant importance in determining ultimate kidney toxicity, we utilized aristolochic acid-I (AA-I), a well-known nephrotoxin and carcinogen, that undergoes extensive hepatic metabolism. We also developed an integrated MPS model with an interconnected liver-on-a-chip populated with hepatocytes , and a kidney-on-a-chip platform using proximal tubule epithelial cells (PTECs). Our results of this proof of concept study demonstrated that hepatocyte-dependent metabolism of AA-I prior to PTEC exposure substantially increased cytotoxicity to PTECs, formation of aristolactam-I (AL-I) DNA adducts in PTECs, and release of KIM-1 and other organ injury biomarkers, indicating that hepatic metabolism apparently contributes more to bioactivation of AA-I than to its detoxification. Additional mechanistic studies provided mechanistic insights into the important role of hepatic biotransformation for the kidney-specific toxicity of AA-I, potentially involved with activation to the AA-lactam intermediate via NADPH:quinone oxidoreductase (NQO1), sulfate conjugation via hepatic sulfotransferases (SULTs), and hepatic export and renal uptake via organic anion transporters (OATs) uptake. This *in vitro/ex vivo* integrated organs-on-chips culture can be used to identify toxicologically relevant organ-organ interactions that may occur *in vivo*, providing a novel approach for investigating the mechanisms that underlay toxicologically important organ-organ interactions.

ACKNOWLEDGMENTS

I'd like to express my sincere appreciation to Drs. Dave Eaton, Ed Kelly and Terry Kavanagh for serving as my advisors during my last four to five years in the toxicology program. I would also like to thank my committee members, Drs. Julia Yue Cui and Danny Shen, and Dr. Jonathan Himmelfarb for their input on the development of my project and their critical review of my dissertation and manuscripts.

During my time at UW, I sought support from many individuals, both in and out of the lab. I'd like to thank many others in other labs for their assistance with a variety of assays and experiments. Specifically, I'd like to thank the Kelly lab and Kavanagh lab, which served as my lab base. I will never forget their hospitality. I also would like to thank the assistance from the members at Mao lab (Dr. Qingcheng Mao at Department of Pharmaceutics) such as Chunying for guiding me the transporter assays and mass-spec analysis. Thanks to the supports and collaborations of Stony Brook University- Drs. Viktoriya Sidorenko and Arthur Grollman.

Over the years in Seattle, I have also formed some wonderful friendships with individuals both within and outside DEOHS: Rachel, Megan, Anna, Alenka, Nino, to name just a few. These friendships helped to sustain me during graduate school and keep me sane. I'm also thankful for all of the fun times with my Seattle friends from Taiwan – we enjoyed many fun times and BBQ parties, which were incredible!!

Last but not least, I'd like to thank my family for their mental and financial support.

TABLE OF CONTENTS

LIST OF TABLES

LIST OF FIGURES

Figure Number Page

List of Abbreviations

MPS: microphysiological system

LDH: lactate dehydrogenase

ALT: alanine aminotransferase

ELISA: enzyme-linked immunosorbent assay

BNF: beta-naphthoflavone

Rif: rifampin

EROD: ethoxyresorufin-O-deethylase

CYPs: cytochrome P450

HNF4α: hepatocyte nuclear factor 4 alpha

MDZ: midazolam

BSEP: bile salt export pump

MRP2: multiple resistance-associated protein 2

PTECs: proximal tubule epithelial cells

AA: aristolochic acid

KIM-1: kidney injury molecule-1

NQO1: NAD(P)H dehydrogenase, quinone 1

XDH: xanthine oxidase

POR: NADPH:CYP reductase

AL-1: aristololactam-I

$SULT_{S:}$ sulfotransferases

OATs: organic anion transporters

AL-I-NOH: N-hydroxyaristolactam I

$AL\text{-}I\text{-}NOSO_3H$: Sulfonyloxyaristolactam

Introduction and Background

The liver is the main organ where xenobiotics and endogenous compounds are metabolized and excreted due to its physiological placement ‘downstream’ from the gastrointestinal tract, high perfusion rate, large size and high concentration of biotransformation enzymes.

To predict a compound’s metabolic fate, including detoxification or bioactivation to a toxic metabolite, it is critical to understand the relative roles of various biotransformation enzymes and transporters expressed in the liver. Since the liver receives nearly all of the blood that perfuses the GI tract, it is anatomically situated to remove xenobiotics absorbed from the gut prior to reaching the systemic circulation– the hepatic first pass effect.

Biotransformation enzymes are often called drug-metabolizing enzymes. These enzymes are involved in xenobiotic (drugs and other chemicals foreign to the body) disposition via the processes of ADME (absorption, distribution, metabolism, and elimination) and are classified as either phase I (generally oxidation, reduction or hydrolysis reactions), phase II (generally conjugation or hydrolysis reactions) or phase III, (transmembrane transporters), based on their metabolic function.

Generally, phase I enzymes are responsible for catalyzing hydrolysis, reduction, and oxidation of xenobiotics. Among the phase I enzymes, cytochromes P450 (CYPs; detailed below) are the largest and most important superfamily: CYP3A4, CYP2D and CYP2C subfamilies are responsible for 50%, 25% and 20% , respectively, of the biotransformation of all drugs [1]. Phase II enzymes can transfer a functional group to xenobiotics- a process called conjugation, including acetylation, methylation, glutathione conjugation, sulfate conjugation, and glucuronidation.

Xenobiotics enter hepatocytes from the portal vein and hepatic artery either by diffusion or through assistance from membrane transporters in the sinusoidal (basolateral) membrane of hepatocytes for subsequent biotransformation.

One result of ADME is to convert toxic xenobiotics into non-toxic, water-soluble compounds which can easily be eliminated - a process called detoxification or inactivation. However, in certain cases, phase I and/or phase II enzymes can transform xenobiotics into more toxic chemicals – a process called bioactivation. The concept of bioactivation has been adapted to the pharmacological idea of prodrug-where the administered parent molecule has little or no pharmacological activity, but one or more metabolites act as the major contributor to the desired pharmacological response. For example, codeine is a morphine prodrug that requires oxidative demethylation by CYP2D6 to form morphine to achieve its pharmacological activity.

Phase I enzymes of pharmacological and toxicological significance: (adapted from Casarett & Doull's Toxicology, 8th Edition [2])

Hydrolysis: Hydrolysis reactions add water across a reactive bond, such as an epoxide. There are multiple different gene products with a wide variety of potential substrates, including: Carboxylesterase, Alkaline phosphatase (ALP), Dipeptidyl peptidase-4, Epoxide hydrolases (microsomal EH; cytosolic EH); Paraoxonase (PON1, 2, and 3)

Reduction: NAD(P)H- quinone oxidoreductases (NQO1 and NQO2), Aldo-keto reductases (AKRs), carbonyl reductase (CR), Cytochrome b5/ NADH-cytochrome b5, NADPH: P450 reductase, Aldehyde oxidase

Oxidation: Examples of enzymes involved in xenobiotic oxidation include: Aldehyde dehydrogenases (ADH1 and 2), Alcohol dehydrogenases (ALDH1), Aldehyde oxidase, Xanthine oxidase (XO), Monoamine oxidase (MAO), Peroxidase-glutathione peroxidase (GSHPx), Flavin-dependent-monooxygenase (FMO3, 4, 5)

Cytochrome P450 (CYPs): are generally considered to be the most important group of oxidative enzymes involved in phase I biotransformation of xenobiotics. There are 56 different human CYP genes, but many are involved only in endogenous metabolic processes. Major human forms involved in xenobiotic biotransformation are: CYP1A1, IA2, 1B1, 2A6, 2A13, 2B6, 2C8, 2C9, 2C18, 2C19, 2D6, 2E1, 2F1, 2J2, 3A4, 3A5, 3A7, 4F3.

Phase II enzymes: Conjugation

UDP-Glucuronosyltransferase (UGTs). There are two major UGT families involved in xenobiotic conjugation, UGT1 and UGT 2. Within the UGT1 family are multiple gene variants that give rise to 10 (UGT1A1 – 1A10) distinct gene products. The UGT2 family has two sub-families, UGT2A (3 members) and UGT2B (4 members.) All UGT enzymes use uridinediphosphoglucuronic acid (UDPGA) as the cofactor. Sulfotransferases are also multigene families of enzymes, with SULT1A, 1B, 1E, and 2A1involved in xenobiotic conjugation. All SULT enzymes use 3' phosphoadenosine-5' phosphosulfate (PAPS) as the cofactor. Glutathione S-transferase (GSTs) are also involved in xenobiotic conjugation, with ~15 different human genes, in 5 classes (GSTA1-5, GSTM1-5, GSTT1 and 2, GSTO1 GSTS1 and GSTZ1). Also GSTs use the tripeptide, glutathione, as a cofactor. Other important conjugation reactions include N-acetyltransferase (NATs- NAT1 and 2), with the cofactor, acetyl coenzyme A (acetyl-CoA), and several methyltransferases with different substrate specificities (O- methyltransferase, N-methyltransferase and S-methyltransferase).

Basolateral Uptake Transporters:

These transporters mediate the hepatic uptake of xenobiotics and endogenous substances such as bile acids and cholesterol. These uptake transporters belong to a multi-gene family of solute carriers (SLCs). In humans, the main uptake transporters

are organic anion transporting peptides (OATPs)- OATP1A2, 1B1,1B3, 2A1, 2B1; the sodium-dependent taurocholate cotransporting protein (NTCP); and the organic cation transporters (OCT) OCT1and OCT2 [3]. Many of these carrier proteins can transport substrates bi-directionally, depending on the substrate concentration gradient.

OATPs are integral membrane proteins with 12 transmembrane helices and are the main drug carrier proteins supporting the sodium-independent hepatic uptake of organic anions [4]. Because of the prominent expression of OATPs on the basolateral membrane of hepatocytes, OATPs are responsible for a critical mechanism of chemical uptake into the liver, including a variety of substrates containing steroidal or peptide structural backbones and/or anionic or cationic chemicals. For example, OATP 1A2 is associated with the uptake of sulfobromophthalein (BSP), BQ-123, [d-Pen^2,d-Pen^5]-Enkephalin (DPDPE), fexofenadine, levofloxacin, ouabain, and methotrexate. OATP 1B1 and -1B3 are the OATP1B isoforms expressed in human livers [5] and can transport bilirubin and its glucuronide conjugates [6]. OATP1B1 not only transports various statin drugs, but also can carry thyroxine, taurocholate, and dehydroepiandrosterone sulfate (reviewed by [7]) while OATP2A1 supports the transport of prostaglandins, including PGE_2 and $PGF_{2\alpha}$ [8].

Chemicals and drugs that belong to small class I organic cations, including tetramethylammonium, tetraethylammonium, tetrabutylammonium, thiamine, choline, dopamine, serotonin, histamine, adrenalin, and noradrenalin, are transported in hepatocytes by OCT1 (reviewed by [3]).

NTCP predominantly transports bile salts and sulfated compounds in the sodium dependent manner in addition to thyroid hormones, estrone 3-sulfate and certain statin drugs such as rosuvastatin and pitavastatin [9-11]. A recent study implicated NTCP as the receptor for hepatitis B and D viruses, showing its clinical importance [12].

Apical Efflux Transporters

These transporters are located on the apical surface of hepatocytes and pump out endogenous metabolites and xenobiotics via biliary excretory processes. These transporters belong to the ATP –binding cassette transporter (ABC) family containing ATP- binding domains that have ATPase activity to provide the energy necessary for active transport of substrates across the cell membrane, most often against a 100-1000-fold concentration gradient (reviewed by [7]). The most abundant and important transporters on the apical side of hepatocytes are the multidrug resistance proteins (MRPs) - MRP2, multidrug resistance-associated proteins (MDRs) - MDR1 and 3, bile salt export pump (BSEP), and breast cancer resistance protein (BCRP/ ABCG2) (reviewed by [7]).

MRP2 is involved in the efflux of both hydrophobic uncharged molecules and water-soluble anionic compounds (reviewed by [3]). MDR1 (also referred to as ABCB1 or P-glycoprotein, P-gp) can transport amphipathic organic cations and neutral compounds across the canalicular membrane to the bile. MDR1 (ABCB1) efflux transporter substrates include: glutathione, glucuronide, and sulfate conjugates; many macrolide antibiotics such as erythromycin, azithromycin, and clarithromycin; and chemotherapeutics such as tamoxifen, doxorubicin, and paclitaxel (reviewed by [3]). MDR3 (ABCB4) can transport phospholipids whereas BSEP primarily transports conjugated bile acids, including taurochenodeoxycholate, taurocholate, tauroursodeoxycholate, glycochenodeoxycholate, and glycocholate. In addition, BSEP can transport pharmaceuticals such as pravastatin (reviewed by [7]).

BCRP transports a highly diverse range of hydrophobic substrates, including chemotherapeutic agents such as mitoxantrone, methotrexate, topotecan and irinotecan. BCRP can also transport hydrophilic conjugated organic anions, particularly the sulfated conjugates with high affinity (reviewed by [13]).

Genetic defects or secondary consequences of hepatobiliary obstruction or destruction can cause cholestasis, which are often involved in impaired function or a sustained inhibition of these apical efflux transporters. Inherited mutations in the human MDR3 gene can cause progressive familial intrahepatic cholestasis type 3 (PFIC-III), a rare disease characterized by an early onset of cholestasis that leads to cirrhosis and liver failure before adulthood [14]. In addition, mutations in BSEP are responsible for PFIC-type 2 patients with high serum bile acid concentrations and low biliary bile acid but normal serum γ-glutamyltranspeptidase activity and cholesterol [15].

Basolateral Efflux Transporters

Removal of endogenous and xenobiotic chemicals from hepatocytes to sinusoidal blood is mediated by transporters on the basolateral side, including MRP3, MRP4 and organic solute and steroid transporter, Ost alpha-Ost beta (OSTα/β).

MRP3 has a high affinity for glucuronide conjugates, which is involved in detoxification and excretion of polar chemicals that have undergone the process of glucuronidation, including morphine-3-glucuronide, bilirubin-glucuronide, etoposide-glucuronide, and acetaminophen-glucuronide. It is suggested that MRP3 has a defense-related function and contributes to the excretion of toxic anions, as expression is upregulated during hepatic injury such as cholestasis as it is associated with bile acid homeostasis in spite of low affinity for bile acids (reviewed in [7]).

MRP4 has a wide range of substrates, including antiviral agents (azidothymidin, adefovir, and ganciclovir), anticancer agents (methotrexate, 6-mercaptopurin, and camptothecins) and cardiovascular agents (loop diuretics, thiazides, and angiotensin II receptor antagonists), as well as endogenous chemicals (steroid hormones, prostaglandins, bile acids, and the cyclic nucleotides cAMP and cGMP). MRP4 has

higher affinity for sulfate conjugates of bile acids and steroids. MRP4 is similar to MRP3, as both are upregulated in cholestasis, suggesting a protective role in preventing hepatotoxicity. Indeed, MRP4-null mice developed cholestasis after bile duct ligation, implying that MRP4 is important in bile acid homeostasis (review by [7]).

OSTα/β proteins are present as heterodimers and/or heteromultimers in the cell membrane. OSTα/β -mediated transport is bidirectional (uptake or efflux) and ATP-independent, depending on the electrochemical gradient. Although it is expressed in high levels in the liver, OSTα/β is also expressed widely in small intestine, colon, kidney, testes, ovaries and adrenal gland, the latter of which is involved in steroid and bile acid homeostasis. The evidence from a study with Ost alpha null mice demonstrated OSTα/β as a target for interrupting the enterohepatic circulation of bile acids. OSTα/β substrates include steroid hormones and endogenous compounds such as estrone sulfate and dehydroepiandrosterone sulfate, bile acids, and PGE_2, as well as the cardiac glycoside digoxin (reviewed by [16]).

The study of hepatic transporter function or chemical toxicity screening has relied on (1) *in vitro/ex vivo* hepatocytes in suspension or two dimensional (2D) plated monolayer cell formats for uptake and/or accumulation efflux assays using radioactive or fluorescent probe substrates and (2) *in vivo* pharmacokinetics studies on mutant animals with deficient in specific transporter genes or transporter gene knockout mice (reviewed by [17]) . There are several *in vitro* methods used to assess human drug metabolism and active transport of drug, including using immortalized cell lines with transient or stable overexpression of transporters. *In vitro* transporter assays can help to determine whether the compound is taken up at the sinusoidal surface by hepatocytes and/or whether its metabolites can be eliminated at the canalicluar membrane for biliary excretion. Uptake and inhibition assays often involve OATP1B1,

-2B1 and -1B3, and biliary efflux assays may include MDR1, MRP2 and BCRP, which can be used to predict compound disposition. The BSEP inhibition assay can be applied to screen whether the compound can lead to cholestasis or hyperbilirubinemia (reviewed by [18]).

Unfortunately, preclinical *in vitro* cell model systems often poorly predict biotransformation and elimination in humans. First, extrapolation from *in vitro* findings to the *in vivo* situation remains complex with poor *in vitro*-to-*in vivo* (IVIV) correlation. In addition, expression levels of phase I/II enzymes and transporters in transformed cell lines such as HepG2 human hepatoma cells are very low and variable (reviewed by [19]). OCT1 and OATP1B1 mRNA were abundantly expressed in human liver tissue whereas these two transporters were expressed at low levels in HepG2 cells [20]. Thus, transporter expression in HepG2 cells did not match the tissue expression pattern. Furthermore, due to overlapping substrate specificities and lack of selectivity with currently available inhibitors, it is challenging to fully understand the role of a given transporter in the disposition of specific drugs. Even though *in vivo* pharmacokinetic studies can provide an integrated analysis of a drug's disposition, preclinical results from transgenic or mutant animal models sometimes fail to predict the clinical outcomes. Expression profiles of transporters in laboratory animals such as rats and mice are different from humans. For example, rodent *mdr1a* and *mdr1b* genes are correlated to the *MDR1* gene in humans. However, functional studies in MDR1, mdr1a, and mdr1b expressing cells demonstrated that substrates for rodent mdr1a and mdr1b are unlikely to be substrates for human MDR1, showing species- dependency in the spectrum of drug efflux activity [21].

Current *in vitro* / *ex vivo* human hepatic cell systems used in chemical toxicity, biotransformation, and transporter studies are briefly reviewed, from traditional assays to the most recently advanced three-dimension (3D) cultures, including

microsomes, cell lines cultured in 2D, primary hepatocyte suspensions, liver slices, sandwich cultures, 3D culture systems, and microphysiological system (MPS) culture.

Human liver subcellular fractions, microsome/supersomes, cytosol fractions, and S9 fractions:

These subcellular fractions contain CYPs and UGT, or NATs, SULTS, and GSTs, are useful for xenobiotic biotransformation research. These assays are traditionally used for *in vitro*-based prediction of metabolic clearance and drug-drug interactions. However, due to the loss of structural integrity of the cell, and the optimization of enzyme kinetic conditions by adding cofactors such as NAPDH and PAPS that are at concentrations not normally encountered, the results using these methods cannot be accurately used for transporter studies and quantitative estimations of *in vivo* human biotransformation.

Cell lines cultured in 2D

The HepG2 cell line is the most frequently used and best characterized immortalized human hepatoma cell line. However, compared to primary human hepatocytes, overall CYPs activity remains low [22]. Expression profile of transporters in HepG2 cells is not highly correlated to human liver tissue so the HepG2 cell line is not a suitable model for transport assays. In general, 2D culture condition cannot provide the optimal microenvironment for cells to establish polarization; thus the use of 2D cell cultures has architectural limitations in transporter assays.

A new human liver cell line derived from a hepatocellular carcinoma – HepaRG recently drew substantial attention in the fields of pharmaceutics and toxicology. HepaRG cells have stem cell-like features, but can be differentiated into either hepatocytes or biliary epithelial cells. Differentiated HepaRG cells expressed high

levels of phase I/II enzymes, and transporters were comparable to freshly isolated human hepatocytes [22]. HepaRG cells can maintain a proliferative state in undifferentiated culture medium for several weeks, and can differentiate into hepatocytes and biliary epithelial cells by adding differentiation culture medium after reaching confluence [22].

Primary human hepatocytes suspension and cultured in 2D

Primary human hepatocyte cultures are a preferred *in vitro* system for predicting *in vivo* drug biotransformation and clearance as they maintain critical metabolic features. After isolation by collagenase perfusion, primary human hepatocytes in suspension are viable for only a few hours but never-the-less can be used in rodent models for kinetic characterization of transporter function. However, this is generally not possible for human hepatocytes. Thus, studies with human hepatocytes rely on establishing primary cultures. Once plated in a monolayer culture, human primary hepatocytes maintain good viability for several days. However, they usually lose cell-specific functions such as albumin production and CYPs expression as both decline quickly over the first 24-48 hours of culture as the cells lose their differentiation status. Due to the scarcity of available human liver tissue and successful cryopreservation techniques, a good supply of human primary hepatocytes is now commercially available. In culture, previously cryopreserved hepatocytes can recover and maintain phase I/II enzyme activity after thawing for at least seven days [23]. Individual donor variation in metabolic enzyme activity due to genetic polymorphisms and other factors can be compensated for by the mixing of hepatocytes from multiple donors to generate homogeneous enzyme activities. Hepatocytes represent the majority of the hepatic cellular mass (about 80%), while other non-parenchymal cells (NPCs), including vascular and biliary epithelial cells

(i.e. cholangiocytes), Kupffer cells and hepatic stellate cells (HSC), provide key physiological functions. For example, cholangiocytes not only can contribute to bile secretion, but also can enable the absorption of ions, bile acids, amino acids, glucose, and other molecules, playing an important role in the modification of hepatic canalicular bile (reviewed by [24]). *In vivo,* Stellate and Kupffer cells have been shown to play an important role in the hepatoxicity of some compounds, and thus the absence non-parenchymal cells in primary culture systems is a potentially serious limitation for toxicology studies. For example, hepatocyte culture usually cannot capture drug-induced immune toxicity because Kupffer cells and HSC can regulate immune such as release of pro-inflammatory cytokines and chemokines, and reactive oxygen species (ROS) [25, 26].

HSC contain approximately 80% of the body's vitamin A (Vit A) with a gradual distribution in the liver lobules that depends on the total Vit A amount and is genetically determined. The number of HSC-elaborated inflammatory and immune regulatory molecules that contribute to liver immunology may be even much greater than known today. cellular levels of inducible NO synthase and TNF-α secretion were suppressed significantly, indicating the posttranscriptional process of generating these proteins might be affected predominantly by these phenolic compounds. Thus, NAC and these phenolic compounds may have therapeutic potential against liver injury by regulating functions of hepatic stellate cells and Kupffer cells.

Precision-cut liver slices

Precision-cut liver slices have several advantages for drug biotransformation and toxicology studies as they maintain the native liver structure with multiple cell types and zonation, and have good *in vitro*/*in vivo* correlations of drug biotransformation features. Cultured liver slices can retain phase II enzyme activity,

albumin production, and gluconeogenesis for up to 20-96 hours and also exhibit good gene expression of the uptake transporters- NTCP and OATP and efflux transporters- BSEP, MDR1 and MRP2 [27].

In spite of the preservation of the overall hepatic architecture, drug biotransformation and intrinsic clearance rates are lower than isolated hepatocytes as necrosis can occur after 48-72 hours while CYPs activities are greatly reduced within 6-72 hours [28].

Sandwich culture

Sandwich cultures with primary human hepatocytes plated between two layers of extracellular matrix (collagen or Matrigel® , derived from Engelbreth-Holm-Swarm sarcoma) were developed to maintain liver-specific functions over longer culture periods. The use of extracellular matrix overlays allows for a favorable cellular attachment environment and is thought to be one of the main reasons why cells polarize in this type of culture. Hepatocyte sandwich cultures with various medium constituents have been shown to maintain albumin secretion, viability, and cuboidal-shape morphology with phase I/II and transporter expression similar to that of liver tissue [29]. Biliary excretion can also be evaluated in sandwich cultures with both basal and inducible biliary enzyme activities that allow assessments of hepatobiliary disposition. Taken together, sandwich cultures can provide a robust means to evaluate hepatic uptake, metabolism, efflux and biliary excretion of target compounds, while closely mimicking *in vivo* characteristics. Compared to other 2D models, sandwich cultures have significant advantages and can be considered as a bridge between 2D and 3D cultures (reviewed by [30]).

Transwell culture for drug efflux

Evaluation of the human hepatocyte uptake and efflux transporters, MDR and MRP2, have been performed in trans-well systems with transfected cell lines, including porcine kidney epithelial cells (LLC-PK1) and Manine-Darby canine kidney epithelial cells (MDCK). Transwell culture cells are grown on a permeable membrane filter that allows for the physical separation of the apical and basolateral domains and has been used to study drug uptake and efflux transporter activity [31].

Co-culture systems, 3D culture systems and MPS culture systems

Traditional *in vitro* methods such as microsomes and suspension cultures usually have too short of a time window to adequately assess overall hepatic biotransformation and transport capabilities, which can lead to imprecisions in the prediction of in vivo human biotransformation/clearance and toxicity. In order to improve the predictability of drug safety and efficacy in clinical development, and to have a clearer perspective of toxicity outcomes, while reducing the use of animals in toxicity assessment, recent research efforts have been focusing on development of advanced *in vitro* models based on the applications of co-culture systems, 3D cultures, and microphysiological system (MPS) cultures that utilize microfluidic flow -- often are referred as organ-on-chips or organoid cultures [32].

The liver is a complex organ, consisting of hepatocytes, NPCs, and various ECM. NPCs play an important role in hepatic physiological functions as well as hepatotoxicity. Many studies have demonstrated that co-cultures of hepatocytes with NPCs can sustain liver-specific function, morphology and expression of liver-specific transcription factors via the activation of cell adhesion molecules and redistribution of cytoskeleton involved in cell-cell and cell-matrix interactions (reviewed in [33]). Several liver organoid cultures based on the application of co-culture have been reported, and some have been commercialized. These include advanced 3D culture

systems based on cellular microenvironment dynamics between ECMs, micro-perfusion flow rates, and co-cultures of various cell types. The MPS model represents an interconnected set of cellular constructs designed to recapitulate the structure and function of human organs [34]. Here, we review current advanced hepatic culture systems:

HepatoPac® is a co-culture system of human hepatocytes with mouse fibroblasts (3T3-J2 fibroblast), commercially available through Hepregen (Medford, MA). This system consists of micro-patterned hepatocyte islands surrounded and stabilized by stromal cells in a 24-well plate format. This culture system can maintain liver-specific function for up to six weeks, including stable albumin secretion, urea synthesis, phase I/II drug biotransformation and formation of bile canaliculi with efflux transporters ([35], reviewed by [36]). Studies with the human HepatoPac® platform have demonstrated an IVIV correlation with hepatic uptake of faldaprevir by multiple transporters (including OATP1B1 and Na^+-dependent transporters) and biotransformation by CYP3A4 [37].

RegeneMed 3-D Liver (San Diego, CA) is a liver tissue co-culture system used for screening hepatic ADME, using the transwell culture approach [38]. NPCs are seeded in a nylon screen sandwich mesh insert with a 140 μm pore size and stabilized for a week, followed by incubation with hepatocytes to form a 3D liver tissue. Liver-specific functions, including production of albumin, fibrinogen, transferrin and urea, can be maintained up to three months, and the induction of CYP1A1, 2C9, and 3A4 activity for up to two months. Co-culture with Kupffer cells allows for study of the inflammatory response as the release of pro-inflammatory cytokines can be observed with lipopolysaccharide (LPS) exposures. Basolateral cell uptake / drug transport activity using ^{3}H-labeled estrone-3-sulphate (E3S) as the tracer has been

demonstrated to occur in this system. Though images of bile canaliculi-like structures were presented, efflux transporter activity or bile excretion were not reported.

The 3D micro-tissue spheroid culture- 3D InSight™ provided by InSphero (Schieren, Switzerland) is a hanging drop co-culture system that uses gravity-forced cellular self-assembly of hepatocytes and NPCs into spheroids using a 96-well format [39]. This 96-well plate format is well suited for high throughput applications and stable viability and liver-specific function such as persistent albumin secretion are preserved over five weeks. MDR1 and BSEP are expressed in this microtissue, evidence that these cultures exhibit cell polarization and bile canaliculi formation. Inflammation-mediated toxicity and chronic toxicity assays with acetaminophen and diclofenac have also been evaluated in this system. However, to date, there are no published data that demonstrate that this system can be applied to transporter assays.

Organovo (San Diego, CA) uses a 3D bioprinting technique to generate small-scale hepatic tissues using human primary cells in a platform called exVive3D™ Liver. This product can maintain stable viability and albumin secretion for up to four weeks and has rifampicin-inducible CYP3A4 activity, as midazolam biotransformation to 1-hydroxy-midazolam was increased by rifampicin pretreatment [40]. As Kupffer cells are also present, this system can respond to immune stimulation (LPS) with the release of pro-inflammatory cytokines [41].

3D liver bioreactors designed by the Charité Universitätsmedizin Berlin are derived from bioartificial livers (BAL) used in the clinic. This hollow-fiber and perfusion based bioreactor provides a continuous mass exchange of culture media and controlled oxygenation with a scaffold for cells to maintain a physiologically relevant environment [42]. This 3D bioreactor is co-cultured with hepatocytes and NPCs and can maintain albumin secretion and CYP activity (CYP1A, CYP2C9 and 3A4) for up to 2-3 weeks, as well as expression of canalicular transporters- MRP2, MDR1, and

BCRP. Limitations of this system for use in pharmacokinetic and drug toxicity testing include a lack of zonation seen in liver tissues and low throughput, as only one condition can be evaluated per system.

HμREL® microdevice, a MPS platform provided by Hurel (Beverly Hills, CA), is an integrated and microfluidic system that assembles multiple units of microfluidic microscale cell culture analogs (μCCA) cultured from hepatic tissue or other organ tissues in parallel. The Hurel plastic biochips are connected to a fluid reservoir and pump system interconnected with a complex set of tubing that serves to recirculate the media. The hepatic co-culture system with NPCs forms a 2-D monolayer and maintains high viability for up to nine days, with higher expression of CYPs, SULT and UGT, and *in vivo*-like hepatic clearance of diclofenac, indomethacin and coumarin, compared to traditional static culture conditions [43]. The formation of the bile canaliculi network was visualized by using carboxy-2′, 7′-dichlorofluorescein diacetate (CMFDA), a fluorescent substrate of BSEP. However, there was no evidence to demonstrate that this system can maintain other hepatic function such as albumin secretion, urea excretion, or transporter activity.

A multiple-well plate platform- LiverChip^{TM} by CN Bio Innovations (Hertfordshire, UK) uses a flow system driven by a pneumatic pump at the bottom of the plate. This system was designed to recapitulate the hepatic microenvironment in terms of fluid flow, oxygen gradient and shear stress (145 μM to 50 μM at a flow of 0.25 mL/min). Compared to 2D static conditions, hepatocytes cultured in this system can maintain CYPs activity (1A2, 2B6, 2C9, 2D6, and 3A4), albumin secretion, expression of phase II-UGT enzymes and transporters (MDR2, MRP2, BCRP) for up to seven days [44]. Hepatocytes co-cultured with liver sinusoidal endothelial cells (LSEC) enriched NPCs fractions can maintain high viability, CYPs activity, albumin secretion and urea excretion for up to 13 days [45]. Kupffer cells incorporated in the

model can release pro-inflammatory cytokines by LPS stimulation. The intrinsic clearance values of hydrocortisone and its metabolites generated in this system correlated well with human data, demonstrating that this system has great potential for high throughput use in hepatic metabolism research [46].

CellAsic (Hayward, CA) has a microfluidic liver sinusoid model with a microporous endothelial-like barrier that mimics liver sinusoids. This platform utilizes a 96-well plate format containing 32 small units that utilized s perfusion system with a flow of 10-20 nL/min and ~250 cells in each unit. Hepatocytes cultured in this system can maintain high viability for up to seven days and respond to drugs [47]. Other liver-specific functions and the characterization of transporters need to be further analyzed.

Vernetti *et al.* developed a human, 3D, microfluidic, four-cell, sequentially layered, self-assembly liver model (SQL-SAL) based on a MPS device platform by Nortis Inc. (Woodinville, WA) [48]. The current SQL-SAL uses a co-culture of primary human hepatocytes along with human endothelial (EA.hy926), immune (U937) and stellate (LX-2) cells in physiological relevant ratios that are viable and functional for at least 28 days under continuous flow. This model can maintain canaliculi structure, phase I/II activity, albumin production and urea excretion. In addition, by the integration of protein-based fluorescence biosensors, the system can be used in reporting drug –induced mechanisms of toxicity (MOT) such as apoptosis and reactive oxygen species (ROS generation for high throughput screening (reviewed by [36])

The above described 3D or liver-on-a-chip platforms generally provide suitable microenvironments for recapitulating most *in vivo* hepatic functions compared to traditional 2D hepatocyte cultures. However, these state-of-the-art *in vitro/ex vivo* technologies still have limitations in accurately predicting human

hepatotoxicity and first pass drug clearance. Further development of advanced 3D hepatic culture systems needs to consider the complexity of the liver, including the co-culture ratio between hepatocytes and NPCs, the source of hepatocytes, and zonation effects. Because the liver has a wide range of diverse functions, hepatic cells show large heterogeneity and plasticity of functions. Oxygen gradients, hormones and ECM all can regulate zonal variations, which are reflected in drug biotransformation capabilities. It would be interesting if these zonation characteristics could be established and sustained on the 3D liver-on-chip systems [49].

Although these 3D models have great potential in pharmacokinetic prediction of first pass drug clearance, additional "proof of concept" studies are needed to validate IVIV correlations using selected clinical drugs or known toxins/toxicants. In addition, most current models are individual liver organ systems, lacking the gastrointestinal and/or renal transport/metabolism modules, which are needed to understand the whole profile of drug ADME *in vivo*.

In this study, we collaborated with Nortis Inc. (Woodinville, WA) to develop a liver MPS model using rat and human hepatocytes (described in Chapter 1). We characterized the viability and hepatic functionality of primary hepatocytes cultured in Nortis® MPS, compared to 2D culture, and the potential of this liver MPS for use in toxicological studies.

Great strides have been made in developing individual organ MPS from various groups, and continued development of integrated MPS models for studying chemical toxicity and metabolic processes is the current focus of several groups. Our group also has developed an integrated liver-kidney MPS system for identifying potentially nephrotoxic liver-metabolized chemicals, by connecting a liver-on-a-chip populated with primary rat or human hepatocytes, to a kidney-on-a-chip device populated with

rat or human proximal tubule epithelial cells (PTECs) in MPS devices developed by Nortis, Inc (Woodinville, WA) [50](described in Chapter 2 & 3).

There are still a number of technical challenges in multiple-organs-on-chips development that remain as important research areas for this new and rapidly growing field of study (reviewed by [34]):

1. Microfluidic volume problems: The physiological relevant scaling of fluid volumes and flow rates that are associated with individual organ microphysiological systems are difficult to acquire, as delicate and reliable engineering systems are required for the connection of reservoirs, pumps, and tubing to deliver accurate flow rates to the cultured cells. Also, the determination of the physiologically relevant flow rate for hepatic cells cultured in MPS is difficult to determine given that the liver is an architecturally complex organ with varying fluid channel areas and perfusion rates that can expose hepatic cells to a wide range of shear forces. One approach to this problem would be to incorporate vascular systems within hepatic or renal chips to allow for cell controlled flow rates between the vascular system and organ-specific cells.

2. Universal cell culture medium: Individual cell types, especially primary cells, require customized media for optimal cell culture performance. A universal culture medium that can sustain multiple cell types from different organs will need to be developed to successfully co-culture cells from multiple organs with an optimal balance of nutrients, osmolality, pH, and supplements.

To address these challenges, the Defense Advanced Research Projects Administration (DARPA), National Center for Advancing Translational Sciences of the National Institutes of Health (NIH-NCATS), FDA, and the Environmental Protection Agency (EPA) have funded several groups for MPS development and organotypic culture models for predictive toxicity and pharmacokinetic study [51, 52].

The European Commission is funding a Body on a Chip project with many collaborating groups between multiple European academic and industrial partners, to achieve the goal of developing a comprehensive *in vitro* model that allows identification of multi-organ toxicity and pharmacogenetics [53].

Chapter 1:

Characterization of Rat or Human Hepatocytes Cultured in Microphysiological Systems (MPS) for Hepatotoxicity Investigations

Abstract:

The liver is the main site for drug and environmental contaminants metabolism, and is one of the most important organs when it comes to predictive evaluation of compounds for efficacy and toxicity, including inactivation of the compound or bioactivation to a toxic metabolite. To improve the predictability of drug safety and efficacy in clinical development, and to have a clearer perspective of the potential human health effects from exposure to environmental contaminants, there is a critical need to accurately model human organ systems such as the liver *in vitro*. We developed a 3-dimensional microphysiological system (MPS) based on a new commercial microfluidic platform (Nortis Inc. Woodinville, WA) that can utilize primary liver cells from several mammalian species (e.g., rat and human). Compared to the conventional monolayer cell culture that typically survives for 5-7 days, primary rat and human hepatocytes in MPS exhibited: higher viability (measured by LDH/ALT release and vital staining), improved hepatic functions, such as albumin production (measured by ELISA), expression of hepatocyte marker-HNF4α and canaliculi structure (measured by immunocytochemistry staining), up to 14+ days. Additionally, induction of Cytochrome P450 1A (via EROD assay) and CYP3A4 (via the formation of luciferin signal from substrate) in human hepatocytes was observed in MPS. These results indicate that hepatocytes cultured in MPS provide a promising approach for evaluating drugs or xenobiotics *in vitro*, where testing over extended periods of time is needed, such as enzyme induction studies.

Introduction

In pharmaceutical drug research and development (R&D) and environmental chemicals risk assessment, systems-level analysis is a pivotal step towards understanding the pharmacokinetics or toxicokinetics of a new chemical entity, that is, how chemicals are absorbed, distributed, metabolized and excreted (ADME) in multi-organ organisms such as experimental animals and humans. Systems-level analysis of these compounds remains largely dependent on time-consuming and expensive *in vivo* animal models. Research using animal models and human subjects have many limitations, including the availability of test subjects, feasibility of testing procedures, and ethical concerns. The goal of these animal studies is to gain knowledge and insights for understanding the response of humans to these compounds. However, the results obtained from animal studies often fail to predict human response [54-57]. Most of the poor translatability associated with extrapolating animal data to humans results from the interspecies differences in pharmacokinetic and pharmacodynamic (PK/PD) behavior between lab animals and humans.

Researchers have been focusing on developing advanced animal-free and/or *in vitro* models such as *in silico* PK/PD modeling, pathway-based toxicity modeling, and microphysiological system (MPS) cultures [32, 58] in order to improve the predictability of toxicity outcomes and reduce the use of animals for systems-level analysis. MPS represents an interconnected set of cellular constructs designed to recapitulate the structure and function of human organs, frequently referred to as "organs-on-chips", " *in-vitro* organ constructs", or "organoids" [34]. Basically, MPS platforms involve a micofluidic device with flow driven by either a perfusion or pneumatic pump through 3D cell constructs with extracellular matrix (ECM) gel. Microfluidics that have low volumes (microliters to attroliter) of fluidics are

embedded inside the system with dynamic fluid flow and spatiotemporal gradients, recapitulating the physical microenvironment of living organs [32]. Currently, the most commonly used *in vitro* model is the monolayer cell culture in plastic flasks or plates using mammalian cells, also known as the conventional two-dimensional (2D) culture. Although conventional 2D culture has provided significant contributions to biological research, it still has limitations compared to the MPS culture, including limited nutrient and metabolite transportation by diffusion, poor mimicry of extracellular concentration *in vivo*, and a failure to recapitulate the heterogeneous tissue microenvironment [34]. Unlike conventional 2D culture, MPS cultures can provide an optimal microenvironment for heterogeneous cell growth and differentiation that more closely mimics the physiological responses of tissues *in vivo* [32, 58-60]. MPS culture profoundly alters cell-cell, drug-cell, drug-drug, and organ-drug interactions *in vitro*, potentially recapitulating *in vivo* physiology and biochemistry that affords MPS a greater potential to more accurately predict chemical toxicity than traditional 2D cultures.

Although still early in the developmental stage, MPS cultures represent a potentially large improvement for *in vitro* systems testing of drugs and toxicants. The liver is the main organ to metabolize drugs and environmental chemicals, and the most important organ when it comes to predictive evaluation of compounds for efficacy and toxicity, including detoxification of the compound or bioactivation to a toxic metabolite. In order to improve the predictability of drug safety and efficacy in clinical development, and to have a clear perspective of the potential human health effects from exposure to environmental chemicals, there is a critical need to accurately model liver function using the MPS approach. Therefore, we developed and validated rat and human ‘liver-on-chip’ *in vitro* models using a commercial MPS (Nortis Inc.). The major goals of this study were to characterize how primary

hepatocytes maintain function in the MPS culture system compared to conventional 2D culture, and to demonstrate that this liver MPS is validated system for assessing chemical toxicity and metabolism *in vitro.*

In this study, we explored how to populate hepatocytes inside the Nortis® MPS chip via chamber or channel seeding (Figure 1). We were most interested in whether the liver MPS model is superior to 2D culture by characterization of cell viability, hepatic functions, enzyme activities, and canaliculi formation of primary rat or human hepatocytes in 3D culture. Our results demonstrated that the liver MPS model of rat or human hepatocytes maintained cell viability up to 14-28 days, compared to 5-7 days for conventional 2D culture. Generally, *in vitro* culture of hepatocytes is associated with dedifferentiation (i.e. decreased hepatocyte-specific functions), including decreased albumin secretion, reduced hepatic enzymatic activity and ammonia metabolism, and loss of hepatocyte polarity [61, 62]. Our liver MPS model also maintained hepatic functions such as albumin production, inducible cytochrome P450 (CYP) - CYP1A and CYP3A4, and hepatic function marker- hepatocyte nuclear factor 4 alpha (HNF4α), a transcription factor regulating many of hepatic genes expression [63], expressed up to at least 14 days. Human liver MPS at culture day 15 possessed canalicular-like structures, including the expression of bile salt export pump (BSEP) and functional bile transporter- multiple resistance-associated protein 2 (MRP2).

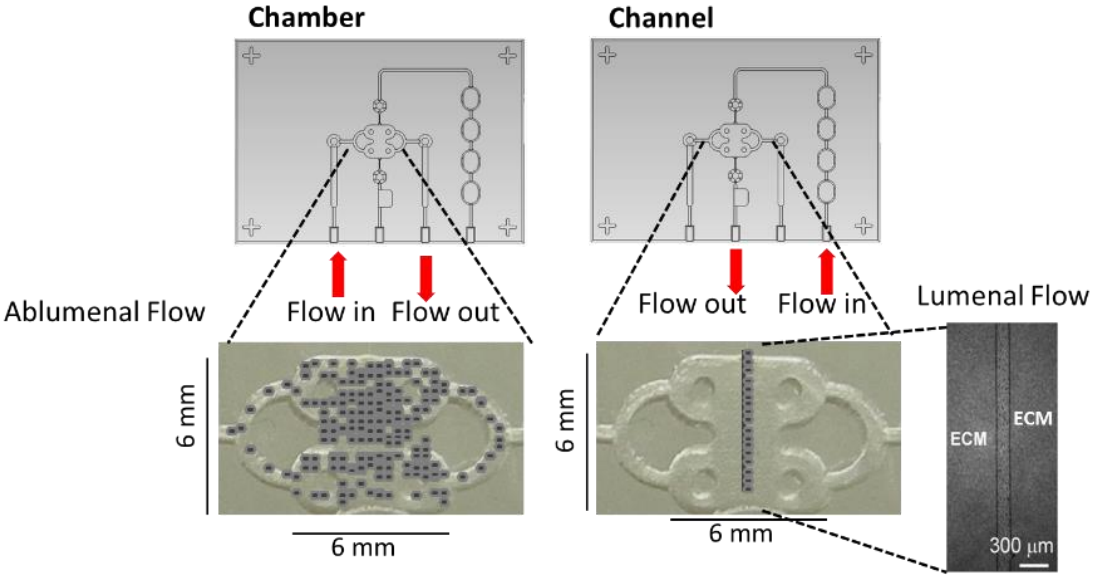

Fig. 1: Methods used to populate the MPS with hepatocytes. Methods of injecting cells included the chamber (ablumenal) and the channel (lumenal) seeding with high concentration (3 mg/mL), or low concentration (1.3 mg/mL) of type I collagen, or Matrigel^{TM} (0.2 mg/ml). Extracellular matrix (ECM) such as type I collagen (6 mg/mL) were used for filling the MPS chips prior to channel seeding. Grey dots represent cells.

Materials and Methods

Source of primary hepatocytes, including rat and human hepatocytes

Freshly-isolated human hepatocytes or cryopreserved human hepatocytes were purchased from Triangle Research Labs (TRL; HUM4037, HUM4038, HUM 4055A, HUM4080 and HUM4096A) or received from The Liver Tissue Cell Distribution System (LTCDS; NIH service; donor 14-018, 15-001,15-002,15-004; all the demographic information of hepatocytes donors is listed in Table 1). Primary rat hepatocytes were isolated by two-step collagenase digestion following isolation from male Sprague Dawley® rats (Charles River Laboratories, Seattle, Washington)[64]. Animals were maintained in ALAC-approved vivarium facilities at the University of

Washington, and all protocols for animal use and care were approved by the UW Institutional Animal Care and Use Committee.

Source	Donor ID	Age	Gender	Race	Cause of Death or Surgery
TRL	HUM 4037	8	Male	Caucasian	Anoxia
	HUM 4038	33	Female	Caucasian	Stroke
	HUM 4055A	54	Female	Caucasian	Stroke
	HUM 4080	47	Female	Caucasian	CVA
	HUM 4096A	34	Female	Caucasian	Anoxia
LTCDS	14-018	Femal	43	Caucasian	persistent biliary stricture and recurrent hepatolithiasis
	15-001	Male	55	Caucasian	carcinoid mets to the liver. There is no history of chemo
	15-002	Femal	37	Caucasian	colon cancer mets to the liver. She has a history of chemo
	15-004	Femal	42	Caucasian	colon CA mets to the liver and pre-op chemotherapy

Table 1: The demographic information of human hepatocytes donors

Cell culture, including conventional 2D culture and MPS culture

Cell culture supplies and materials were obtained from Thermo Fisher Scientific (Waltham, MA), except for the aflatoxin toxicology experiments, where tissue culture medium from Triangle Research Labs (TRL)/Lonza was used. Primary rat or human hepatocytes were cultured in 2D configuration on 24-well plates coated with type I collagen, or were seeded into Nortis™ devices for MPS culture (Figure 1). For the 2D culture, primary rat or human hepatocytes were seeded at a density of 1 x 10^6 cells/mL into type I collagen coated plates. For MPS culture via chamber seeding (Fig 1A), 0.2 to 0.3 mL of a cell suspension at a density of 1 x 10^6 hepatocytes/mL mixed with type I collagen (final conc. 3 or 1.3 mg/mL) was injected into each device via ablumenal ports. All devices were pre-coated with 0.1 mg /mL of collagen type I in PBS with 0.1% acetic acid at 37℃ for 1 hour. For MPS culture via channel seeding (Fig. 1B), 2 to 5 μL of a cell suspension at a density of 10^7 hepatocytes/mL was injected into each chip with pre-gelled collagen type I (6 mg/mL) via the injection port using a sterile 5 μL Hamilton #65 syringe. Plating medium composed of William's E medium supplemented with 5% fetal bovine serum (FBS), 100 mg/ml penicillin streptomycin, 100 nM dexamethasone, 1 μg/mL of Gibco® Fungizone® , 100x diluted ITS+ (final

concentration of insulin/transferrin/selenium was 6.25 μg/mL), and 0.2 mM glutaMAX supplement were used. After 4 hours, the hepatocytes were switched to maintenance media (the same formula as plating media but without FBS), and lumenal or ablumenal flow was initiated at flow rates between 5 and 30 μL/hr using an infusion syringe pump (KD Scientific Inc. model# KDS220). Following maintenance of cells at 37 ℃ in a 5% CO_2 incubator overnight, cells were subsequently maintained in an incubator in a humidified atmosphere at 37℃ in 5% CO_2/95% air. The effluent media from the MPS cultures and conditioned media from 2D cultures were collected at various time points and stored at -80 ℃ for later measurement of LDH or ALT, and albumin.

LIVE/DEAD® staining

The LIVE/DEAD® viability/cytotoxicity kit (Life Technologies, Waltham, MA) was used to distinguish viable cells from dead cells according to the manufacturer's specifications. Briefly, 5 μL of 4 mM calcein AM, 20 μL of 2 mM ethidium homodimer-1 (EthD-1) and 100 μL of 5 mg/mL 4',6-diamidino-2-phenylindole (DAPI) were diluted in 10 mL of pre-warmed D-PBS. Adequate volumes of diluted reagents were added to 2D culture plates or perfused through the MPS chips at 0.5 μL/min for 20 minutes and then incubated for 10 minutes at 37 ^{0}C. After the staining procedure, MPS devices or 2D plates were imaged using fluorescent microscopy (Nikon Eclipse Ti-S inverted microscope equipped with a spinning disk confocal apparatus, 3i-Intelligent Imaging Innovations, Denver, CO) to localize red and green fluorescence.

Immunocytochemistry (ICC) staining

Primary antibodies- HNF4 (mouse monoclonal [K9218], ab41898, Abcam) and BSEP (mouse monoclonal (F-6), sc-74500. Santa Cruz Biotechnology) were used. Cells were fixed with 4% formaldehyde in PBS. After antigen retrieval with warm citrate buffer (10 mM citric acid, 0.05% Tween 20, pH 6.0) for 20 minutes, samples were permeabilized with PBST (PBS plus 0.1% Tween 20) for 1 hour, and blocked with 1% bovine serum albumin (BSA) and 10% serum in PBSG (10 mg/mL glycine, 0.1% Tween 20) for an additional 1 hour. The samples were then incubated with primary and secondary antibodies followed by washing, using a standard ICC protocol. Secondary antibodies were goat anti-Mouse IgG (H+L) Secondary Antibody, Alexa Fluor® 488 conjugate (Thermo Fisher Scientific, Waltham, MA). Diluted ProLong Gold Antifade Mountant with DAPI reagents (catalog# P-36931, ThermoFisher Scientific) were used in the final step of staining. Cells were imaged using fluorescent microscopy with the Nikon Eclipse Ti-S microscope for detecting the intensity of green and blue fluorescence.

Measure of Lactate Dehydrogenase (LDH) release

Cell viability was assessed through lactate dehydrogenase (LDH) release using the CytoTox 96® Non-Radioactive Cytotoxicity Assay (Promega, Madison, WI) following the manufacturer's suggested protocol. Standard curves (amount of LDH per hepatocytes) and volume of media were used to normalize the results. In order to normalize cell death to 'percent viability' values, (% = experimental LDH release/ maximum LDH release) in condition media or effluents at different time points, the maximum LDH release of MPS model was obtained from lysate of hepatocytes freshly-seeded MPS chip. Results of viability % were calculated from the equation- viability $\%_{(time=n)} = 100\% - \sum \text{cell death}\%_{(time=n).}$

Measure of Alanine Aminotransferase (ALT) and albumin levels and albumin

The ALT activity kit (Sigma-Aldrich Co. Catalog # MAK052-1KT) was used according to the manufacturer's protocol. ALT activity was determined by a coupled enzyme assay, which results in a colorimetric (570 nm) product, proportional to the pyruvate generated. Standard curves of pyruvate were included for normalizing ALT activity. Human Albumin ELISA Kit (ab108788, Abcam) was used to measure albumin level in effluents of MPS culture and conditioned media of 2D culture. For purposes of comparing 2D and MPS cultures, activity assessment were normalized to the amount of cells seeded in the respective *in vitro* systems (1×10^6 cells in 2D vs. 0.02×10^6 in MPS).

Enzyme activities measurements

Various assays were used to measure CYP1A1/2 and CYP3A4 activities. To induce enzyme activities, cells were pre-treated with -naphthoflavone (BNF; CYP1A; Sigma-Aldrich Co. Catalog # N3633), rifampicin (Rif, CYP3A4; Sigma-Aldrich Co. Catalog #R3501), and 0.1% DMSO vehicle control for 72 hours prior to performing the enzyme activity assays. BNF is an aryl hydrocarbon receptor (AhR) ligand used as a CYP1A1/2 inducer [65]. Rif is a potent activator of the pregnane X receptor (PXR) ligand-activated transcription factor, and is used as a prototypical CYP3A4 inducer [66].

Ethoxyresorufin-O-deethylase (EROD, CYP1A) kinetic confocal assay:

Figure 2 shows a conceptual diagram of the EROD kinetic confocal assay. Cells in MPS (Fig. 1A) or in 2D culture plate (Thermo Scientific™ Nunc™ Lab-Tek™ II Chamber Slide™ System) were incubated with dicumarol (25 μM), verapamil (100 μM), and probenecid (1mM) in HBSS++ for 30 minutes prior to the assay. Cells cultured in MPS were perfused with HBSS++ reaction buffer, which contains 7-ethoxyresorufin (10 μM), dicumarol (25 μM), verapamil (100 μM) and probenecid

(1mM), at a flow of 100 μL/min for 30-40 minutes. Cells plated in 2D plate were incubated with 0.5 ml of the same reaction buffer. The average fluorescence intensity in a randomly-selected area (100x) was monitored by an ACAS (adherent cell analysis and sorting) Ultima Laser Cytometer (Meridian Instruments, Okemos, Michigan) equipped with an argon ion laser and image analysis software (MetaMorph) every minute starting with the reaction buffer incubation or perfusion (ex = 514 nm, em > 570 nm). Representative images of Δ fluorescence intensity were presented in pseudocolor mode. Final results of fluorescence intensity were analyzed from 10 randomly-selected cells in the visual field. area.

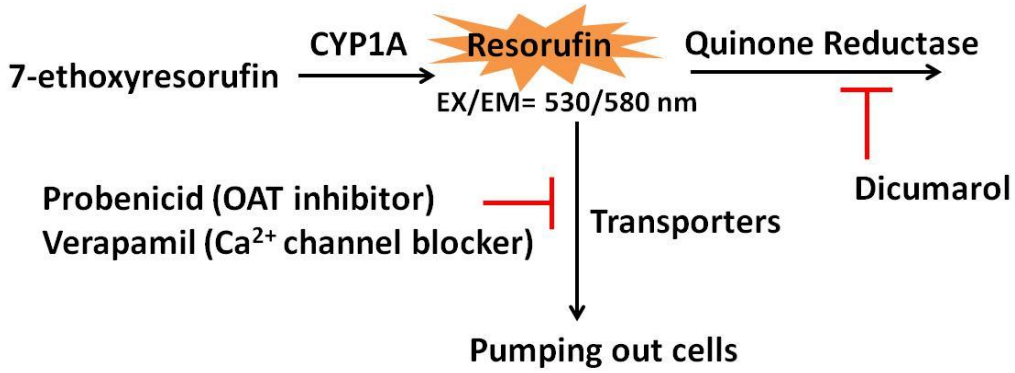

Fig. 2: A conceptual diagram of EROD kinetic confocal assay.

CYP3A4 Glo: CYP3A4 enzyme activity was measured using the P450-GloCYP3A4 kit according to the manufacturer's instructions (Promega, Madison, WI), as modified by Choi et al. [67]. Briefly, cells were incubated with luciferin-IPA (3 μM) under static state (2D) or continuous flow (MPS) at 50 μL/hour for 4-6 hours at 37 ^{0}C. Culture supernatants (2D) and effluent media (MPS) were collected every hour starting 2 hours before, during, and after the incubation with luciferin-IPA. Collected samples were incubated with luciferin detection reagent for 20 minutes at room temperature. Relative luminescence units (RLUs) were measured on a luminescence plate reader. The quantification of the luciferin produced was determined by a calibration curve of various concentrations of d-luciferin.

Analysis of midazolam (MDZ) metabolite (1-OH-MDZ) in effluents: Cells cultured in MPS were incubated with media containing 100 μM MDZ for 4 hours via a flow rate of 5 μL/min. Effluent medium was collected and analyzed for MDZ and 1-OH-MDZ by selective ion gas chromatography-negative chemical ionization mass spectrometry (GC /NCI-MS) according to Paine et al. [68].

Monitoring of canalicular structures

Chloromethyfluorescein diacetate (CMFDA, CellTracker™ Green CMFDA Dye, Invitrogen, Carlsbad, CA), a fluorescent substrate for the bile transporter -MRP2, to examine canalicular structure in our liver MPS model [34]. The stock solution was diluted to a final working concentration of 25 μM in serum free medium. Pre-warmed CMFDA working solution was perfused through the MPS in a cell culture incubator for 15 minutes at a flow rate of 5 μL/min, followed by culture media for 3 minutes at a flow rate of 5 μL/min. After the procedure, chips were imaged using fluorescent microscopy to determine green fluorescence.

Statistical analysis

GraphPad Prism 6 was used to plot and analyze results. All results were from three independent experiments of hepatocyte cultures (total N=3). Average ± standard deviation and the two-tailed t-test for independent samples were used to compare two groups.

Results

Comparison of cell viability between conventional 2D culture and MPS

Primary rat hepatocytes maintained a differentiated morphology (e.g., an epithelial cell-like appearance) for up to 14-28 days in culture in MPS (Figure 3).

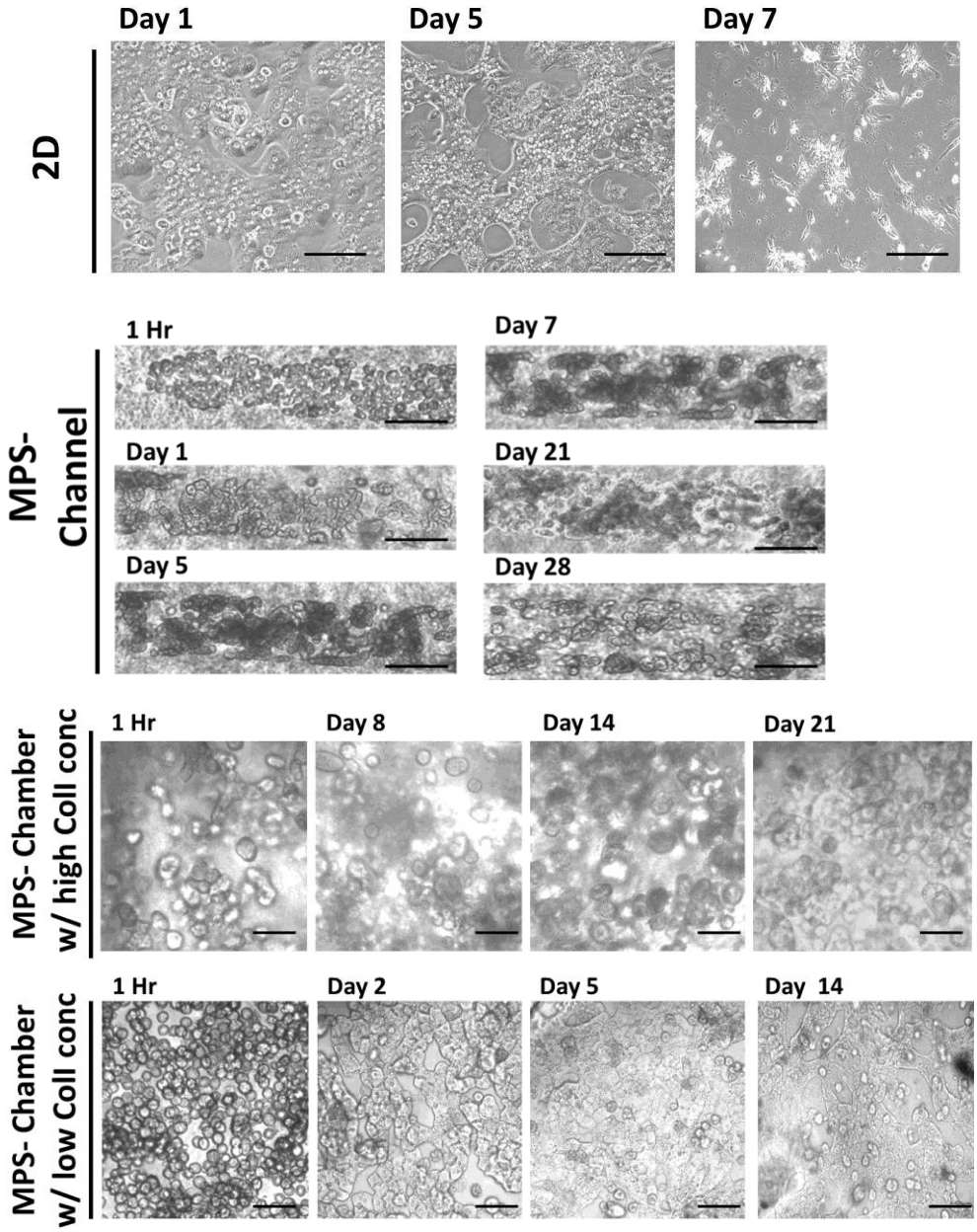

Fig. 3: Morphologies of rat hepatocytes cultured in 2D or MPS over time. Phase contrast pictures show primary rat hepatocytes cultured in conventional 2D culture (6-well or 24-well plate) **(top)** and MPS, (middle) including seeding in the channel, and seeding in the chamber with high concentration (3 mg/mL), or low concentration (1.3 mg/mL) of type I collagen up to 28 days (bottom).

LIVE/DEAD® staining showed that rat hepatocytes in conventional 2D culture survived for a maximum of 6 -8 days (Figure 4). In contrast, cells in the MPS had higher viability with epithelial cell-like morphology up to 28 days.

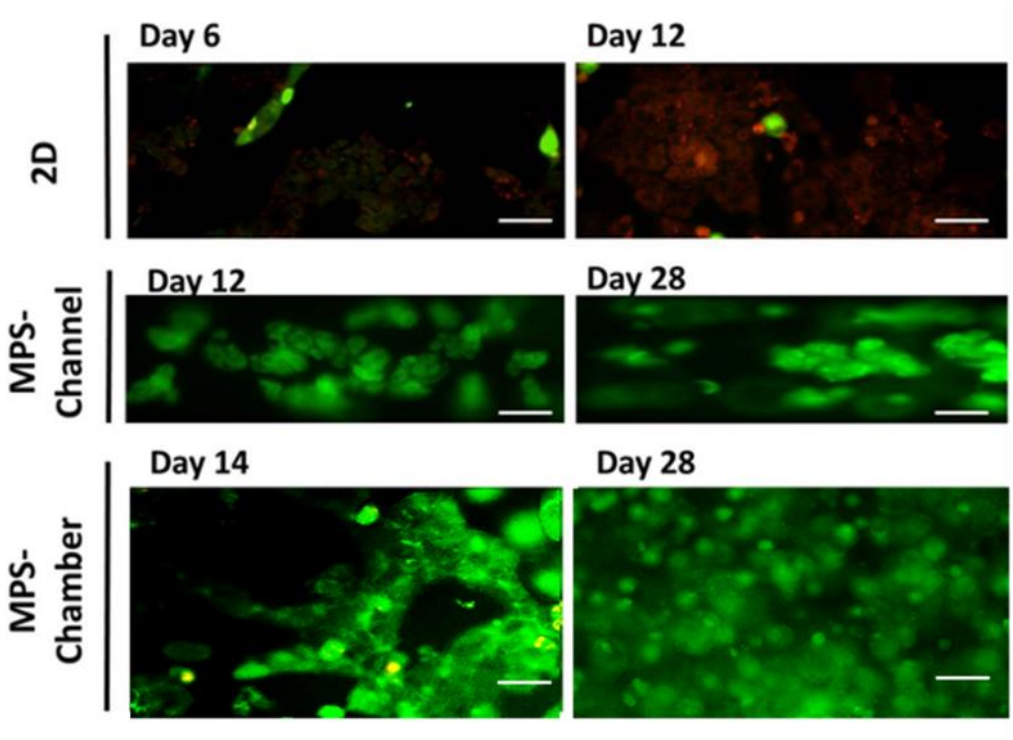

Figure 4. LIVE/DEAD® vital staining of rat hepatocytes at different cultured periods. Cells were incubated in 2D or MPS culture for up to 28 days (red= ethidium homodimer-1stained dead cells; green= live cells that can metabolize calcein AM to calcein; bar=50 μm; 200x magnification).

One significant advantage of using MPS culture is the ability to measure cytotoxicity biomarkers such as LDH and ALT released in effluents collected at different days without terminating the culture. In clinical medicine, such serum markers of hepatocellular injury play a crucial role in evaluating hepatotoxicity, which also can be applied to *in vitro* preclinical studies [69]. Cell viability on the day of seeding (day 1, represented as 100 ± 8.0% viability measured using LDH released by lysing whole cells in a parallel chip) can be cumulatively subtracted by the measurement of LDH

released in effluents on following culture days. The LDH release data (Fig. 5) show that MPS cultures of rat hepatocytes maintained 82.4 ± 7.0% viability up to 28 days, compared to 2D cultures which only had 27.9 ± 8.4% viability on day 8. This difference in viability between 2D and MPS was statistically significant (p <0.05) after culturing for 2 days.

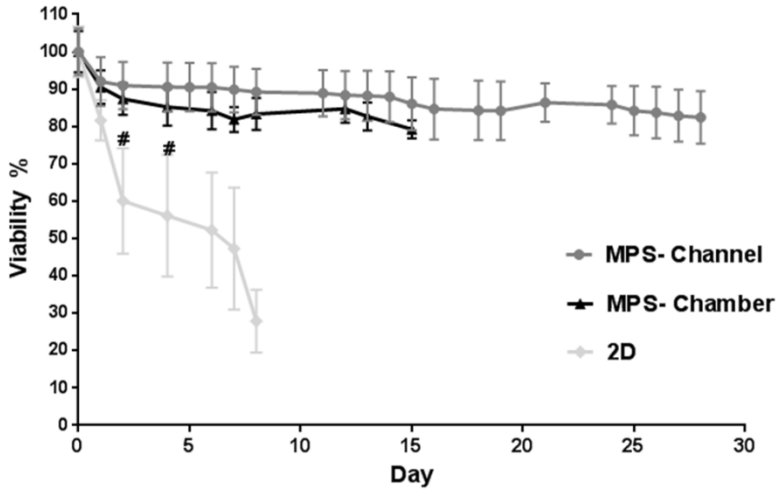

Fig. 5: Viabilities of rat hepatocytes cultured in 2D or MPS over time.
Lactate dehydrogenase (LDH) released to media in rat hepatocytes cultured in 2D or MPS over time. LDH release measurements were used to determine viability over time (% to seeding number = 100 ± 8 % of viability). Results presented as mean ± SD from 3-4 independent experiments, including 5-6 MPS chips on different days (over 24 h collection of effluxes) and 6 wells of 2-well chamber slides (t-test, #, p< 0.01).

Similar results were observed in human hepatocytes. Human hepatocytes maintained differentiated hepatocyte morphology (Fig. 6) with ~80% viability up to 15 days in culture in MPS compared to a small percent of live cells at day 8 in 2D culture (Fig 7).

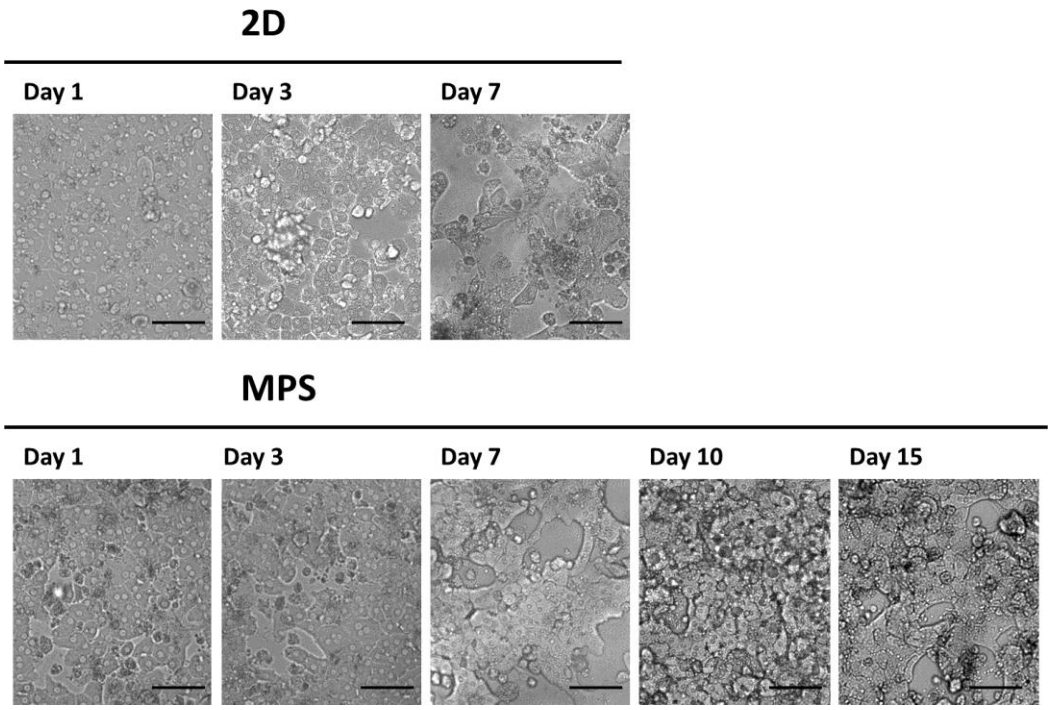

Fig. 6. Morphologies of human hepatocytes cultured in 2D or MPS over time. Phase contrast pictures show primary human hepatocytes (donor: HUM4038) in conventional 2D culture (top) and MPS culture (bottom). Bar=100 μm; 200x magnification.

Based on cell morphology and LIVE/DEAD® staining, the few viable cells seen in 2D culture on day 8 were non-parenchymal cells (Fig. 7). These cells were considered neither hepatocytes nor epithelial cell-like cells.

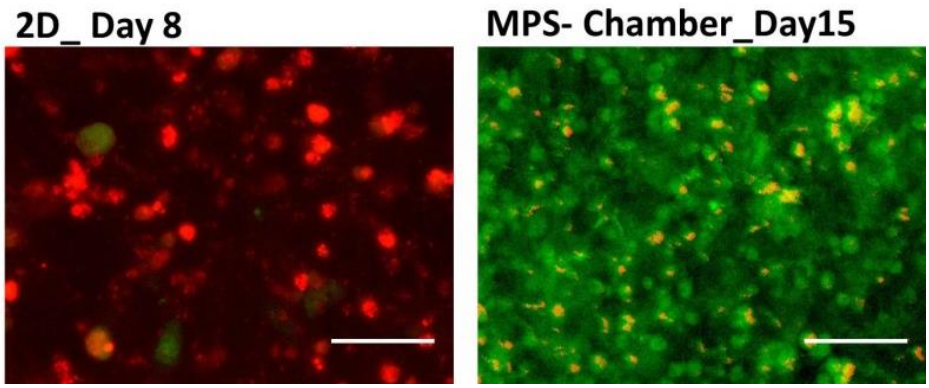

Figure 7. LIVE/DEAD® vital staining of freshly isolated human hepatocytes. Cells were from donor 14-018 cultured in 2D on day 8 and in MPS on day 15 (MPS chamber culture with low concentration of type I collagen; bar =50 μm).

The level of ALT in effluents or culture media was used as a surrogate for damaged and dead cells when comparing the viability of human hepatocytes for 2D vs. MPS

culture. Human hepatocytes from three different donors in conventional 2D culture had a higher level of ALT release (normalized to medium volume and cell seeding number) compared to cells in MPS culture (Fig. 8).

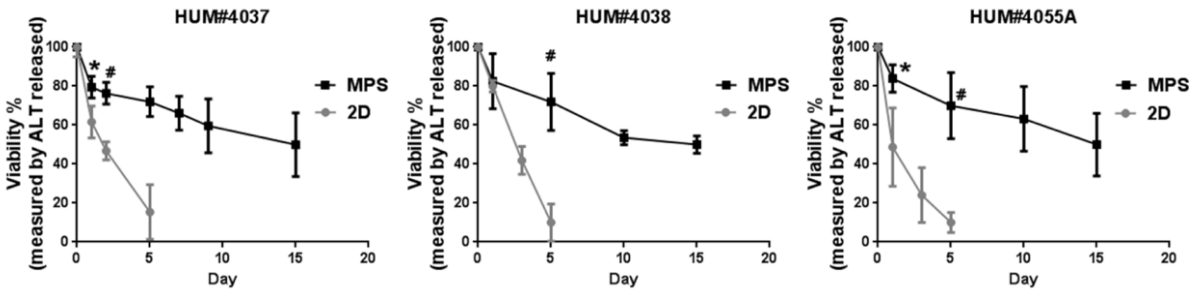

Figure 8. Percent Viability determined by alanine transaminase (ALT) release from human hepatocytes cultured in 2D or MPS. Human hepatocytes were from the donors of HUM#4038 and HUM#4055A, cultured up to 15 days. Results presented as mean ± SD from 3 MPS chips and 3 wells of 2-well chamber slides in 3 independent experiments. Each sample had triplicated data in each assay (t-test, *, $p< 0.05$, #, $p< 0.01$).

Comparison of hepatic functioning between 2D and MPS cultures using primary hepatocytes

Due to limited cell numbers in channel-seeded MPS (approximate 2000 cells/ chip), we decided to use chamber seeding in MPS (20,000 – 25,000 cells/chip) for testing hepatic functions.

HNF4α expression: ICC staining of HNF4α, a marker for liver function and differentiation, was performed to compare the conventional 2D culture and MPS. Figure 9A shows that 59 ± 11.8 % of rat hepatocytes in MPS expressed HNF4α on day 7 compared to only 12.4 ± 58 % in 2D culture (p <0.01). Human hepatocytes in MPS culture not only maintained higher expression level of HNF4α on day 5, compared to 2D culture (Figure 9B, p <0.01), but also human hepatocytes in MPS maintained 74.74 ± 0.05 % of HNF4α expression on day 14.

A.

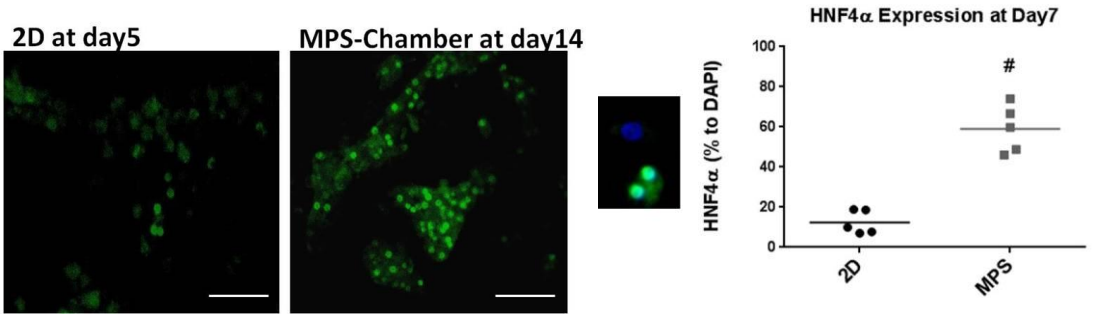

B.

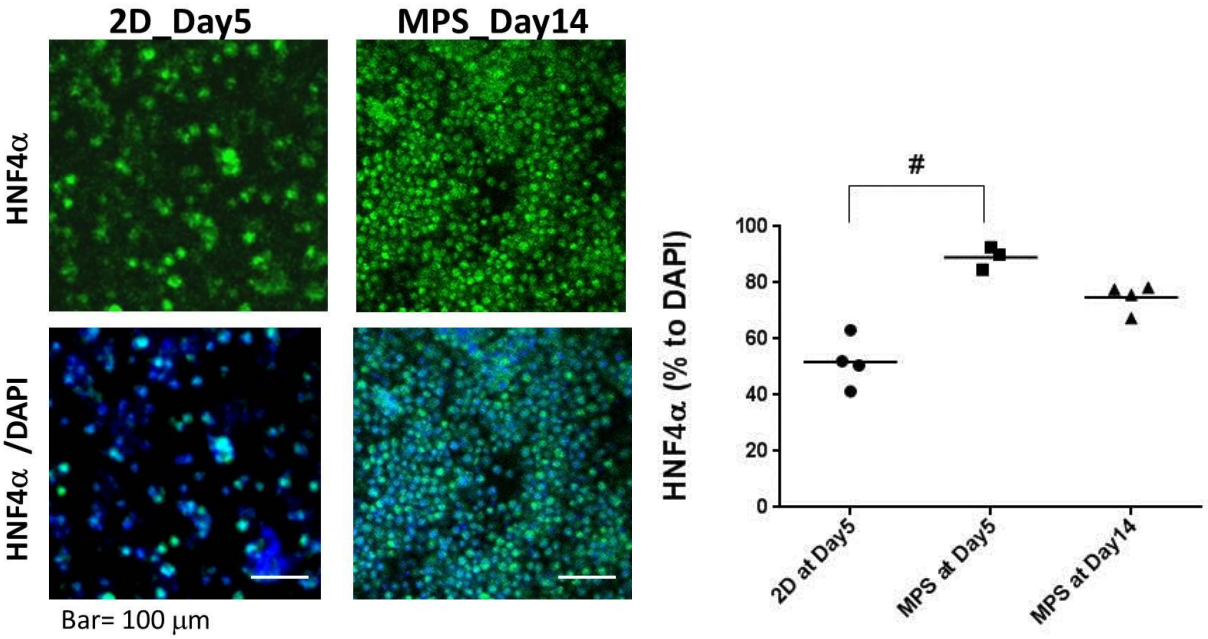

Fig. 9: The protein expression level of HNF4α in primary hepatocytes cultured in 2D or MPS: (A) HNF4α expression in rat hepatocytes cultured in 2D on day 5 and in MPS on day 14 (bar=100 μm; 200x magnification), and quantitative result of 2D versus MPS on day 7 (counted HNF4α % to counted DAPI nuclear staining). **(B)** Human hepatocytes (HUM#4080) cultured in 2D or MPS. Results presented as mean ± SD from 3-4 MPS chips and 4-5 wells of 2-well chamber slides. Each sample was counted within 5 randomly selected fields under 100x magnification. Significant differences were calculated from 2D versus MPS data using t-test (#, $p < 0.01$).

Albumin production: Albumin production is one of the major physiological functions of the liver *in vitro* [61]. ELISA results show that human hepatocytes in MPS

culture had higher albumin production (Figure 10) up to day 15 after normalization to the seeding cell number (10^6 cells: 0.5 x 10^6 cells for 2D; 0.02 x 10^6 cells for MPS).

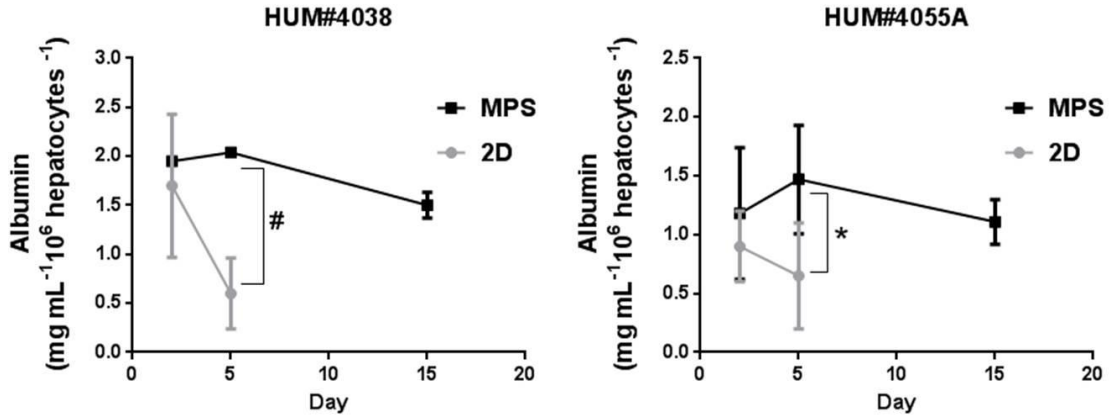

Fig. 10: Albumin production of human hepatocytes cultured in 2D or MPS over time. Cells from the donors of HUM#4038 and HUM#4055A cultured up to 15 days. Results presented as mean ± SD from 3 MPS chips and 3 wells of 2-well chamber slides in 3 independent experiments. Each sample had triplicated data in each assay (t-test, *, $p< 0.05$, #, $p< 0.01$).

Measurement of CYP1A1/2 activities: CYP1A activities from cells cultured in MPS were measured through the EROD kinetic confocal assay, a real-time confocal monitoring for 30-40 minutes using fluorescence intensity. The quantitative results of EROD assay, represented as △fluorescent intensity, show that induced enzyme activity was detectable in cells cultured in MPS. Figure 11 that rat hepatocytes pre-treated with BNF and cultured in MPS demonstrated BNF-inducible and dose-dependent CYP1A activity on day 7.

A.

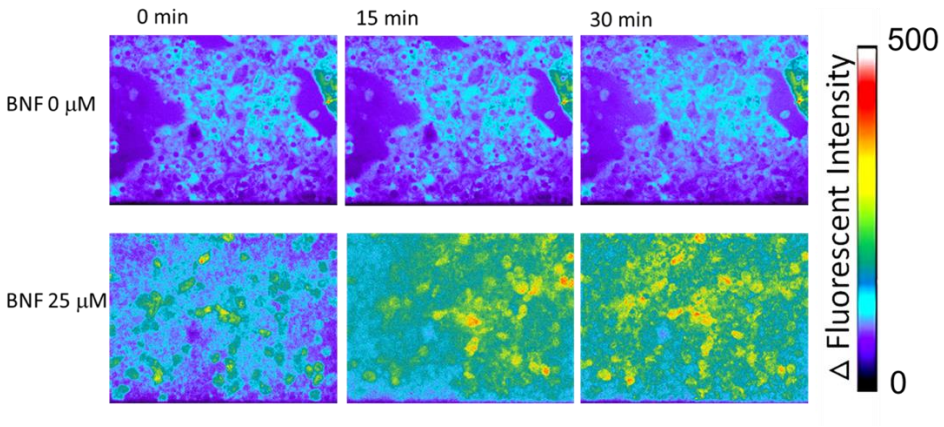

B

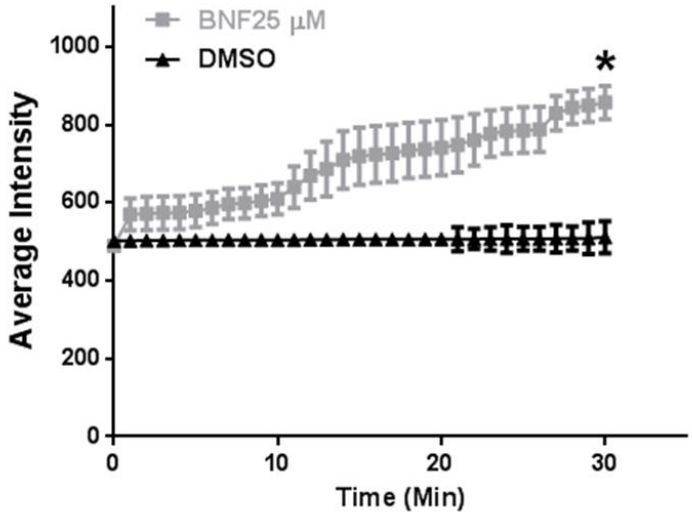

Fig. 11: CYP1A1/2 activity in primary rat hepatocytes cultured in MPS using EROD kinetic confocal assay. Cells cultured in MPS expressed BNF-inducible CYP1A1/2 after a perfusion of EROD subtract within 40 minutes. **(A)** EROD activity of rat hepatocytes cultured in MPS with or without BNF treatment for 72 hours.

Human hepatocytes in MPS also showed extensive induction of CYP1A with pretreatment with BNF over 72 hrs. Human hepatocytes in the MPS showed significantly greater responsiveness to BNF than cells in 2D culture (Fig 12).

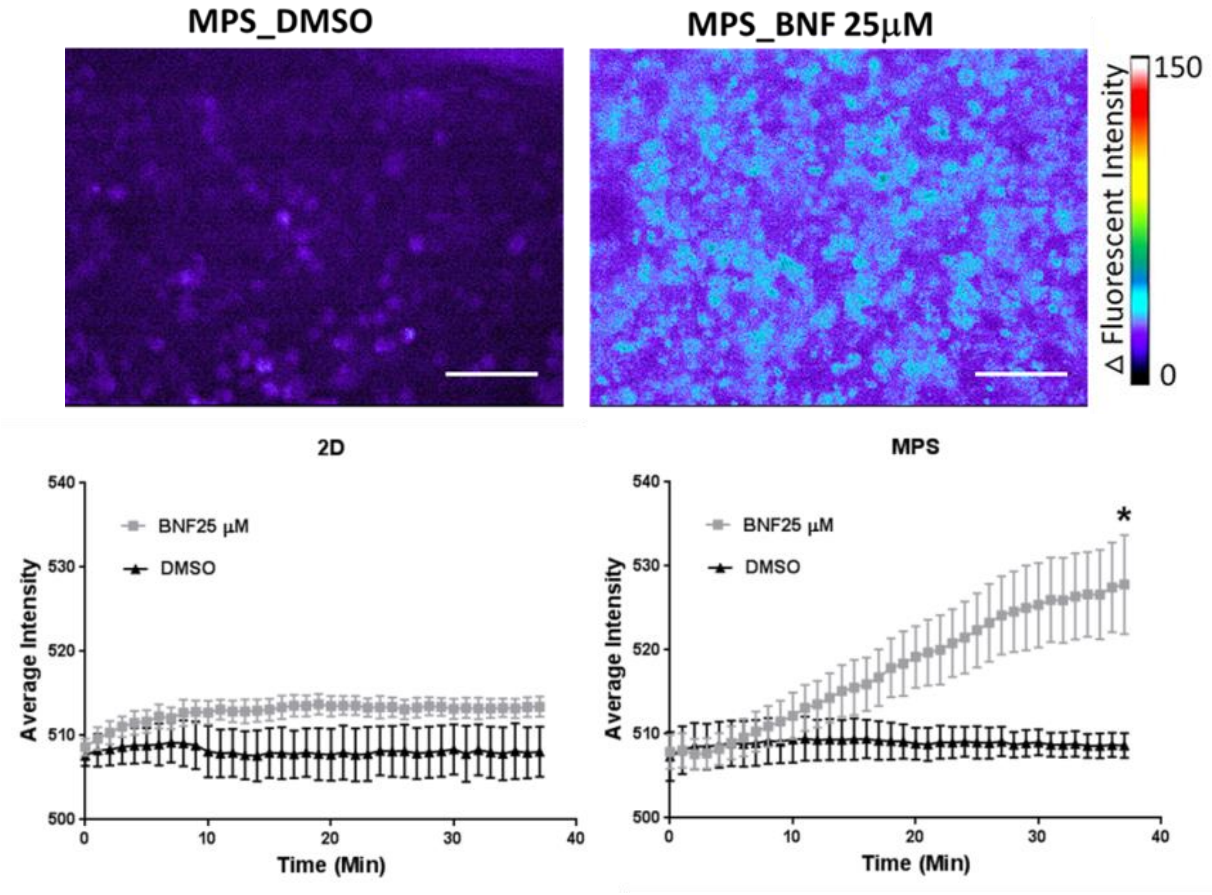

Fig. 12: CYP1A1/2 activity in primary human hepatocytes cultured in MPS using EROD kinetic confocal assay. EROD activity of human hepatocytes cultured in MPS with or without BNF treatment for 72 hours. Cells from donor of HUM#4038 cultured in MPS expressed BNF-inducible CYP1A1/2 after a perfusion of EROD subtract for 40 minutes (bar = 100 μm). Results presented as mean of average intensity from 3 MPS chips in 3 independent experiments. Each sample was analyzed for average intensity of 10 randomly selected cells under 100x magnification (t-test, *<0.01).

Repeated induction of CYP1A was evident by sequential 3 day treatment, followed by 3 days with no exposure, and induction repeated. This protocol found that CYP1A1/2 activities were repeatedly inducible in human hepatocytes cultured in MPS on day 5, day 10, and day 14 (Figure 13).

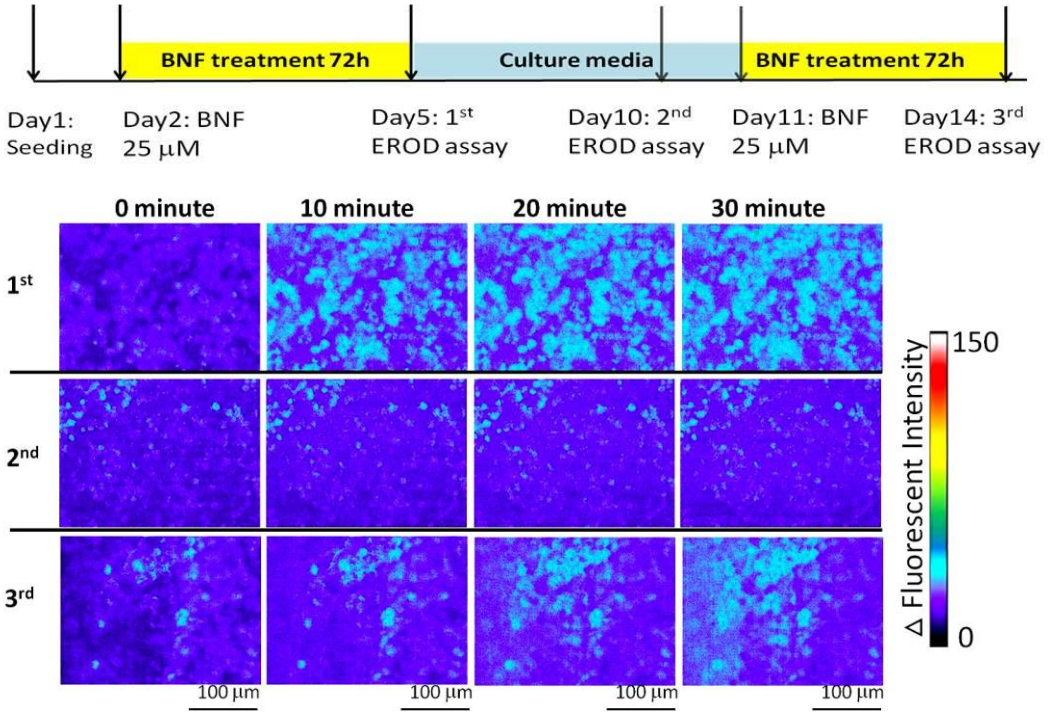

Fig. 13: Repeated induction CYP1A1/2 in primary human hepatocytes cultured in MPS using EROD kinetic confocal assay over 14 days. Repeatedly BNF-induced CYP1A1/2 in human hepatocytes cultured in MPS up to 14 days. An experimental flow chart of repeated BNF treatment and dates of performing EROD assays. Hepatocytes were from donor of HUM#4038 cultured in MPS. Repeatedly BNF-induced CYP1A1/2 was measured for 0, 10, 20, and 30 minutes on day 5, and repeated on day 10, and day 14 (bar = 100 μm).

Measurement of CYP3A4 activities: CYP3A4 is responsible for 30-50 % of drug and chemical metabolism, including the metabolism of midazolam (MDZ) and 25-OH-Vitamin D3 [70]. Inducible CYP3A4 activity was measured either by a luminescence reporter assay using the CYP3A4-specific bioluminescent substrate, luciferin-IPA [67], or by quantifying metabolites in effluents before and after inducing CYP3A4 with rifampicin (5 μM) for 72 hours. Results were calculated as area under the curve (AUC) of metabolite formation for the 6 hours following a 4-hour incubation with the parent compound, luceferin-IPA (3μM). The AUC values were normalized to the cell seeding number (50 x 10^4 cells in a 24-well plate for 2D; 2 x

10^4 cells in a MPS chip). Figure 14 shows that human hepatocytes in MPS had higher CYP3A4 activities on day 5 and day 9 compared to 2D culture.

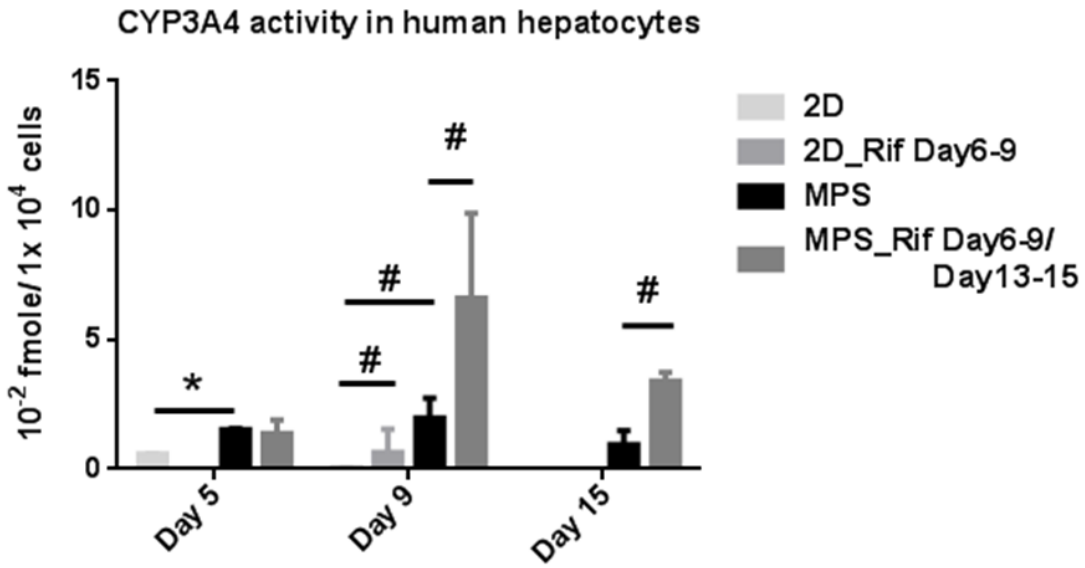

Fig. 14: CYP3A4 activity in primary hepatocytes cultured in 2D or MPS over time. The CYP3A4 'Glo® subtrate:' was used. Cells were pre-treated with rifampicin (Rif) 5 μM for 72 hours. Results presented as CYP3A4 metabolite formation normalized to the total culture areas of 2D or MPS (1.9 cm^2 of one well in 24 –well plate for 2D; 0.32 cm^2 for MPS) from 3 wells of 24-well plate or 3 MPS chips in 3 independent experiments (t-test. *, $p < 0.05$, $^\#$, $p < 0.01$).

Even though CYP3A4 activities decreased somewhat over time in MPS culture, human hepatocytes still exhibited enzymatic activities after 15 days in culture. Additionally, rifampicin–treated human hepatocytes in MPS (5 μM during days 6-9) had approximately 3-fold increased CYP3A4 activity compared to the DMSO-treated control. Qualitative LC-MS/MS data (Figure 15) showed that the CYP3A4 metabolite 1-OH-MDZ increased by about 3-fold after rifampin treatment for 72 hours. All results of CYP3A activity support that its activity was maintained through day 15 in cells cultured in MPS.

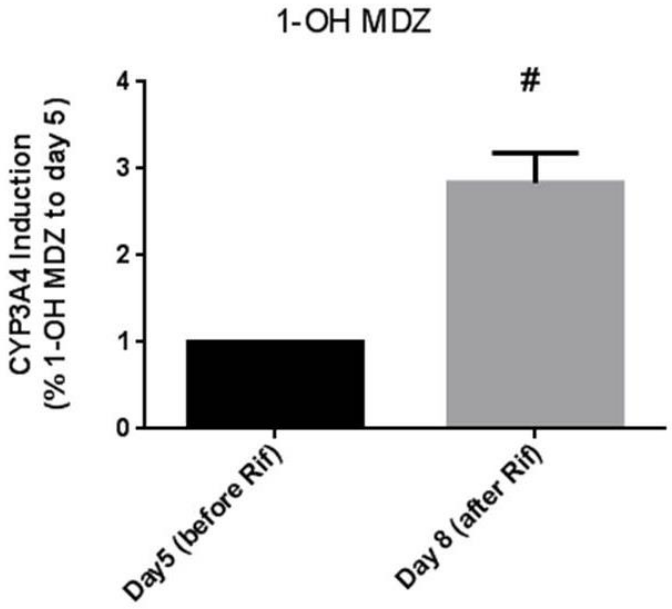

Figure 15. Midazolam (MDZ) hydroxylation in MPS system: Cells were pre-treated with rifampicin (Rif) 5 μM for 72 hours.100 μM MDZ in culture media was perfused though MPS for 4 hours. All the effluents before and after Rif treatment were collected for analysis of 1-OH MDZ. The 1-OH-midazolam formation was quantitative analyzed and was presented as the fold change compared to prior to Rif treatment. Human hepatocytes were from donors 15-001, 15-002, and 15-004. (t-test, *, $p< 0.05$, $^{\#}$, $p< 0.01$).

Investigating canaliculi structure and cell polarity in primary hepatocytes cultured in MPS

The primary human hepatocytes cultured in MPS maintained canaliculus-like structures (Figure 16A) up to 15 days in culture. ICC data (Figure 16B) show that cells cultured in MPS expressed BSEP and a bile duct-like structure on day 15 in culture, indicating that primary human hepatocytes maintained cell polarity in MPS culture. In order to investigate whether hepatocytes formed canalicular structures, we used chloromethyfluorescein diacetate (CMFDA), a fluorescent substrate for the bile transporter Multidrug Resistance-associated Protein (MRP2), to examine canalicular

structures in our liver MPS model [71]. Figure 16C showed canalicular structures was detected in human MPS model at day 15 in culture by CMFDA.

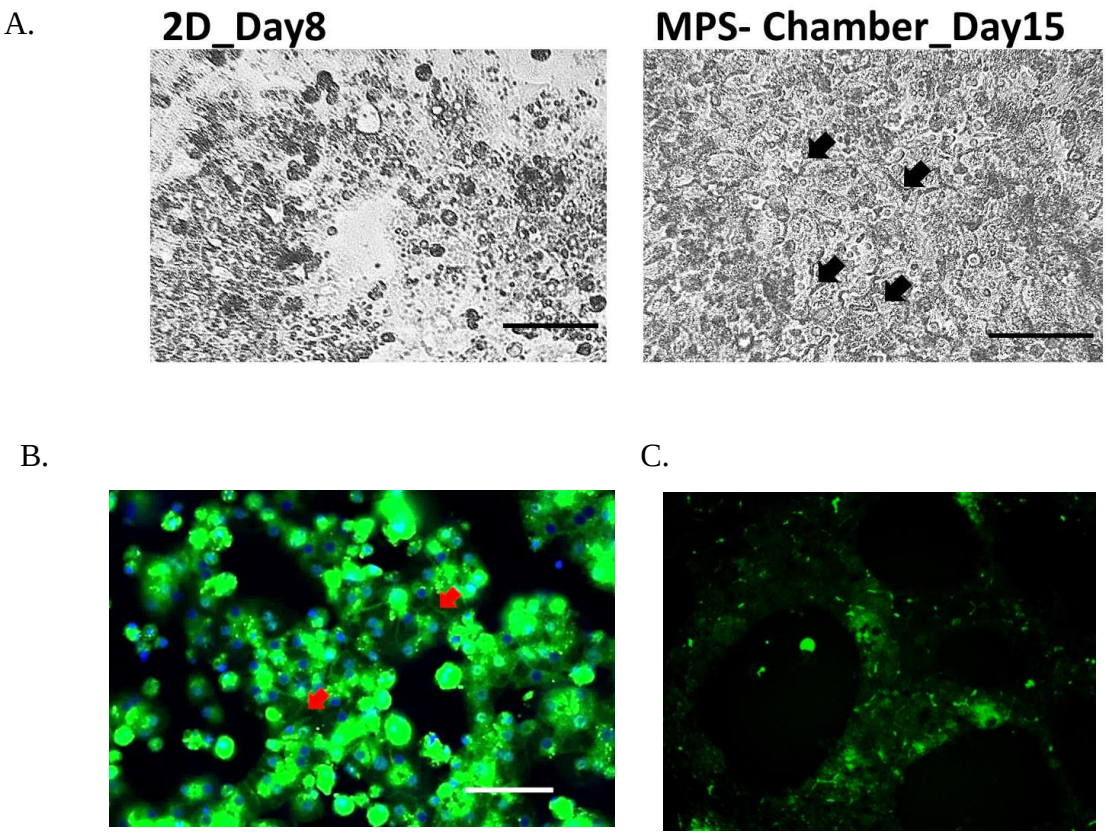

Fig. 16: Canalicular–like structures in human hepatocytes cultured in MPS on day 15. (A) Phase contract pictures showed human hepatocytes from donor 14-018 in 2D culture on day 8 and in MPS on day 15. **(B)** ICC of BSEP in hepatocytes from donor 14-018 in cultured in MPS on day 15 (bar=100 μm; 200x magnification). **(C)** Canaliculi structure was detected by CMFDA tracer in HUM4097B in culture in MPS on day 15. Black, white and red arrows indicated canaliculus-like structures.

Discussion

MPS platforms offer a new opportunity for reducing animal usage in pharmaceutical and toxicological research and provide an improved *in vitro* culture system for predicting the toxicity and efficacy of drugs and environmental chemicals. Many laboratories, research institutes, and government organizations are promoting the development of various organ-on-chips with different scaffolds, models, and cell

types [52]. However, there are many challenges to the broader use of MPS culture, including costs, scaling the flow rate for integrating multiple organs-on-chips, adsorption of hydrophobic compounds to chip matrix, and scarcity of primary human cells. In order to facilitate the usage of MPS culture for toxicity prediction, more evidence is needed to demonstrate that MPS culture provides benefits over conventional 2D culture. Towards this end, we must better characterize MPS culture by determining 1) if the microenvironment in MPS mimics cell growth *in vivo*, and 2) if the results using MPS culture better recapitulate the human response to drugs or environmental chemicals, compared to results using conventional 2D culture.

In this study, the results from our liver MPS model show that MPS culture offers an adequate microenvironment to maintain growth of primary rat and human hepatocytes with high viability and maintenance of crucial hepatic functionalities for at least 14 days. By comparison, 2D culture could only sustain cell growth for 7 days. Additionally, human hepatocytes cultured in the MPS also formed canalicular structures and maintained high levels of HNF4α expression, albumin production and inducible CYP1A activity. Even though CYP3A4 activity in human hepatocytes decreased on day 14 of MPS culture, hepatocytes in MPS retained the rifampicin-induced activity of CYP3A4. Furthermore, maintenance of CYP metabolic capacity was demonstrated in this MPS system through our aflatoxin (AFB) experiments (results not shown in this dissertation). Our work indicates that we can expose human hepatocytes to AFB, a toxicant that needs to be bioactivated, and detect hepatic cytotoxic effects of the highly reactive adduct-forming metabolites formed during AFB CYP metabolism. A possible next step of our study is to create a liver MPS model that is composed of multiple hepatic cells types, including endothelial cells, Kupffer cells, and stellate cells [72], with acinus and vascular structures, for

capturing immune responses. A liver MPS model with multiple cell types may also prolong viability and functionality for long-term *in vitro* culture [73-75].

Why is the MPS culture superior to the conventional 2D culture? Numerous studies [67, 76-78] have reported that a microfluidics system can maintain cell viability and functionality for a longer period in culture compared to cell culture without any flow. In addition, ECM gels, such as collagen or Matrigel, are often used in MPS culture. Using ECM gels can enhance cellular function and improve tissue organization, thereby better mimicking the natural architecture of tissues, cell structure and polarization [79, 80]. Several studies have found that ECM can provide an appropriate mechanical microenvironment for cell growth, tissue differentiation and maintenance of tissue functionalities [81-83]. The combination of ECM gel and the microfluidic system makes MPS a more representative *in vitro* organ-specific, biochemical and mechanical microenvironment for organoid type culture. A representative example is the kidney-on-a-chip microphysiological system that mimics renal physiology by reconstructing the proximal tubule of the kidney [50].

Even though MPS culture provides a promising future for pharmacology, toxicology and systems biology, there are still challenges that must be addressed [34]. For example, using polydimethylsiloxane (PDMS), a major material for fabricating MPS chips, can potentially confound the delivery of drug or toxicants in the MPS culture if the compounds are highly hydrophobic [84] because PDMS has been found to adsorb hydrophobic compounds ($\log P > 2.62$; [85]). Researchers have been working to solve this adsorption problem by using chemical surface modifications such as glass coating [86] [87]. In addition, these cutting-edge models are relatively expensive and are more labor intensive than traditional 2D cultures. However, in contrast to 2D cell culture, once individual organ chips are well-fabricated and tested, it should be possible to connect several organs into a multiple-organ MPS and then

validate these systems with well-known toxicants. In order to address these challenges, we and several other groups are supported by the Defense Advanced Research Projects Administration (DARPA), the National Center for Advancing Translational Sciences of the National Institutes of Health (NIH-NCATS), FDA, and the Environmental Protection Agency (EPA) [51, 52].

Chapter 2

Development of an Integrated Rat Liver- Kidney Microphysiological System (MPS) to Investigate Organ-Organ Interactions Using Aristolochic Acid- I (AA-I)

Abstract

To develop improved *in vitro/ex vivo* models for identifying potentially nephrotoxicity chemicals, we initially developed an integrated rat liver–kidney dual organ microphysiological systems (MPS) by connecting a kidney-on-a-chip platform using rat proximal tubule epithelial cells (PTECs) and a liver-on-a-chip using rat hepatocytes grown in MPS developed by Nortis, Inc. To test the hypothesis that hepatic clearance of a nephrotoxic chemical might have significant importance in determining ultimate kidney toxicity, we utilized aristolochic acid-I (AA-I), a well-known nephrotoxin and carcinogen, that undergoes extensive hepatic metabolism. Interestingly, using LIVE/DEAD® vital stain data to quantify the extent of nephrotoxicity after 24 hour treatment, hepatocyte exposure substantially increased toxicity in PTECs compared to direct exposure of the PTECs to AA, indicating that hepatic metabolism apparently contributes more to bioactivation of AA than to detoxification. We also detected increased levels of kidney injury molecule-1 (KIM-1), a kidney tubular injury marker, and alanine aminotransferase (ALT), a biomarker of liver and /or kidney injury, in effluents of liver→kidney MPS group after 25 μM AA treatment for 24 hours. In addition, inhibition of hepatic NAD(P)H dehydrogenase, quinone 1 (NQO1) with dicumarol attenuated AA-I toxicity in PTECs. These results demonstrate that *in vitro/ex vivo* bioactivation of AA potentially via NQO1 in the liver impacts its nephrotoxicity, and support the hypothesis that *in vitro/ex vivo* integrated MPS culture systems can be used to identify toxicologically relevant organ-organ

interactions that may occur *in vivo*, which also is an initial success for us to develop a human dual organ-on-a-chip system.

Introduction

Numerous laboratories have developed a variety of microphysiological systems (MPS) using human cells to recapitulate human organ functions with the support of by the Defense Advanced Research Projects Administration (DARPA), the National Center for Advancing Translational Sciences of the National Institutes of Health (NIH-NCATS), Food and Drug Administration (FDA), and the Environmental Protection Agency (EPA) [52, 88]. Such systems have great potential to improve toxicity testing used for preclinical drugs and xenobiotics. A representative example is lung-on-a-chip system by Harvard University reconstitutes the mechanically active alveolar-capillary barrier of the human lung [60]. With the increasing development of organ-on-chips, well-designed *in vitro* studies utilizing such systems could be transformative for future toxicology studies. Although much work has been accomplished with individual organ-based MPS models, there have been relatively few advances in utilizing combined or integrated multiple organs MPS approaches to identify toxicologically relevant organ-organ interactions *in vitro*.

Recent studies from our group describe a novel kidney-on-a-chip MPS that recapitulates renal physiology by reconstructing the proximal tubule of the kidney using human proximal tubule epithelial cells (PTECs) in the Nortis ® MPS [50, 89] as an *in vitro/ex vivo* model for predicting xenobiotic clearance in the kidney. In addition to the kidney, the liver is also a critical organ for predictive evaluation of the toxicity and efficacy of drugs and xenobiotics that can be bioactivated and/or be detoxified by hepatic biotransformation. We have also developed a liver MPS model using primary rat hepatocytes cultured in the Nortis ® MPS (described in Chapter 1). Our rat liver

MPS model maintains viability and functional enzymatic activities for at least 14 days in culture. In this study, we described a novel approach to evaluate whether two Nortis® MPS devices, one containing liver cells and the other PTECs, connected in series, can identify putative inter-organ interactions that occur *in vivo*. To test this general hypothesis, we chose to examine whether hepatic metabolism would alter the nephrotoxicity induced by aristolochic acid-I (AA-I), a toxin found in plants of *Aristolochiaceae* family [90].

Plant-derived AA is a mixture of nitrophenanthrene carboxylic acids, the primary forms being 8-methoxy-6-nitrophenanthro-(3,4-d)-1,3-dioxolo-5-carboxylic acid (AA-I) and the 8-demethoxylated form of AA-I (AA-II)[91]. Historically, exposure to AA has been associated with chronic renal failure, generally referred to as aristolochic acid nephropathy (AAN) or Balkan endemic nephropathy (BEN) [92]. These individuals have subsequent high risk for developing upper urinary tract urothelial carcinomas (UTUC) [93]. The International Agency for Research on Cancer (IARC) has classified herbal remedies containing AA as a Group 1, carcinogenic to humans [94]. Although AA-I and AA-II both are carcinogenic in rodents and mutagenetic in bacteria and mammalian cells, only AA-I displays nephrotoxic properties in rodents [95, 96]. Based on studies in experimental animals, oral administration of AA to rats caused a dose- and time-dependent tumor response in chronically exposed rats (1-10 mg/kg body weight for 3- 6 months or 0.1 mg/kg body weight for 12 months). Exposed animals developed a variety of benign or malignant tumors, including forestomach, kidney, renal pelvis, urinary bladder, ear duct, thymus, small intestine, and pancreas [97-99], via activation of the c-Ha-ras oncogene.

AA-I- induced cytotoxicity is associated with the activation of caspase 3/7[100]- AA-I can induce cell injury via activation of caspases. Li *et al.*, study [101] suggested the secretion of transforming growth factor-β (TGF-β) 1 in AA-I stimulated

apoptosis in human kidney (HK)-2 cells [102]. AA also has been identified its toxicity to induce apoptosis via STAT3-dependent posttranslational modification and p53 activation [103]. Results of Y. H. Hsin *et al*., study demonstrated that AA can induce intracellular Ca^{2+} concentration, leading to mitochondria stress and release of cytochrome C [104]. Increased ROS level also has been found in AA-I-treated renal tubular epithelial Madin-Darby canine kidney (MDCK) cells [105].

AA-I undergoes extensive hepatic metabolism by several enzymes, including various cytochrome P450 enzymes (CYPs: CYP1A1 and 1A2; CYP1A2 is a liver specific form) and NAD(P)H dehydrogenase, quinone 1 (also known as NAD(P)H: quinone oxidoreductase (NQO1)[106-110]. AA-I has been shown to cause genotoxicity *in vitro* and *in vivo* via bioactivation. Previous studies in our laboratory demonstrated that induction of CYP1A1/2 can detoxify AA-I to non-toxic metabolite- 8-hydroxy aristolochic acid, AA Ia [111]. Previous studies have suggested that when AA-I (the predominant form of AA) is not detoxified via CYP-mediated oxidative O-demethylation to AA-Ia in the liver, it is instead activated to a toxic metabolite-aristolactam-I(AL-I) via reduction of the nitro moieties of the phenanthrane ring by one or more enzymes with nitroreductase activity, including potentially NQO1, xanthine oxidase (XDH), NADPH:CYP reductase (POR), and CYP1A1/2 [112, 113].

However, the exact mechanisms of how and which hepatic enzymes activate or detoxify AA-I remain unclear because the results from *in vitro* and *in vivo* studies were inconsistent [114]. For example, the NQO1 inhibitor-dicumarol largely eliminated the genotoxicity of AA-I in kidney cells *in vitro* [115] [116], but dicumarol can also induce NQO1 protein expression level *in vivo,* which could increase AA-I activation to the genotoxic lactam metabolite [115, 117].

A.

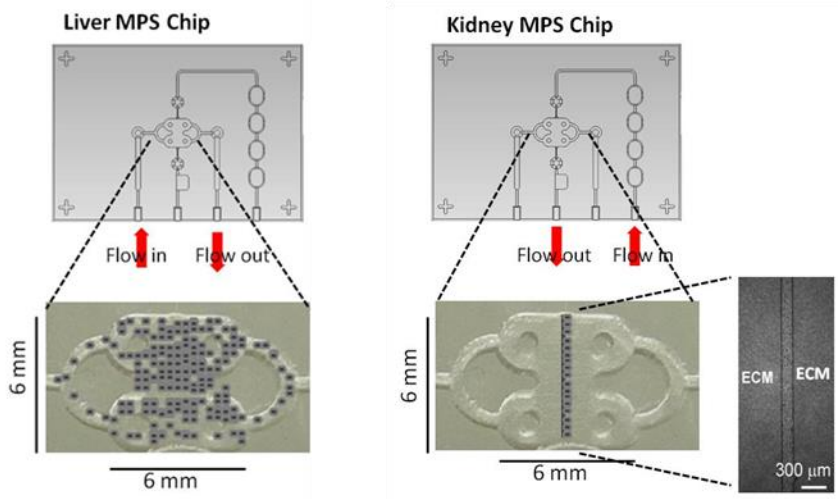

B.

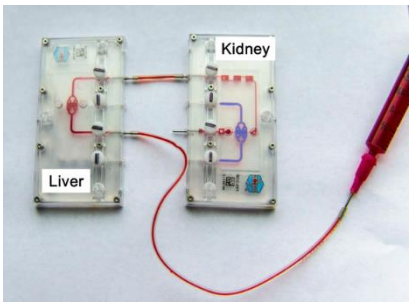

Fig. 17. Integrated Liver- kidney MPS models. (A) Individual kidney MPS chip vs. liver MPS chip. PTEC cells were injected into MPS filled with type I collagen (6 mg/mL) to form tubular structure as the kidney MPS chip. Hepatocytes were seeded through the whole chamber with Matrigel® (0.23 mg/ml) overlay on the top as the liver MPS chip. Liver MPS and kidney MPS were separately maintained with flow rates until the treatment. Grey dots represent cells. **(B)** Flow routes of liver-kidney MPS models were connected with C-Flex® tubing indicated by the red dye.

The integrated MPS model (Liver→kidney, shown in Figure 17) described herein represents a novel *in vitro* approach for investigating liver-kidney interactions in renal toxicity of AA-I, and provides a mechanistic approach to understand the role of hepatic

bioactivation and/or detoxification in AA-I nephrotoxicity. First, we were interested in whether the integrated liver→kidney MPS model can be used effectively to understand sequential effects from AA-I exposure. To that end, we used primary rat cells, including hepatocytes and PTECs, for the initial development. Based on our results using this novel integrated MPS model, we conclude that overall biotransformation of AA-I by hepatic enzymes increases, rather than decreases, the toxicity of AA-I in kidney, as indicated by an increase in cytotoxicity and increase in the release of the organ-specific injury biomarker- Kidney Injury Molecule-1 (KIM-1) [118] and liver injury marker (alanine aminotransferase, ALT) [119] in liver → kidney effluents. In clinical medicine, KIM-I is a more specific biomarker in urine for ischemic tubule injury than other biomarkers such as leucine aminopeptidase, alkaline phosphatase, α-glucosidase, and γ-glutamyl transpeptidase (GGT). A meta-analysis reported by Xinghua Shao et al. showed that the estimated sensitivity of urinary KIM-1 for the diagnosis of acute kidney injury was 74.0% (95% CI, 61.0%–84.0%), and specificity was 86.0% (95% CI, 74.0%–93.0%), suggesting urinary KIM-1 is a promising biomarker for early detection of acute kidney injury with considerable predictive value [120]. ALT is considered as liver specific injury biomarker but higher ALT levels are associated with acute kidney injury in patents [121] and laboratory animal models [122].

In addition, we provide further evidence to suggest that hepatic NQO1 is involved in the bioactivation of AA-I, based on the results from dicumarol and AA-I co-treatment. Dicumarol attenuated AA-I induced toxicity. This study demonstrates that an integrated MPS model can be used effectively to investigate the organ interactions between liver and kidney *in vitro/ex vivo.* This approach may be of substantial value to pre-clinical toxicity screening for chemicals, and for identifying mechanisms for potentially important organ-organ interactions. The most important

aspect of this study is that it provides a foundation for developing an integrated dual organ MPS model using human cells.

Materials and Methods

Animals

Adult male Sprague Dawley® rats, 40-60 days-old, were used for kidney and rat liver tissues (Charles River, Seattle, WA). Animals were maintained in ALAC-approved vivarium facilities at the University of Washington, and all protocols for animal use and care were approved by the UW Institutional Animal Care and Use Committee.

Isolation of PTECs and PTECs culture in MPS chips

Cell culture supplies and materials were from Thermo Fisher Scientific (Waltham, MA). Rat PTECs were isolated from rat kidneys using *in vitro* collagenase digestion [123]. Isolated PTECs were grown in a 2D flask with PTEC culture media, including MEM/F12 media supplemented with 2.5 mM glutamine, 100x-diluted ITSA, 50 nM hydrocortisone and 100x –diluted antibiotic-antimyotic. After expanding cells in 2D monolayer culture, PTECs were re-suspended using 0.01% trypsin, and then injected into Nortis® MPS chips pre-filled with collagen type I (6 mg/mL at tail collagen type I; Ibidi, Madison, WI). The MPS platform used in these studies was developed by Nortis Inc. (Woodinville, WA) and details of its construction have been reported by Tourovskaia et al [124]. After cell injection and stabilization overnight at 37℃, 5% CO_2 incubator, the MPS chips were connected with C-Flex tubing ® and PTEC culture media-loaded syringe at a flow rate of 0.5 μL/min controlled by infusion/syringe pumps (KD Scentific Inc. model# KDS220). PTECs in MPS chips can be maintained for more than two weeks prior to subsequent treatments [89].

Source of hepatocytes and hepatocytes culture in MPS chips

Primary rat hepatocytes were isolated by two-step collagenase digestion following isolation [64]. All MPS chips used for hepatocytes seeding were pre-coated with 0.1 mg /mL of collagen type I in PBS with 0.1% acetic acid at 37℃, 5% CO_2 incubator

for 1 hour. For plating hepatocytes into MPS culture, 0.1 to 0.2 mL of a cell suspension at a density of 2 x 10^6 hepatocytes/mL was injected into each chip via the abluminal ports. Hepatocyte plating medium consisted of William's E medium supplemented with 5% fetal bovine serum (FBS), 100 mg/ml penicillin streptomycin, 100 nM dexamethasone, 1 μg/mL of Gibco® Fungizone® 100x diluted ITS+, and 0.2 mM glutaMAX. After 4 hours of plating, the hepatocytes were overlaid with Matrigel® (Corning®, final conc. 0.23 mg/ml) in maintenance medium (the same formula for plating medium but without FBS) via abluminal ports. Following maintenance of cells at 37℃, 5% CO_2 incubator overnight, cells in MPS chips were held at 37℃with 5% CO_2 in a sterile incubator, and were maintained in maintenance medium with abluminal flow at flow rates between 5 to 10 μL/hr via infusion/syringe pumps (KD Scientific Inc. model# KDS220). Hepatocytes in MPS chips were maintained with high viability up to 5-7 days prior to the further treatments.

AA-I treatment in cells cultured in MPS

AA-I and dicumarol were purchased from Sigma Aldrich Co. LLC (St. Louis, MO; catalog #A5512 and catalog # M1390). Probenecid (water soluble) was purchased from ThermoFisher Scientific (catalog# P36400).

PTECs cultured in MPS were checked for cell confluency and tubule morphology before AA-I treatment. Only kidney MPS with 95 -100% confluence were used for further treatments. Two groups of cells cultured in MPS were subjected to AA-I treatment: 1) kidney-only group that has only PTECs cultured in MPS chips, and 2) liver→kidney group that includes MPS chips with 3D cultured hepatocytes connected upstream of another MPS chip with PTECs. The connection of liver→kidney MPS model utilized C-Flex® tubing (Fig. 17B; flow is from abluminal liver chip into luminal kidney chip). Cells cultured in the MPS were treated with AA-I with/without

dicumarol in the treatment media (mixtures of PTEC culture media and hepatocytes maintenance media at volume ratio of 50: 50) for 24 hours at a flow rate of 1.5 μL/min. After AA-I treatment, LIVE/DEAD® staining was used to analyze AA-I-mediated cell death in hepatocytes and PTECs (shown in Figure 18). Quantitative results of cytotoxicity, measured as percent of viable cells, were calculated from the ratio of dead cells (red fluorescent-stained cells from LIVE/DEAD® staining) and detached cells to the total cell number (Hoechst 33342 stained cells) (Figure 18, N=5). Effluents were collected and stored in -80 ℃ for later analysis of organ –specific injury biomarkers.

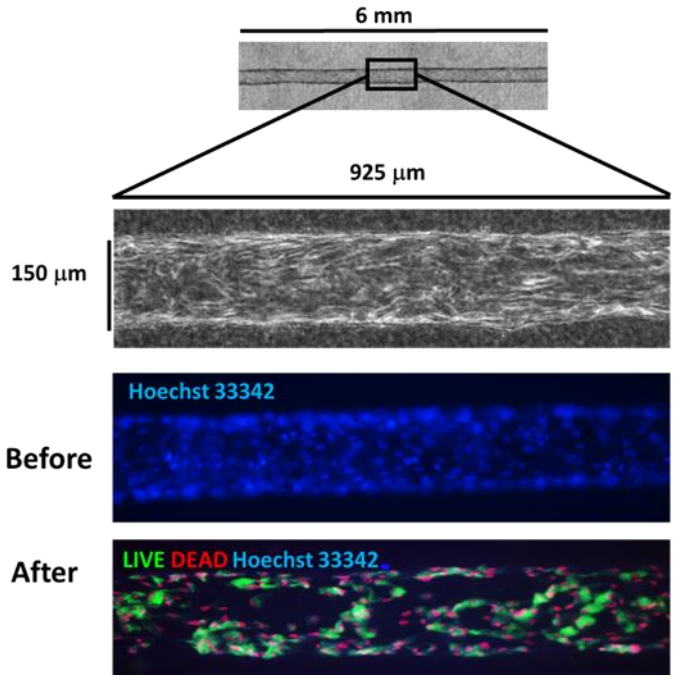

$$\text{Cytotoxicity\%} = \frac{\#\text{ of Dead cells} + \#\text{ of lost cells } (\Delta\text{Hoechst 33342})}{\#\text{ of Original cells } (\text{Hoechst 33342})}$$

Fig. 18. Method used to quantify cytotoxicity. The population of PTECs-formed kidney tubule-like network of cells with 95-100% confluence, 6 mm in length. A randomly picked microscopy image of kidney tubule with a 100x magnitude (Hoechst 33342 stained, 222 ± 5 rat cells vs. had 209 ± 9 human cells, N=5) in an area of 150 x 925 μm^2 (wide x length) is shown. All kidney MPS chips were checked for confluency before the treatment. Only kidney MPS chips with 95-100% confluence were used. After AA-I exposure, LIVE/DEAD® staining was performed and imaged

under a microscope with a 100x magnification from a randomly picked area of kidney tubule to assess cytotoxicity. Cytotoxicity % was calculated from an equation of [# of dead cells + # of lost cells]/ [# of initial total cells] in a field with size of 150 x 925 μm^2.

LIVE/DEAD® staining

The LIVE/DEAD® viability/cytotoxicity kit and Hoechst 33342 (Life Technologies) were used to distinguish live cells from dead cells according to manufacturer's specifications. Briefly, calcein AM (final conc. 2 μM), EthD-1 (final conc. 4 μM) and Hoechst 33342 (final conc.0.1 μg/ml) were diluted in pre-warmed D-PBS. Adequate volume of diluted reagents was perfused through the MPS chips at 5 μL/min via a luminal port of kidney MPS for 20 minutes and then was incubated for 10 minutes at 37 ^{0}C. After the staining procedure, chips were imaged using fluorescent microscopy (Nikon Eclipse Ti-S and inverted spinning disk microscope, 3i-Intelligent Imaging Innovations, Denver, CO) to calculate the numbers of dead cells (red stained cells) and Hoechst 33342-stained cells. All results were repeated with 3-4 independent experiments (N=4-7). Representative images are shown in the Results.

Analysis of organ-specific injury biomarker- KIM-1 and ALT

Meso Scale Discovery immunoassay kits (Meso Scale Diagnostic, Inc.) were used to measure KIM-1 (rat) in effluents following the manufacturer's suggested protocol. The levels of ALT were measured by Phoenix Central Laboratory (Mukilteo, WA, USA)

Statistical Analysis

GraphPad Prism 6 was used to plot and analyze results. All results of MPS culture were from three to four independent experiments of AA treatment. The two-tailed t-test for independent samples was used to compare two groups.

Results

Hepatic metabolism bioactivates AA-I toxicity in the rat MPS model

The results from LIVE/DEAD® stain (Figure 19) with primary rat cells showed that AA-I treatment resulted in greater kidney cell mortality in liver→ kidney group compared to kidney-only group, indicating that hepatic metabolism substantially increased AA-I toxicity in PTECs.

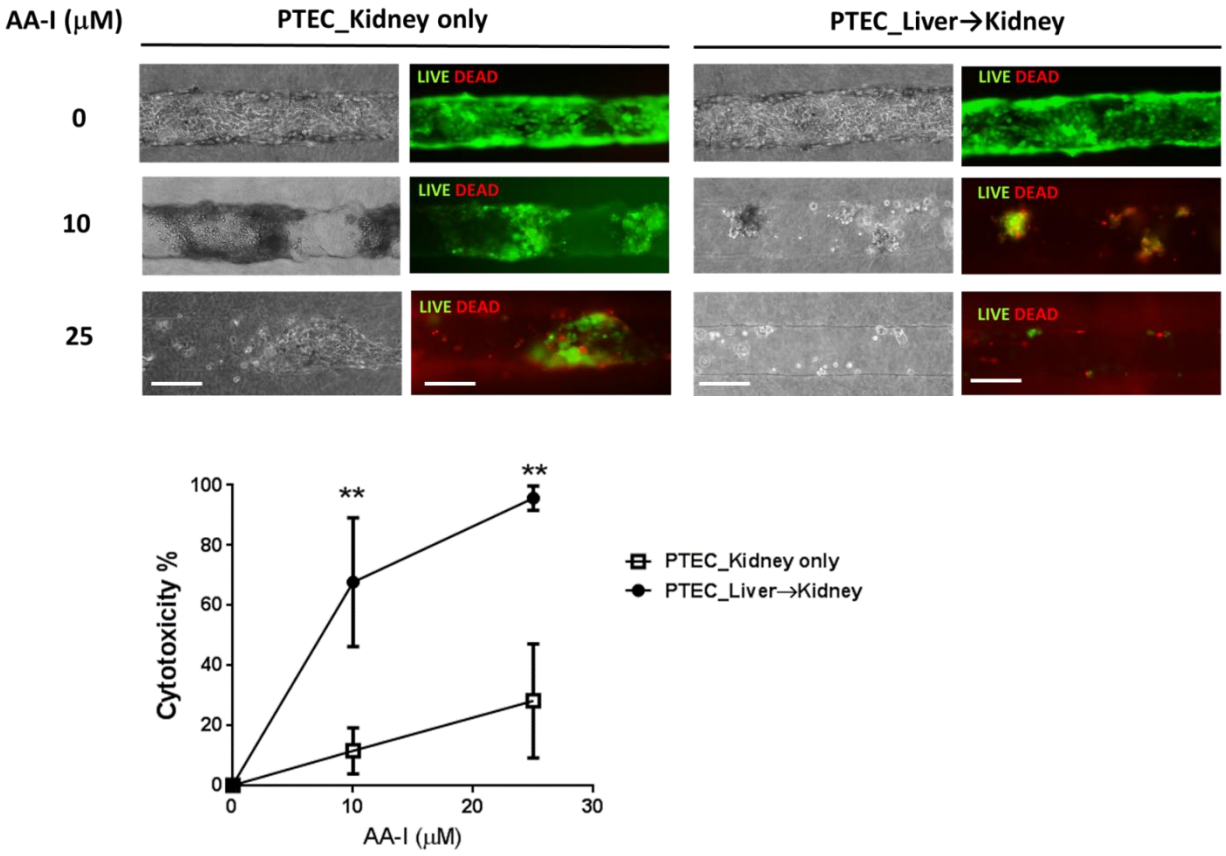

Fig. 19. AA-I toxicity with or without hepatic metabolism in rat kidney MPS. (A) Phase contrast pictures and LIVE/DEAD® staining showed rat PTECs cultured in MPS after AA-I treatment for 24 hours, and cytotoxicity% (N=4-7). Statistic significant was calculated between Kidney only group and Liver→ kidney group using t-test (*: $p<0.05$; **: $p< 0.01$). Bar = 150 μm

Quantitatively, the ratio of dead cells (red fluorescent-stained cells) and detached cells to initial total cells number, indicated that AA-I treatment was significantly more toxic

in PTECs with pre-hepatic metabolism (liver→ kidney group) compared to PTECs directly exposed to AA-I (kidney-only group) (Figure 12).

Hepatic metabolism of AA-I increases release of kidney-specific injury biomarkers into effluents from PTECs

In addition to cellular images and fluorescent probes, organ-specific injury biomarkers in effluents can be used to evaluate organ-specific toxic responses. Utilization of such biomarkers provides another advantage of using MPS culture to recapitulate *in vivo* fluid dynamics such as the transport of metabolites into urine. To that end, we found that the KIM-1, a kidney-specific biomarker of kidney toxicity, was increased in effluents of rat liver→kidney MPS group after 25 μM AA-I treatment for 24 hours (Figure 20A; 2.1- fold compared to the vehicle control with 15 ± 6.8 pg/mL, $p < 0.01$; 2.0- fold compared to kidney only group at 25 μM with 16.9 ± 7.6 pg/mL; $p < 0.05$). ALT, which is increased in response to liver, and also is associated with acute kidney injury toxicity *in vivo*, also showed an increased level in effluents of rat liver→ kidney MPS group after 25 μM AA-I treatment for 24 hours (Figure 20, about 3-fold compared to the vehicle control 6 ± 2.5 U/L; a 2.1-fold increase compared to kidney only group at 25 μM with 8.8 ± 2.0 U/L; $p < 0.01$). Rat ALT levels in liver→ kidney group at 10 μM AA-I were also increased slightly, compared to kidney only group at 10 μM AA-I. However, rat ALT levels in the hepatocytes only group did not increase as increased treatments of AA-I concentration.

A. **B.**

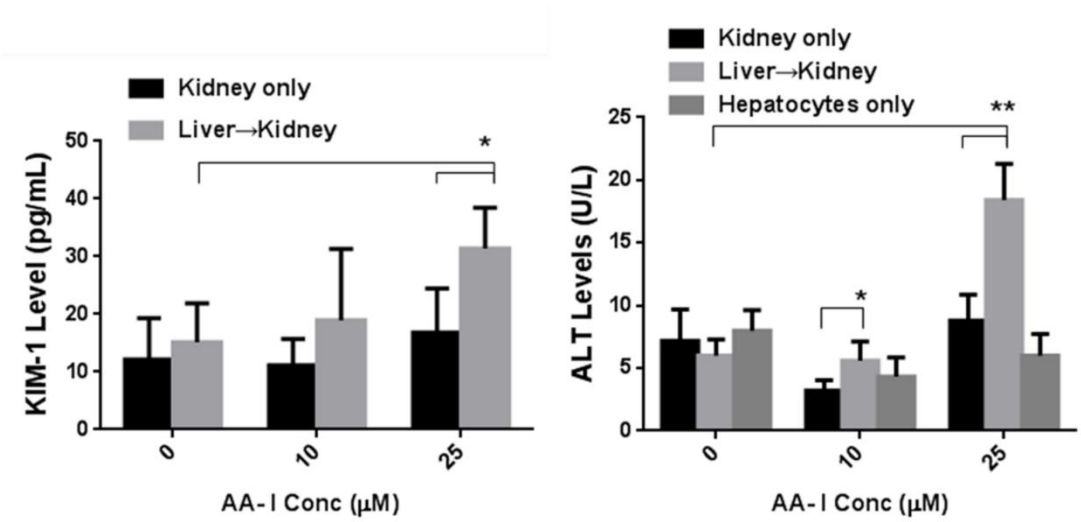

Fig. 20: Detection of organ-specific injury biomarkers in effluents of an AA-I treated MPS model. (A) Released levels of kidney injury biomarkers- KIM-1 and **(B)** ALT were detected from the effluents of rat MPS models (N=3-7). KIM-1 and ALT levels were presented as average ± SD. Statistic significant was calculated using t-test (*: $p<0.05$; **: $p< 0.01$).

Co-treatment of liver and kidney cells with the nitroreductase inhibitor, dicumarol, attenuates AA-I nephrotoxicity

In the pathway of AA-I biotransformation to toxic metabolite(s) (Figure 21), the first step is bioactivation of AA-I, which requires nitroreduction. Although several nitroreductases may have this potential, NQO1 is often considered to be the most important nitroreductase involved in AA-I activation [125].

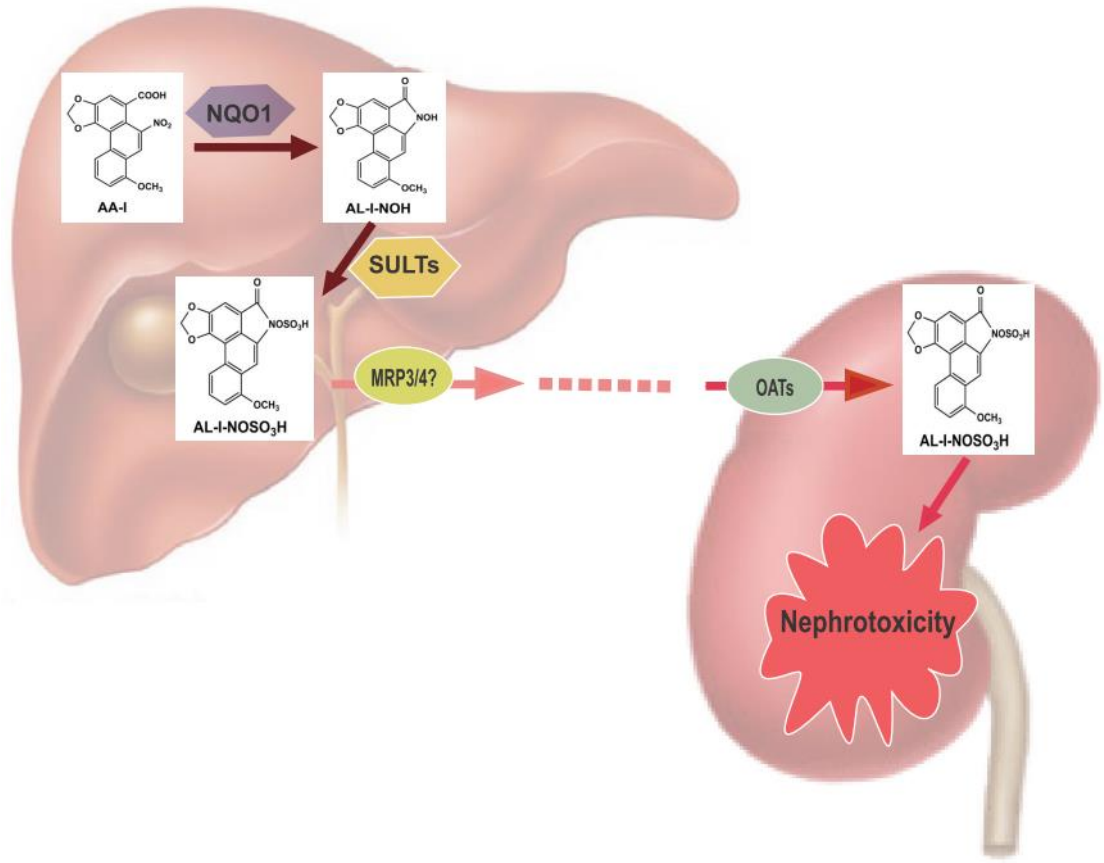

Fig. 21: AA-I metabolic pathway under the interaction of liver and kidney. Activated metabolite of AA-I: Sulfate conjugated AL-I metabolite (AL-I-$NOSO_3$) is formed by hepatic enzymes, including NQO1 and SULTs. AL-I-$NOSO_3$ is taken up by kidney via apical transporters- OATs, including OAT4, causing DNA adduct- induced nephrotoxicity.

To test this hypothesis, we co-treated cells in the MPS system with both AA-I and the nitroreductase inhibitor, dicumarol [126, 127], for 24 hours to investigate whether dicumarol can prevent AA-I toxicity. Although dicumarol is not a specific inhibitor of NQO1 [128], 10 μM dicumarol treatment for 24 hours reduced by 70% the NQO1 activity in 2D cultures of liver and reduced the formation of toxic AA metabolites- AL I and AL Ia in human hepatocytes, based on our data in 2D cell culture (data not shown). The result of LIVE/DEAD® stain of PTECs demonstrated that 10 μM dicumarol attenuated 25μM AA-I-induce cytotoxicity in liver→ kidney groups of rat

cells by 42.8% (Figure 22, 10 μM dicumarol did not cause significant toxicity in PTECs, data not shown).

A. **B.**

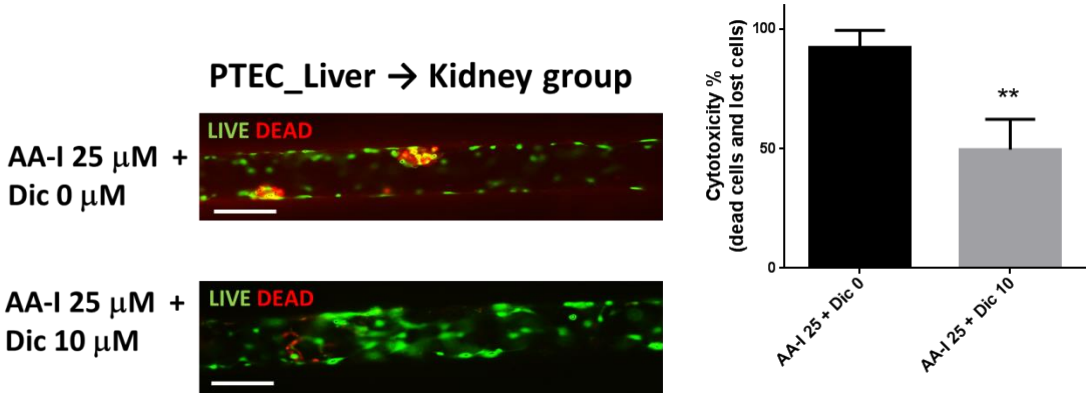

Fig. 22: Dicumarol (NQO1 inhibitor) mediated reduction of AA-I toxicity in an integrated rat MPS model. LIVE/DEAD® staining showed rat PTECs cultured in MPS after dicumarol (Dic, 10 μM) and AA-I (25 μM) co-treatment for 24 hours (N= 5). **(B)** Quantitative results were presented as average ± SD. Statistic significant were calculated using t-test (**: $p < 0.01$). Bar = 150 μm

Discussion

This proof of principle study utilizing AA- I treatment in the rat liver→kidney MPS model supports the utility of this new approach for studying chemical toxicity in multiple organs, and organ-organ interactions *in vitro/ex vivo*. In addition, due to the scarcity and high cost of available primary human cells, the successful development of this rat *in vitro* duel organ model is the fundamental step for us to establish an integrated human liver→kidney MPS model. We found that passing AA-I through hepatocytes prior to kidney PTECs caused substantially greater toxicity in PTECs compared to direct AA-I exposure, demonstrating that hepatic metabolism contributes significantly to overall bioactivation of AA-I. Bioactivation of AA-I requires NQO1 or potentially other nitroreductases in this rat model.

The metabolic pathway of AA-I toxicity is associated with the activity of CYPs, NQO1 and other 'phase II' conjugating enzymes [114]. *In vitro*, *ex vivo*, and *in vivo* studies [116, 129, 130] demonstrate that NQO1 is the most efficient enzyme for activation of AA to cytotoxic and potentially carcinogenic metabolites. The metabolic pathway modulating AA toxicity and its carcinogenic effects is a dynamic and complex balance between bioactivation and detoxification of AA, and is influenced by oxygen concentration [114]. It has been hypothesized that when AA-I is not detoxified via oxidative O-demethylation to AA-Ia in the liver, it is instead activated to a toxic metabolite by one or more enzymes with nitroreductase activity. The results from *Cyp1a* knockout mice [131] and CYP1A-humanized mice [108] show that CYP1A activates AA I under anaerobic conditions, while CYP1A detoxifies AA I via *O*-demethylation into AA Ia under oxidative conditions.

NQO1 is critical in transferring two electrons into AA-I and has been postulated to be the primary cytosolic nitroreductase involved in AA-I activation [125]. *In vivo*, administration of dicumarol attenuated AA-I nephrotoxicity and decreased renal AL-1 levels [116]. A study of Stiborova et al. showed that dicumarol acts as an NQO1 inhibit *in vitro* and as an NQO1 inducer if administered to rats [115]. Although dicumarol is generally used as a pharmacological inhibitor to study the functions of NQO1 in cells and bioactivation of drugs, dicumarol has several "off-target" effects such as extensive protein binding, mitochondrial uncoupling and increased production of intracellular superoxide, confounding the results of using dicumarol in pharmacological studies [128]. Most *in vivo* studies have demonstrated a role for NQO1 in AA-I activation using dicumarol. For example, Chen *et al.* demonstrated that inhibition NQO1 Activity *in vivo* by dicumarol can suppress nitroreduction of AA-I and can attenuates AA-I nephrotoxicity in male C57BL/6 mice [116]. However, Stiborova *et al.* found that dicoumarol treatment prior to AA-I administration

increased reductive activation of AA-I, followed by the enhanced genotoxicity in Wistar rats. Stiborova *et al.* also found that dicumarol induced NQO1 mRNA/protein expression in rats. The discrepancy that is observed from the effect of dicumarol probably needs a further *in vivo* research such as using NQO-1 knockout animal models [114]. Recently, an *in vitro* study found that AL-I DNA adducts levels in AA-I exposed human cell line with genetic knockdown of NQO1 remain unchanged, compared to cells expressed normal NQO1 levels [132]. However, it is possible that a compensatory up-regulation of other nitroreductases, such as POR and XDH, could be involved in the activation of AA-I in the absence of NQO1. Our results suggested that NQO1 and/or other NR reaction is critical for AA-I bioactivation. Dicumarol is an effective inhibitor of NQO1, it also is an inhibitor of XDH [133].

Using MPS meets the principle of 3Rs in animal testing. First, using MPS can reduce animal usage. For example, we can generate at least 200 liver MPS by sacrificing one rat used in hepatocytes isolation. Second, MPS is a refined system to better capture human responses to xenobiotics. The ultimate goal of using MPS is to replace the animal usage.

In conclusion, net hepatic bioactivation of AA resulted in enhance toxicity to the kidney in liver→kidney rat MPS model, which is potentially mediated via hepatic NQO1-dependent AL-I formation. Based on this proof-of-concept study, our rat liver→kidney MPS model provides a new and validated approach to identify mechanistically-based organ-organ interactions important in toxicity.

Chapter 3

Microphysiological Systems (MPS) to Identify Organ-Organ Interactions in Toxicology: Hepatic Metabolism Enhances Nephrotoxicity of Aristolochic Acid-I in Human Dual Organ Models

Abstract

The specific activation and detoxification pathways for the natural phytochemical, aristolochic acid-I (AA-I), a well-known nephrotoxin and carcinogen in humans, in liver and/or kidney are not fully understood. We hypothesized that passing AA-I through a liver-on-a-chip prior to introducing the outflow into a kidney-on-a-chip would alter its nephrotoxicity. Our results of this proof of concept study demonstrated that hepatic parenchymal cell metabolism of AA-I prior to kidney exposure substantially increased cytotoxicity to human proximal tubular epithelial cells (PTEC), formation of aristolactam-I (AL-I) DNA adducts in PTEC, and release of kidney injury biomarker- KIM-1. These results demonstrated that hepatic metabolism contributes more to bioactivation of AA-I than to detoxification. Additional mechanistic studies provided insights into the important role of hepatic biotransformation for the kidney-specific toxicity of AA-I, potentially involving activation to the AA-lactam intermediate via NAD(P)H dehydrogenase, quinone 1 (also known as NADPH:quinone oxidoreductases, NQO1), sulfate conjugation via hepatic sulfotransferases (SULTs), and hepatic export and renal uptake via organic anion transporters (OATs), especially OAT4. This *in vitro*/*ex vivo* integrated organs-on-chip culture systems can be used to identify toxicologically relevant organ-organ interactions that may occur *in vivo*, providing a novel approach for investigating the mechanisms that underlie toxicologically important organ-organ interactions in human tissues.

Introduction

While great strides have been made in developing individual organ-based MPS models, the integration of two or multiple organ systems to model complex metabolic process is the current focus of several groups. The HμREL® microdevice platform is one example of integrated MPS models, that assembles multiple microscale cell cultures units (μCCA) of hepatic tissue with other organ tissues in parallel. Used in combination with a mathematical modeling approach (PK–PD modeling), this novel platform provides improved predictability for drug biotransformation, clearance, and toxicity [134, 135]. The efficacy or toxicity of naphthalene, doxorubicin, nanoparticles, have been tested in this devices [83, 136-138]. Another example- Integrated Discrete Multiple Organ Co-culture (IdMOCTM) by *In Vitro* ADMET Laboratories (Columbia, MD) uses the "wells-in-a-well" concept, interacting multiple cell types via the overlying medium. This model can mimic multiple organs in a human body interacting via the systemic circulation [139].

Our group also has developed an integrated liver-kidney MPS system for identifying potentially nephrotoxic liver-metabolized chemicals, by connecting a liver-on-a-chip containing primary hepatocytes, to a kidney-on-a-chip device containing proximal tubule epithelial cells (PTECs) in MPS devices developed by Nortis, Inc (Woodinville, WA) [50]. After we successfully developed the integrated dual organ MPS model using primary rat cells (described in Chapter 2), we initiated the development of an integrated human dual organs model for testing AA-I toxicity to investigate whether the bioactivation of AA-I can be observed in human cells, and to study the underlying mechanisms of AA-I bioactivation between liver and kidney.

Consumption of*Aristolochia* species-derived herbal compounds that contain relatively high levels of AA can cause aristolochic acid nephropathy (AAN; also

referred to as Chinese Herb Nephropathy (CHN)). The consequence of AAN is a rapidly progressive renal fibrosis. AAN was initially observed in a group of Belgian woman who had ingested AA as a part of a weight loss regimen. These individuals are at high risk (~50%) for developing upper urinary tract urothelial carcinomas (UTUC) [93]. AAN cases have also been found in other locations of Europe and Asia [140]. Balkan endemic nephropathy (BEN) is also associated with a high risk of urothelial cancer, seen in certain rural areas of Serbia, Bosnia, Croatia, Bulgaria and Romania, and has also been linked to dietary exposure to AA [93, 141]. Based on the strong evidence of causality in epidemiological investigations, the International Agency for Research on Cancer (IARC) has classified herbal remedies containing AA as Group 1, "carcinogenic to humans" [94]. Aristolactam-I (AL-I) DNA adducts, including 7-(deoxyadenosin-N6-yl) aristolactam I (dA-AL-I), 7-(deoxyguanosin-N2-yl) aristolactam I (dG-AL-I), have been detected in urothelial tissues of AAN and BEN patients [93, 142, 143]. The formation of AL-I DNA adducts can lead to A to T transversion mutations [144]. High levels of dA-AL-I adducts in renal cortex tissues and A:T to T:A transversions in TP53 genes in tumor cells both are biomarkers of AA exposure founded in Balkan endemic nephropathy [93, 145] and UTUC cases reported in Taiwan [146].

AA-I undergoes extensive hepatic metabolism by several enzymes, including cytochrome P450 enzymes (CYPs: CYP1A1 and 1A2; CYP1A2 is a liver specific form) and NAD(P)H dehydrogenase, quinone 1 (also known as NADPH:quinone oxidoreductases, NQO1)[106-110]. Previous studies in our laboratory demonstrated that human liver microsomes with an induction of CYP1A1/2 can detoxify AA-I to non-toxic metabolite- 8-hydroxy aristolochic acid, AA-Ia [111]. AA-Ia is a substrate for nitroreduction (NR) and subsequent glucuronide and sulfate conjugation, forming soluble, excreteable metabolites [147-149]. NR of AA-I produces an active metabolite

of AA-I, hydroxylamine [N-hydroxyaristolactam I (AL-I-NOH)] that is the immediate precursor of the electrophilic cyclic nitrenium ion that can form AL-I DNA adducts [140, 150, 151]. AL-I-NOH is formed via reduction of the nitro moieties of the phenanthrane ring by one or more enzymes with nitroreductase activity, including potentially NQO1, xanthine dehydrogenase (XDH), NADPH:CYP reductase (POR), and, at low oxygen tension, CYP1A1/2 [112, 113].

However, the exact mechanisms of how and which hepatic enzymes activate or detoxify AA-I remain unclear because the results from *in vitro* and *in vivo* studies have been inconsistent [114]. Recently, the potential involvement of sulfotransferases (SULTs) in AA-I bioactivation was demonstrated (*98). In vitro* N-hydroxyaristolactams are sulfonated with high efficiency by murine and human SULTs [110]. The sulfate conjugates are unstable and reactive, and readily form AL-I DNA adducts [110]. In humans, SULT1A1, appears to play a critical role of AA-I bioactivation in formation of sulfonyloxyaristolactam (AL-I-$NOSO_3$, a highly unstable and reactive metabolite with a half-life of 15-20 min in water and buffer) and AL-I DNA adducts. These *in vitro* results are supported by evidence with human cell lines treated with a SULT inhibitor, and by SULT1A1 gene knockdown experiments [132].

Organic anion transporters (OATs), a group of membrane transporters carrying negative charged drugs and other organic compounds, mediate high-affinity transport of AA-I and AA-I metabolites in kidney, and are likely to be involved in the site-selective toxicity and renal elimination of AA-I [152, 153]. In humans, the OAT family of membrane transporter proteins has eight members that have been identified, and six are expressed in kidney, including OAT1, OAT2, OAT3, OAT4, urate transporter 1 (URAT1), and OAT10 (reviewed in [154]). The most abundant forms of OATs in kidney are OAT1, -2, -3, -4 and URAT1. The genes of OAT1, -3, -4 and URAT1 are found to occur in pairs in the genome, suggesting they are also closely

linked genetically. In kidney, OAT1, 2 and 3 are located in the basolateral membrane of proximal tubule whereas OAT4 is typically expressed in the apical membrane. OAT4 also has been confirmed to favor the formation of sulfate conjugates [155] and thus has the most potential for transporting sulfate conjugated AA-I metabolite into kidney.

The integrated human MPS model (Liver→kidney) described herein represents a novel *in vitro* approach for investigating liver-kidney interactions in renal toxicity of AA-I, and provides a mechanistic approach to understand the role of hepatic bioactivation and/or detoxification in AA-I nephrotoxicity. Based on our results using this novel integrated MPS model of dual human organs, we conclude that overall biotransformation of AA-I by hepatic enzymes increases, rather than decreases, the toxicity of AA-I in kidney, as indicated by an increase in cytotoxicity, increased formations of AL-I DNA adducts, and increase in the release of the organ-specific injury biomarker- Kidney Injury Molecule-1 (KIM-1) in liver → kidney effluents. The results from human cells were similar to these from rat cells (Chapter 2), suggesting that rat cells are a reasonable model for predicting human response to AA-I exposure. In addition, we provide further evidences to suggest that hepatic NQO1 and SULTs are the major enzymes for bioactivation of AA-I, based on the results from dicumarol and AA-I co-treatment. Dicumarol attenuated AA-I induced toxicity. Furthermore, direct exposure of PTECs to the active form of AA-I, AL-I-$NOSO_3$, in our MPS model caused severe cytotoxicity in PTECs without pre-hepatic metabolism (kidney only group). The OAT inhibitor, probenecid, inhibited the toxicity of the active AA-I metabolite in human kidney MPS, supporting the hypothesis that formation and subsequent active transport of the sulfate conjugate into PTECs is necessary for AA-I nephrotoxicity, especially via OAT4. This study demonstrates that an integrated MPS model can be used effectively to investigate the organ interactions between liver and kidney *in vitro/ex vivo.* This approach may be of substantial value to pre-clinical

toxicity screening for chemicals, and for identifying mechanisms for potentially important organ-organ interactions.

Materials and Methods

Isolation of PTECs and PTEC culture in MPS chips

Cell culture supplies and materials were from Thermo Fisher Scientific (Waltham, MA). Following institutional IRB approval, human PTECs were isolated from surgically-dissected kidney tissues from human donors (Demographic information of PTEC donors Him 20, Him 23, Him 25, Bio 13, and Bio 26 is listed in Table 2). Isolated PTECs were grown in a 2D flask with PTEC culture media, including MEM/F12 medium supplemented with 2.5 mM glutamine, 100x-diluted ITSA, 50 nM hydrocortisone and 100x –diluted antibiotic-antimyotic. After expanding cells in 2D monolayer culture, PTECs were re-suspended using 0.01% trypsin, and then injected into Nortis® MPS chips filled with collagen type I. After cell injection and stabilization overnight at 37℃, 5% CO_2 incubator, the MPS chips were connected with C-Flex tubing ® and PTEC culture media-loaded syringe at a flow rate of 0.5 μL/min controlled by infusion/syringe pumps (KD Scentific Inc. model# KDS220). PTECs in MPS chips can be maintained for more than two weeks prior to the further treatment [89].

Source of hepatocytes and hepatocytes culture in MPS chips

Freshly-isolated human hepatocytes or cryopreserved human hepatocytes were purchased from Triangle Research Labs (TRL; HUM4096A and HUM4097B) or were received from The Liver Tissue Cell Distribution System (LTCDS; NIH service; donor 15-002) following IRB protocol review and approval (demographic information of hepatocytes donors is listed in Table 2). All MPS chips were pre-coated with 0.1

mg /mL of collagen type I in PBS with 0.1% acetic acid at 37℃, 5% CO_2 incubator for 1 hour.

Human Cryopreserved Hepatocytes from TRL:

Sample Number	Age	Sex	Race	BMI	Tobacco Use	Alcohol Use	HIV, HBV, HCV Serology	Cause of Death
HUM4096A	34	Female	Caucasian	25	No	Yes	Negative	Anoxia
HUM4097A	53	Female	Caucasian	35	No	Yes	Negative	Anoxia

Human Fresh-isolated Hepatocytes from LTCDS:

Sample Number	Age	Sex	Race	Cause of Surgery
15-002	Femal	37	Caucasian	colon cancer mets to the liver. She has a history of chemo

Human PTEC:

PTEC ID#	Sex	Age	Race	Cause of Surgery
Him-20	Male	62	Caucasian	Transitional cell carcinoma - no kidney tumor. Other active medical problems: HTN, DM, hyperlipidemia, but normal renal function
Him-23	Male	62	Hispanic	
Him-25	Male	49	Caucasian	Presented with renal mass—path shows clear cell renal CA. No other active medical problems
Bio 13	Male	57	Caucasian	
Bio 26	Male	38	Caucasian	

TABLE 2: Demographics information for human hepatocytes and PTEC donors

For plating hepatocytes into MPS culture, 0.1 to 0.2 mL of a cell suspension at a density of 2 x 10^6 hepatocytes/mL were injected into each chip via the abluminal ports. Hepatocyte plating medium was William's E media supplemented with 5% fetal bovine serum (FBS), 100 mg/ml penicillin streptomycin, 100 nM dexamethasone, 1 μg/mL of Gibco® Fungizone® 100x diluted ITS+, and 0.2 mM glutaMAX. After 4 hours of plating, the hepatocytes were overlaid with Matrigel® (Corning®, 0.23 mg/ml) in maintenance medium (the same formula for plating medium but without FBS) via abluminal ports. Following maintenance of cells at 37℃, 5% CO_2 incubator overnight, cells in MPS chips were held at 37℃with 5% CO_2 in a sterile incubator, and were maintained in maintenance medium with abluminal flow at flow rates between 5 to 10

μL/hr via infusion/syringe pumps (KD Scientific Inc. model# KDS220). Hepatocytes in MPS chips were maintained with high viability up to 5-7 days prior to the further treatment.

AA-I treatment in cells cultured in MPS

AA-I and dicumarol were purchased from Sigma Aldrich Co. LLC (catalog #A5512 and catalog # M1390). AL-I-$NOSO_3$ was synthesized from Dr. Viktoriya Sidorenko's lab (Stony Brook University, NY [110]). Probenecid (water soluble) was purchased from ThermoFisher Scientific (catalog# P36400).

PTECs cultured in MPS were checked for cell confluency and tubule morphology before AA-I treatment. Only kidney MPS with 95 -100% confluence were used for further treatments. Two groups of cells cultured in MPS were subjected to AA-I treatment: 1) kidney-only group that has only 3D PTECs cultured in MPS chips, and 2) liver→kidney group that has MPS chips with 3D cultured hepatocytes connected upstream of another MPS chip with PTECs. The connection of liver→kidney MPS model utilized C-Flex® tubing (Fig. 10 in Chapter 2 ; flow is from abluminal liver chip into luminal kidney chip). Cells cultured in the MPS were treated with AA-I, AL-I-$NOSO_3$, with/without dicumarol or probenecid in the treatment media (mixtures of PTEC culture media and hepatocytes maintenance media at volume ratio of 50: 50) for 24 hours at a flow rate of 1.5 μL/min. After AA-I treatment, LIVE/DEAD® staining was used to analyze AA-I-mediated cell death in hepatocytes and PTECs. Quantitative results of cytotoxicity, determined as the percentage of viable cells, were calculated from the ratio of dead cells (red fluorescent-stained cells from LIVE/DEAD® staining) and detached cells to the total cell number (Hoechst 33342 stained cells). Effluents were collected and stored in -80 ℃ for later analysis of organ –specific injury biomarkers.

LIVE/DEAD® staining

The LIVE/DEAD® viability/cytotoxicity kit and Hoechst 33342 (Life Technologies) were used to distinguish live cells from dead cells, and total cell number (Hoechst 33342) according to manufacturer's specifications. Briefly, calcein AM (final conc. 2 μM), EthD-1 (final conc. 4 μM) and Hoechst 33342 (final conc.0.1 μg/ml) were diluted in pre-warmed D-PBS. Adequate volume of diluted reagents was perfused through the MPS chips at 5 μL/min via a lumenal port of kidney MPS for 20 minutes and then was incubated for 10 minutes at 37 ^{0}C. After the staining procedure, chips were imaged using fluorescent microscopy (Nikon Eclipse Ti-S and inverted spinning disk microscope, 3i-Intelligent Imaging Innovations, Denver, CO) to calculate the numbers of dead cells (red stained cells) and Hoechst 33342-stained cells. All results were repeated for 3-4 independent experiments (N=4-7). The most representative images are shown in the Results.

Immunocytochemistry staining for AL-I DNA adducts in kidney MPS and NQO1 in liver MPS

Rabbit anti- AL-I DNA antibody were generated from Dr. Thomas Rosenquist's lab (Stony Brook University, NY). Before the staining, 4% formaldehyde fixed kidney MPS were bleached with 0.3% H_2O_2 for 5 minutes and were under the antigen retrieval procedure (boiled 10mM Tris-HCl pH 9, 1mM EDTA buffer) for 10 minutes at a flow rate of 10 μL/min. Regular ICC staining procedure, including blocking, primary antibody incubation, washing, and secondary antibody incubation, were performed using reagents-loaded syringes, controlled at flow rates between 5 to 10 μL/min via infusion/syringe pumps (KD Scientific Inc. model# KDS220). Tyramide SuperBoost™ kits (goat anti rabbit IgG^2 and Alexa Fluor™ 647 labeled tyramide were included, ThermoFisher Scientific) were used to enhance the signal of AL-I

DNA adducts, following by the manufacturer's protocol. Diluted ProLong Gold Antifade Mountant with DAPI reagents (catalog# P-36931, ThermoFisher Scientific) were used in the final step of mounting. Kidney MPS chips stained with secondary antibody only (without incubated with the primary antibody)were used to check for nonspecific binding. All results of ICC staining were repeated (N=3). Representative images were shown in the Results.

Immunocytochemistry staining for NQO-1 in liver MPS

Anti-NQO1 antibody (rabbit polyclonal, ab34173, Abcam) was used. Cells were fixed with 4% formaldehyde in PBS. After antigen retrieval with warm citrate buffer (10 mM citric acid, 0.05% Tween 20, pH 6.0) for 20 minutes, samples were permeabilized with PBST (PBS plus 0.1% Tween 20) for 1 hour, and blocked with 1% bovine serum albumin (BSA) and 10% serum in PBSG (10 mg/mL glycine, 0.1% Tween 20) for an additional 1 hour. The samples were then incubated with primary and secondary antibodies followed by washing, using a standard ICC protocol. Secondary antibodies were goat anti-rabbit IgG (H+L) Secondary Antibody, Alexa Fluor® 488 conjugate (Thermo Fisher Scientific, Waltham, MA). Diluted ProLong Gold Antifade Mountant with DAPI reagents (catalog# P-36931, ThermoFisher Scientific) were used in the final step of staining. Cells were imaged using fluorescent microscopy with the Nikon Eclipse Ti-S microscope for detecting the intensity of green and blue fluorescence.

OAT4 uptake of AL-I-NOSO$_3$ assay

Cell Culture: Stably transfected COS-7/OAT4 cells and parental non-transfected COS-7 cells were generously provided by Dr. Guofeng You of the Department of Pharmaceutics at Rutgers University, New Jersey. The cells were cultured at 37℃ and 5% CO_2 in Dulbecco's modified Eagle's medium (Gibco, Carlsbad, US) supplemented with 10% fetal bovine serum (VWR, Radnor, US) and

Antibiotic-Antimycotic (Gibco). In the case of COS-7/OAT4 cells, the cells were maintained in the presence of additional G418 at a concentration of 200 μg/ml.

Uptake Assay: For uptake measurements, COS-7/OAT4 cells and mock control COS-7 cells were seeded on BioCoat collagen I-coated 24-well plates at a density of 5×10^4 cells/well and cultured for 2 days. Cells were then washed once with 1 ml of Hanks' balanced salt solution (HBSS, from Gibco) and pre-incubated at 37℃ with 0.5 ml HBSS in the presence or absence of probenecid at a final concentration of 2 mM for 10 min. Uptake was initiated by adding 0.5 ml HBSS containing AL-I-$NOSO_3$ (0.5 μM) or the OAT4 model substrate estrone-3-sulfate (1 μM) in the presence or absence of probenecid at a final concentration of 2 mM, and incubation was continued for 6 min at 37℃. The uptake reaction was stopped by rapidly washing the cells with ice-cold HBSS. Cells were then lysed for 5 min with 0.5 ml acetonitrile containing 32 ng/ml estradiol-3-sulfate (internal standard). Cell extracts were centrifuged at 14,000 rpm for 5 min and the supernatant was evaporated to dryness immediately and kept on dry ice. The residuals were reconstituted in 100 μl methanol/water (1:1, vol/vol) immediately prior to LC-MS analysis. Estradiol-3-sulfate added in cell extracts was used as an internal standard. Cells used for BCA protein assay were solubilized with 0.2 ml 0.1 N NaOH. The amount of AL-I-$NOSO_3$ or estrone-3-sulfate in cell extracts normalized to protein content was presented as cellular uptake activity.

LC/MS Analysis: Chromatographic separation was achieved using a Waters Symmetry C_{18} (2.1 × 50 mm, 3.5 μm) column (Waters) on an Agilent 1200 LC system. The elution was performed at a flow rate of 0.3 ml/min with the mobile phase containing methanol, acetonitrile and 10 mM ammonium acetate (native pH) at a ratio of 30:14:56 (vol/vol/vol). Mass spectrum analysis was carried out using a negative mode electrospray ionization method on an Agilent 6410 triple quadrupole tandem mass spectrometer. The ionization and fragmentation parameters were set as follows:

capillary voltage, 3000 V; gas temperature, 350℃; gas flow rate, 11 L/min; nebulizer: 35 psi; fragmentor: 135 V. Single ion monitoring (SIM) at m/z 388 was applied for detection of AL-I-$NOSO_3$. Since deuterated AL-I-$NOSO_3$ was not available, estradiol-3-sulfate was used as an internal standard for quantification of AL-I-$NOSO_3$.

Analysis of organ-specific injury biomarker- KIM-1

Meso Scale Discovery immunoassay kits (Meso Scale Diagnostic, Inc.) were used to measure KIM-1 (rat and human) in effluents following the manufacturer's suggested protocol.

Statistical Analysis

GraphPad Prism 6 was used to plot and analyze results. All results of MPS culture were from three to four independent experiments of AA treatment (Table 3). The two-tailed t-test for independent samples was used to compare two groups.

Experiments	Cell Types	N=1	N=2	N=3	N=4	N=5	N=6
LIVE/DEAD® stain of AA-I treatment	Hepatocytes:	15-002	HUM 4096A	HUM 4096A	HUM 4097B		
	PTEC:	Him 20	Him 25	Him 25	Bio 13		
ICC of AL-I DNA Addcuts in AA-I treated	Hepatocytes:	HUM 4097B	HUM 4097B	HUM 4096A			
	PTEC:	Bio 13	Bio 26	Him 23			
KIM-I	Hepatocytes:	15-002	HUM 4096A	HUM 4096A	HUM 4096A	HUM 4096A	HUM 4096A
	PTEC:	Him 20	Him 25	Him 20	Him 25	Him 25	Him 25
LIVE/DEAD® stain of AA-I + Dic treatment	Hepatocytes:	HUM 4097B	HUM 4097B	HUM 4096A	HUM 4097B	HUM 4097B	
	PTEC:	Bio 26	Bio 26	Him 23	Bio 13	Bio 13	
LIVE/DEAD® stain of AL-I-NOSO3 treatment	Hepatocytes:	HUM 4097B	HUM 4097B	HUM 4096A	HUM 4097B	HUM 4097B	
	PTEC:	Bio 26	Bio 26	Him 23	Bio 13	Bio 13	
ICC of AL-I DNA Addcuts in AL-I-NOSO3 treated	Hepatocytes:	HUM 4097B	HUM 4097B	HUM 4097B			
	PTEC:	Bio 26	Bio 13	Bio 13			
LIVE/DEAD® stain of AL-I-NOSO3 + Pro treatment	Hepatocytes:	HUM 4097B	HUM 4097B	HUM 4096A	HUM 4097B	HUM 4097B	HUM 4097B
	PTEC:	Bio 26	Bio 26	Him 23	Bio 13	Bio 13	Bio 26

TABLE 3: List of human cells used in different experiments

Results

Hepatic metabolism bioactivates AA-I toxicity in human MPS models

AA-I treatment caused greater toxicity in PTECs with pre-hepatic metabolism than with direct exposure in human cells. More human PTECs were lost (e.g., cells detached due to death) and dead in the liver→ kidney group after AA-I treatment compared to the kidney-only group (Figure 23).

A.

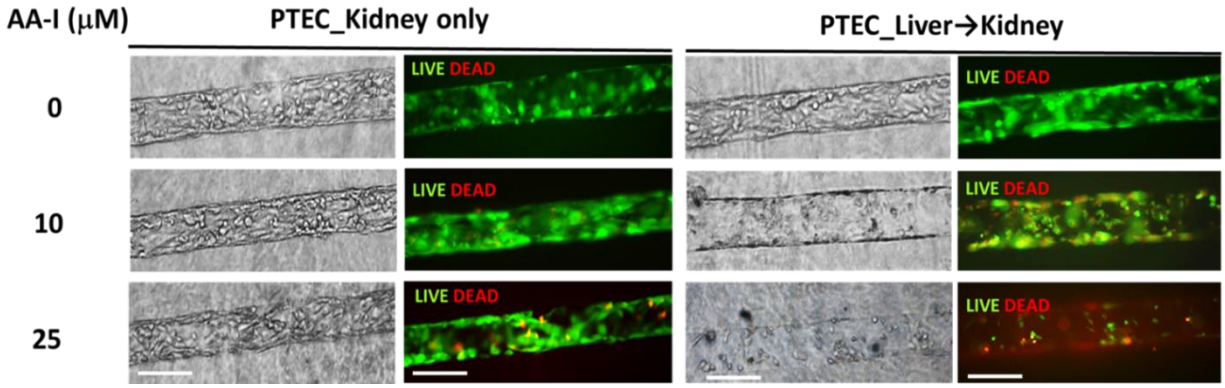

B.

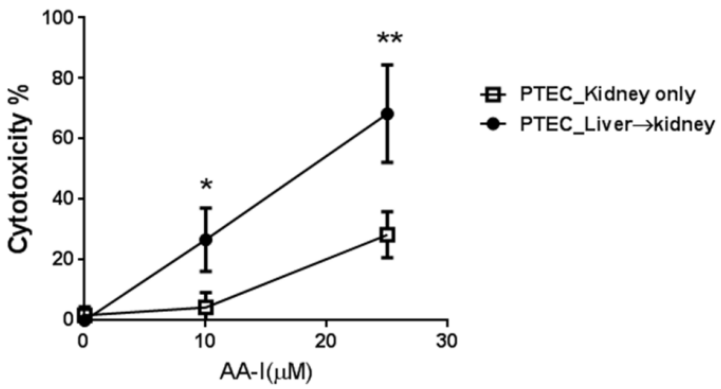

Fig. 23. AA-I cytotoxicity with or without hepatic metabolism in human kidney MPS. (A) Phase contrast pictures and LIVE/DEAD® staining showed human PTECs cultured in MPS after AA-I treatment for 24 hours. (B) Results expressed as cytotoxicity%. All experiments were independently repeated at least for three times (N=4-7). Human cells used in the representative images of LIVE/DEAD® staining were HUM 4096A (hepatocytes) and Him20 (PTECs). Statistical significance was calculated between Kidney only group and Liver→ kidney group using t-test (*: $p<0.05$; **: $p< 0.01$). Bar = 150 μm

Remaining PTECs inside the tubule of the liver→ kidney group also had a greater extent of cell death after 24 hours of AA-I treatment, especially at 25 μM AA-I (Figure 23, data of LIVE/DEAD® stain). AA-I treatment was significantly more toxic in PTECs with pre-hepatic metabolism (liver→ kidney group) compared to PTECs that were directly exposed to AA-I (kidney-only group) (Figure 23, $p < 0.05$ at 10 μM; $p < 0.01$ at 0.01 at 25 μM in liver→ kidney group compared to kidney-only group).

Hepatic activation of AA-I increases the amount of AL-DNA adducts in PTECs

The formation of AL-I DNA adducts is a useful biomarker to demonstrate AA-I genotoxicity. ICC staining of AL-I DNA adducts in human PTECs (Figure 24) demonstrated more AL-I DNA adducts in PTECs with pre-hepatic metabolism at 10 μM AA-I, compared to PTECs directly exposed to AA-I.

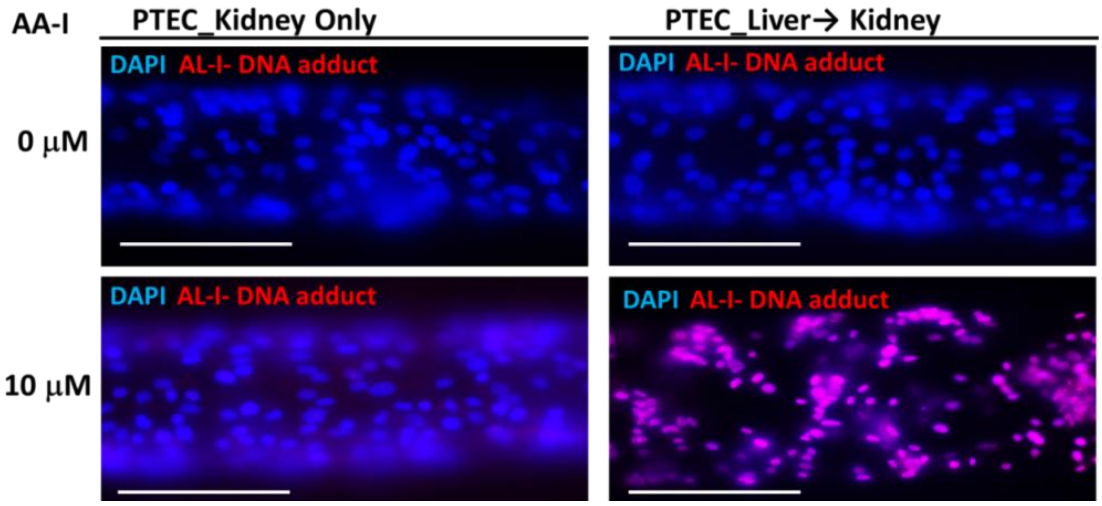

Fig. 24. AA-I-DNA adducts with or without hepatic metabolism in human kidney MPS. ICC results of AL-I DNA adducts in AA-I 0 and 10 μM treated PTECs in MPS without or with hepatic metabolism (N=3). Representative images of AL-I DNA adducts were from an experiment of HUM 4097B, and Bio 13.

Taken together, these results suggested that hepatic biotransformation of AA-I causes an approximately 5-fold net increase in toxicity to both rat and human PTECs, when compared to direct exposure to PTECs.

Hepatic metabolism of AA-I increases release of kidney-specific injury biomarkers into effluents from PTECs

In addition to cellular images and fluorescent probes, organ-specific injury biomarkers in effluents can be used to evaluate organ-specific toxic responses. Utilization of such biomarkers provides another advantage of using MPS culture to recapitulate *in vivo* fluid dynamics such as the transport of metabolites into urine. Human KIM-1 was also increased in effluents of liver→kidney MPS group after 25 μM AA-I treatment for 24 hours (Figure 25; 2.5- fold compared to the vehicle control with 56.4 ± 13.7 pg/mL; 3.2- fold compared to kidney only group at 25 μM with 43.3 ± 12.2 pg/mL; $p < 0.01$

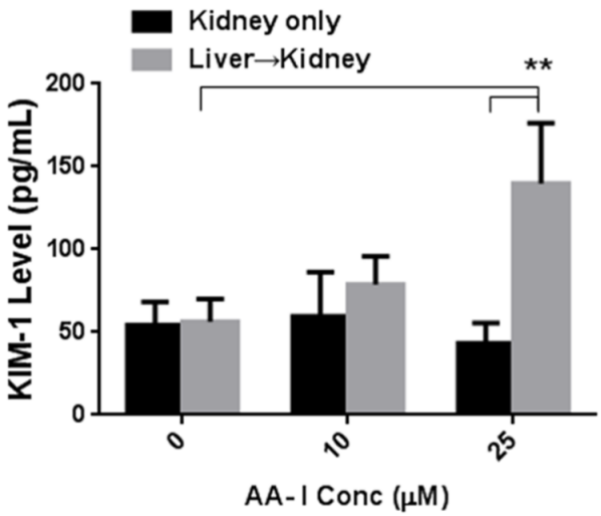

Fig. 25: Detection of organ-specific injury biomarker KIM-1 in effluents of AA-I treated MPS models. Level of KIM-1 was detected from effluents of human MPS models (N=5-6; PTECs were form the donor Him20, Him25, and hepatocytes were from HUM4096A). Levels were presented as average ± SD. Statistic significant was calculated using t-test (**: p< 0.01).

Co-treatment of liver and kidney cells with the nitroreductase inhibitor, dicumarol, attenuates AA-I nephrotoxicity

In the pathway of AA-I biotransformation to toxic metabolite(s) (Figure 21 in Chapter 2), the first step is bioactivation of AA-I, which requires nitroreduction. Although several nitroreductases may have this potential, NQO1 is often considered to be the

most important nitroreducatse involved in AA-I activation [125]. To test this hypothesis, we co-treated cells in the MPS system with both AA-I and the nitroreductase inhibitor, dicumarol, for 24 hours to investigate whether dicumarol can prevent AA-I toxicity. NQO1 levels are not highly expressed in normal hepatic tissues but can be induced by liver injury [156]. We found that AA-I exposure greatly induced NQO1 expression in human hepatocytes cultured in MPS (Figure 26). Although dicumarol is not a specific inhibitor of NQO1, 10 μM dicumarol treatment for 24 hours reduced by 70% the NQO1 activity in 2D cultures of liver and reduce the formation of toxic AA metabolites- AL-I and AL-Ia in human hepatocytes, based on our data in 2D cell culture (data not shown).

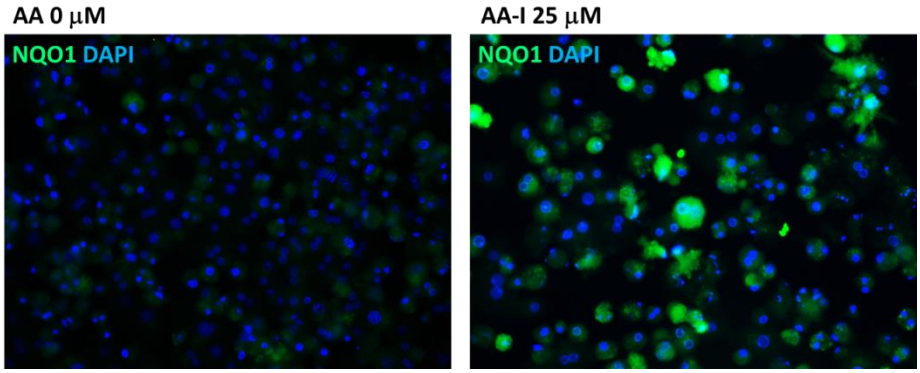

Fig. 26: AA-I induced NQO1 expression in human hepatocytes. ICC staining of NQO1 in human hepatocytes (HUM4096A) cultured in MPS with or without AA-I treatment for 24 hours.

The result of LIVE/DEAD® stain of PTECs demonstrated that dicumarol at 10 μM attenuated 25μM AA-I-induce cytotoxicity in liver→ kidney groups of human cells by 39% (Figure 27; 10 μM dicumarol did not cause significant toxicity in PTECs, data not shown). Dicumarol also tended to decrease AA-I toxicity in the kidney only group of human cells, but the result was not significantly different (p= 0.206).

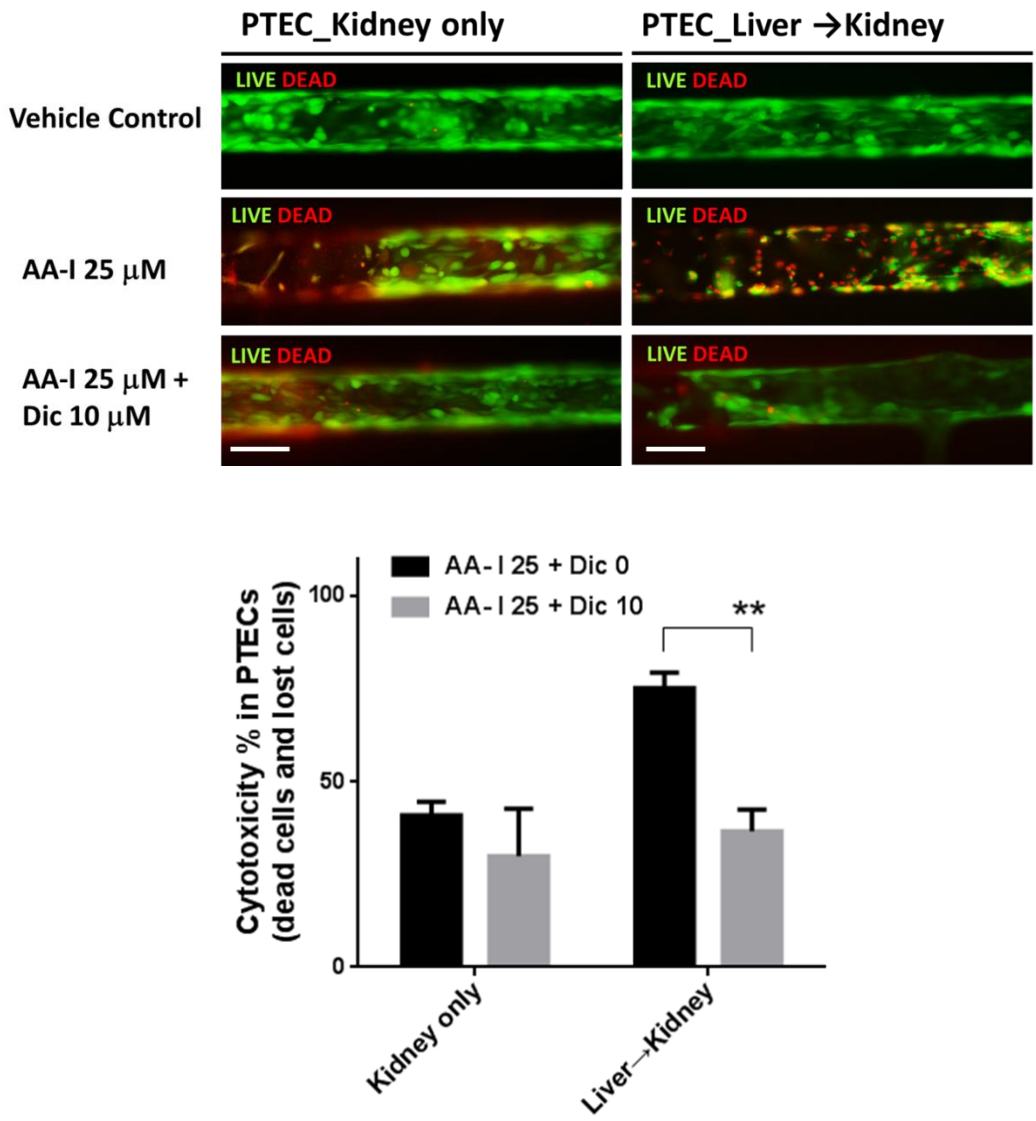

Fig. 27: Dicumarol (NQO1 inhibitor) –mediated reduction of AA-I toxicity in an integrated human MPS model. LIVE/DEAD® staining showed human PTECs cultured in MPS after dicumarol and AA-I co-treatment for 24 hours (N= 5).

Quantitative results were presented as average ± SD. Statistical significance was calculated using t-test (**: $p < 0.01$). Human cells used in the representative images of LIVE/DEAD® staining were HUM4097B and Bio 26. Bar = 150 μm

Sulfate conjugated AL-I metabolite (AL-I-$NOSO_3$) are directly toxic to human PTECs, and this is not modified by hepatic metabolism

To demonstrate that AL-I-$NOSO_3$ is the bioactivated form of AA-I metabolite, we treated human cells with synthetic AL-I-$NOSO_3$. The results from LIVE/DEAD® stain

(Figure 28) with primary human cells showed that AL-I-$NOSO_3$ treatment resulted in the similar levels of cytotoxicity in PTECs with and without pre-hepatic metabolism (55% ± 10% in liver →kidney group vs. 40.7% ± 7.6% in kidney only group at 10 μM of AL-I-$NOSO_3$; not significantly different; p = 0.239).

A.

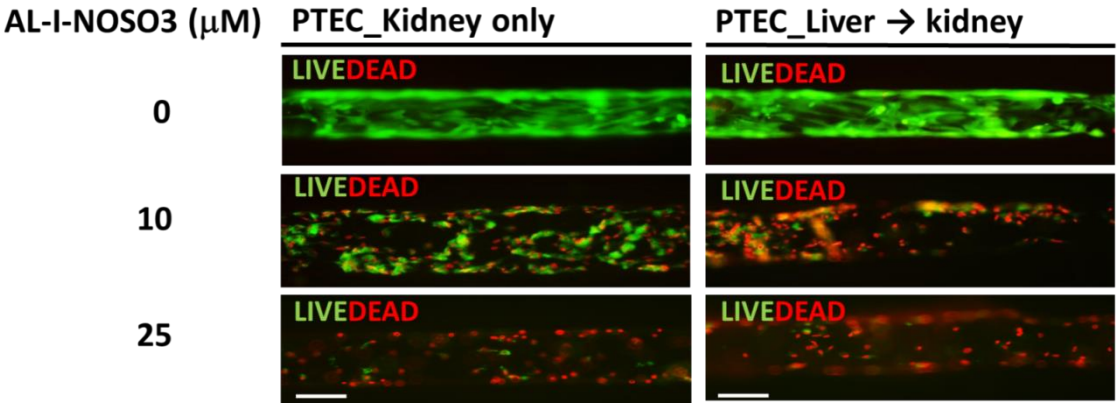

B.

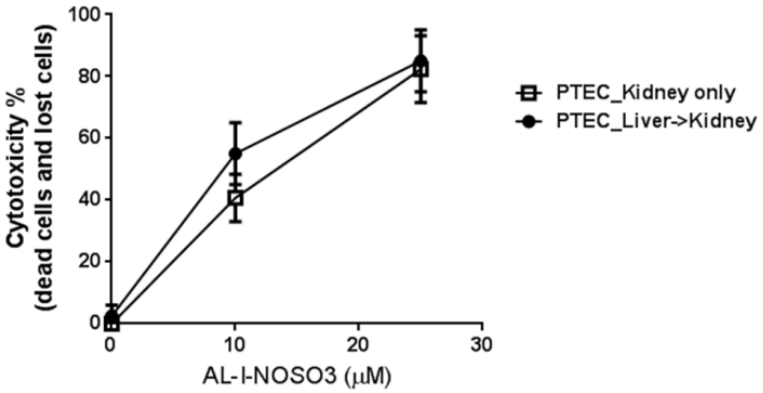

Fig. 28: Sulfate conjugated AL-I metabolite (AL-I-$NOSO_3$) toxicity in human MPS models. (A) LIVE/DEAD® staining showed human PTECs cultured in MPS after AL-I-$NOSO_3$ treatment for 24 hours, and cytotoxicity% (N= 5). Cells used in the representative images of LIVE/DEAD® staining were HUM4097B and Bio 26. Cells used in AL-1 DNA images were HUM4097B and Bio 13. Bar = 150 μm.

This bioactivated metabolite also caused the similar levels of AL-I DNA adducts in PTECs in the kidney only group at 10 μM AL-I-$NOSO_3$ (Figure 29), compared to liver→ kidney group. The results support the hypothesis that AL-I-$NOSO_3$ is the bioactived, nephrotoxic metabolite of AA-I.

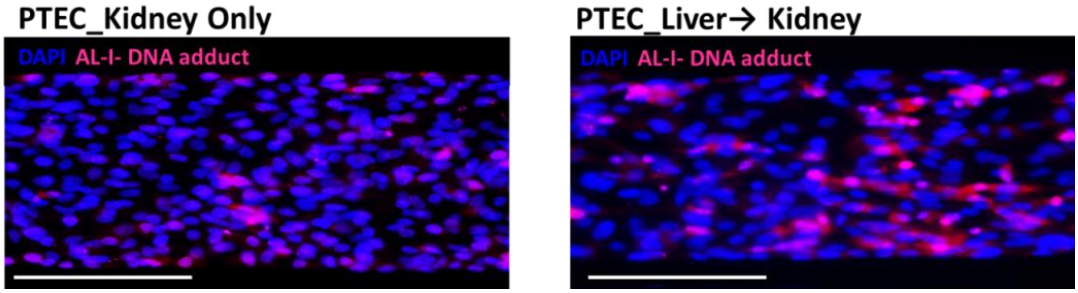

Fig. 29. AL-I-$NOSO_3$ –DNA adducts with or without hepatic metabolism in a human liver-Kidney MPS. ICC results of AL-I DNA adducts in AL-I-$NOSO_3$ 10 μM treated PTECs in MPS without or with hepatic metabolism (N=3). Cells used in AL-1 DNA images were HUM4097B and Bio 13. Bar = 150 μm.

The OAT inhibitor probenecid attenuates AL-I-$NOSO_3$ toxicity

Since AL-I-$NOSO_3$ is water soluble and not able to readily diffuse across cell membranes, we were interested in which renal membrane transporter is involved in the uptake of AL-I-$NOSO_3$ into PTECs. Previous studies have provided evidence that OATs are involved in the site-selective toxicity and renal elimination of AA-I [152, 153]. To investigate this hypothesis, we co-treated the liver→kidney or kidney only MPS containing human cells with AL-I-$NOSO_3$ and the OATs inhibitor- probenecid for 24 hours. The result of LIVE/DEAD® staining showed that probenecid at 2 mM attenuated 25 μM AA-I-induced cytotoxicity in human cells by 50-60% (Figure 30, 51.5% in kidney only group and 63% in liver→ kidney group; Probenecid 2 mM did not cause significant toxicity in PTECs, data not shown).

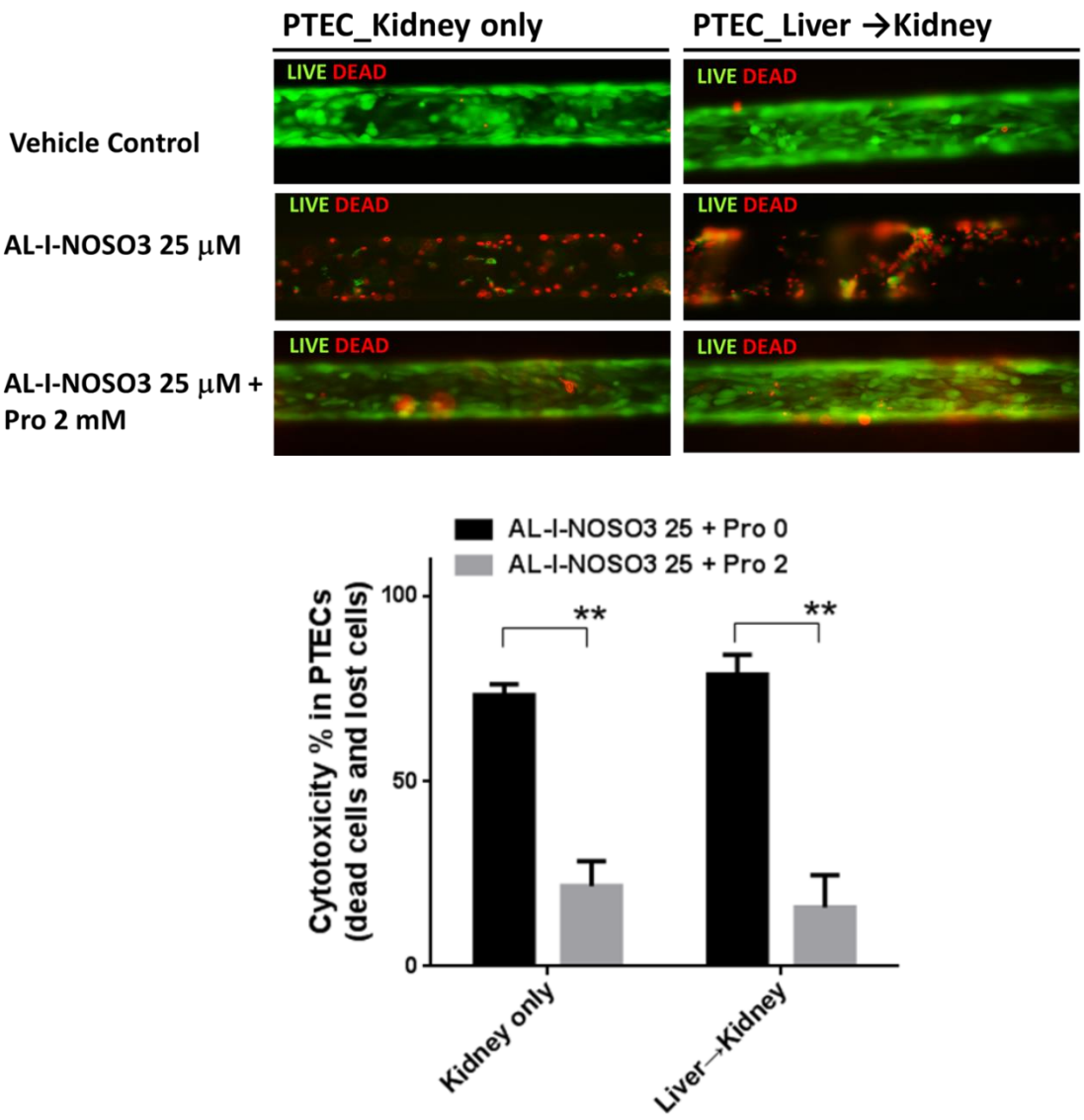

Fig. 30: Probenecid (OATs inhibitor)-mediated inhibition of AL-I-NOSO$_3$ toxicity in a human MPS model. LIVE/DEAD® staining showed human PTECs cultured in MPS after probenecid (Pro, 2 mM) and AL-I-NOSO$_3$ (25 μM) co-treatment for 24 hours (N= 5-7). Cells used in the representative images were HUM4097B and Bio 26. Bar = 150 μm. Quantitative results were presented as average ± SD. Statistic significant was calculated using t-test (**: p< 0.01).

After incubation of cells with AL-I-NSO$_3$ at 0.5 μM, cellular uptake of AL-I-NOSO$_3$ in OAT4 cells was 4-5-fold greater compared to that in non-transfected COS-7 cells. In the presence of probenecid, OAT4-mediated uptake of AL-I-NOSO$_3$ was completely abrogated. The results suggest that AL-I-NOSO$_3$ is a substrate of OAT4

and OAT4-mediated uptake of AL-I-$NOSO_3$ can be effectively inhibited by probenecid(Figure 31), suggesting PTEC can take up the sulfate conjugate of AA-I metabolite via OAT4.

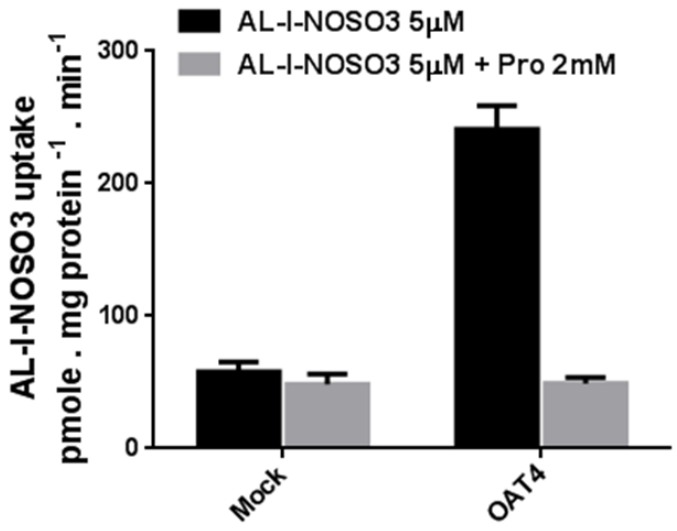

Fig.31: OAT4 uptake of AL-I-$NOSO_3$ in OAT4-overexpressed Cos7 cells. Uptake of AL-I-$NOSO_3$ in COS-7 cells. Cellular uptake of AL-I-$NOSO_3$ (0.5 μM) in COS-7/OAT4 and COS-7 cells was determined as described in Materials and Methods. The open bars represent intracellular AL-I-$NOSO_3$ levels in the absence of probenecid. The solid bars represent intracellular AL-I-$NOSO_3$ levels in the presence of 2 mM probenecid. Results shown are means ± SD from three independent experiments. The differences in intracellular AL-I-$NOSO_3$ levels between COS-7/OAT4 and COS-7 cells and between with and with probenecid are statistically significant: ** $p < 0.01$ by the t-test.

Discussion

This proof of principle study utilizing AA- I treatment in the liver→kidney MPS model supports the value of this new approach for studying chemical toxicity in multiple organs, and organ-organ interactions *in vitro/ex vivo*. Our results demonstrate that the toxicity of AA-I in rat cells is similar to human cells in our system, supporting in this example that rat cells are a reasonable model predicting in AA-I toxicity in humans (all the IC 50_S in Table 4; results of $IC50_S$ were extrapolated). We found that passing AA-I through hepatocytes prior to kidney PTECs caused substantially greater toxicity in PTECs compared to direct AA-I exposure, demonstrating that net hepatic metabolism contributes significantly to overall bioactivation of AA-I. Bioactivation of AA-I requires NQO1 or potentially other nitroreductases, and the products of this are then subject to sulfate conjugation via SULTs. We demonstrated that the active form of AA-I metabolite, AL-$INOSO_3$ is apparently formed in hepatic tissues and then transported out of liver and then taken up into kidney tissue via one or more OAT membrane transporter(s). OAT1, OAT2, and OAT3 are localized in the proximal tubule basolateral membrane (reviewed in [157]), whereas OAT4 is typically expressed in the apical membrane, and thus has the most potential in transporting sulfate conjugated AA-I metabolite into kidney. The lumen of PTECs tubule in MPS model is the location of direct exposure to AA-I and other compounds, that is simulated to the apical part of the proximal tubule. Moreover, OAT4 also has been confirmed to favor sulfate conjugates [155]. Xue X *et al*. study found that AA-I induced nephrotoxicity was suppressed in Oat1 and Oat3 knockout mice, compared to this in the wild-type mice, that supported that OATs have a critical role in AA-I renal accumulation and toxicity [158].

Cells	Group	Compound	IC50 (mM)	95% CI (mM)
Rat	PTEC (Kidney only)	AA-I	66.52	38.3 to 115.5
	PTEC (Liver →Kidney)		5.35 **	2.79 to 10.24
Human	PTEC (Kidney only)	AA-I	77.52	50.25 to 119.6
	PTEC (Liver →Kidney)		17.84 **	10.67 to 29.84
	PTEC (Kidney only)	AL-I-NOSO3	9.521	6.111 to 14.83
	PTEC (Liver →Kidney)		8.407	5.310 to 13.31

Table 4: IC_{50} of AA-I and AL-I-$NOSO_3$ for 24 hours exposure in PTECS without or with hepatic metabolism MPS models (** $p < 0.01$ compared to kidney only group)

Conjugation is generally considered to be the final step of biotransformation of xenobiotics in the process of converting absorbed nonpolar xenobiotics into water-soluble metabolites that can be excreted via kidneys or bile, and is traditionally associated with inactivation or detoxification. However, SULT-mediated genotoxic effects from polycyclic aromatic hydrocarbons and various aromatic hydroxylamines have demonstrated the cytotoxic and mutagenic effects of some sulfate conjugates. For example, sulfate conjugates of N-hydroxy arylamines, N-hydroxy heterocyclic amines, and hydroxymethyl polycyclic aromatic hydrocarbons are genotoxic and cytotoxic (reviewed in [159, 160]). Sulfate conjugation is electron-withdrawing and may be cleaved via heterolytic processes, leading to highly reactive electrophiles that are both mutagenic and carcinogenic. AL-I-NOH, considered to be the major precursor of reactive cyclic nitrenium species and of AL-I-DNA adducts, has been shown to require further activation by SULTs, in particular of SULT1A1, to efficiently react with DNA [110, 132]. SULTs are abundantly expressed in the liver but expressed with low levels in the kidney [161]. Our study supports the hypothesis that AL-I-$NOSO_3$, an unstable and highly reactive sulfate conjugate, is the most toxic metabolite of AA-I and is formed via hepatic SULTs, and is subsequently transported out of the liver and actively taken into kidney proximal tubular cells via OATs,

including OAT4, thereby explaining the kidney-specific toxicity and carcinogenicity of AA-I.

In conclusion, hepatic bioactivation of AA-I produced more toxicity and AL-I DNA adducts in kidney in liver→kidney MPS model, which is potentially through hepatic NQO1 and SULTs activities. We also demonstrated the toxicity of AL-I-$NOSO_3$ in PTECs, supporting that sulfation of AA-I N-OH metabolite leads to bioactivation rather to detoxification. The activated AA-I metabolite AL-I-$NOSO_3$ is actively transported into PTECs by OAT4 in kidney. Based on this proof- of - concept study, our integrated liver→kidney MPS model provides a novel and validated approach to identify mechanistically-based organ-organ interactions important in toxicity *in vitro*.

References

1. Nebert, D.W. and D.W. Russell, *Clinical importance of the cytochromes P450.* Lancet, 2002. **360**(9340): p. 1155-62.
2. Anzenbacher, P. and E. Anzenbacherova, *Cytochromes P450 and metabolism of xenobiotics.* Cell Mol Life Sci, 2001. **58**(5-6): p. 737-47.
3. Faber, K.N., M. Muller, and P.L. Jansen, *Drug transport proteins in the liver.* Adv Drug Deliv Rev, 2003. **55**(1): p. 107-24.
4. Kalliokoski, A. and M. Niemi, *Impact of OATP transporters on pharmacokinetics.* Br J Pharmacol, 2009. **158**(3): p. 693-705.
5. Kullak-Ublick, G.A., et al., *Organic anion-transporting polypeptide B (OATP-B) and its functional comparison with three other OATPs of human liver.* Gastroenterology, 2001. **120**(2): p. 525-33.
6. Niemi, M., M.K. Pasanen, and P.J. Neuvonen, *Organic anion transporting polypeptide 1B1: a genetically polymorphic transporter of major importance for hepatic drug uptake.* Pharmacol Rev, 2011. **63**(1): p. 157-81.
7. Klaassen, C.D. and L.M. Aleksunes, *Xenobiotic, bile acid, and cholesterol transporters: function and regulation.* Pharmacol Rev, 2010. **62**(1): p. 1-96.
8. Kanai, N., et al., *Identification and characterization of a prostaglandin transporter.* Science, 1995. **268**(5212): p. 866-9.
9. Visser, W.E., et al., *Study of the transport of thyroid hormone by transporters of the SLC10 family.* Mol Cell Endocrinol, 2010. **315**(1-2): p. 138-45.
10. Ho, R.H., et al., *Drug and bile acid transporters in rosuvastatin hepatic uptake: function, expression, and pharmacogenetics.* Gastroenterology, 2006. **130**(6): p. 1793-806.
11. Fujino, H., et al., *Transporter-mediated influx and efflux mechanisms of pitavastatin, a new inhibitor of HMG-CoA reductase.* J Pharm Pharmacol, 2005. **57**(10): p. 1305-11.
12. Yan, H., et al., *Sodium taurocholate cotransporting polypeptide is a functional receptor for human hepatitis B and D virus.* Elife, 2014. **3**.
13. Ni, Z., et al., *Structure and function of the human breast cancer resistance protein (BCRP/ABCG2).* Curr Drug Metab, 2010. **11**(7): p. 603-17.
14. Falguieres, T., et al., *ABCB4: Insights from pathobiology into therapy.* Clin Res Hepatol Gastroenterol, 2014. **38**(5): p. 557-63.
15. Kubitz, R., et al., *Autoimmune BSEP disease: disease recurrence after liver transplantation for progressive familial intrahepatic cholestasis.* Clin Rev Allergy Immunol, 2015. **48**(2-3): p. 273-84.

16. Ballatori, N., et al., *OST alpha-OST beta: a key membrane transporter of bile acids and conjugated steroids.* Front Biosci (Landmark Ed), 2009. **14**: p. 2829-44.
17. Zhang, Y., C. Bachmeier, and D.W. Miller, *In vitro and in vivo models for assessing drug efflux transporter activity.* Adv Drug Deliv Rev, 2003. **55**(1): p. 31-51.
18. Sahi, J., *Use of in vitro transporter assays to understand hepatic and renal disposition of new drug candidates.* Expert Opin Drug Metab Toxicol, 2005. **1**(3): p. 409-27.
19. Brandon, E.F., et al., *An update on in vitro test methods in human hepatic drug biotransformation research: pros and cons.* Toxicol Appl Pharmacol, 2003. **189**(3): p. 233-46.
20. Hilgendorf, C., et al., *Expression of thirty-six drug transporter genes in human intestine, liver, kidney, and organotypic cell lines.* Drug Metab Dispos, 2007. **35**(8): p. 1333-40.
21. Yamazaki, M., et al., *In vitro substrate identification studies for p-glycoprotein-mediated transport: species difference and predictability of in vivo results.* J Pharmacol Exp Ther, 2001. **296**(3): p. 723-35.
22. Hart, S.N., et al., *A comparison of whole genome gene expression profiles of HepaRG cells and HepG2 cells to primary human hepatocytes and human liver tissues.* Drug Metab Dispos, 2010. **38**(6): p. 988-94.
23. Richert, L., et al., *Gene expression in human hepatocytes in suspension after isolation is similar to the liver of origin, is not affected by hepatocyte cold storage and cryopreservation, but is strongly changed after hepatocyte plating.* Drug Metab Dispos, 2006. **34**(5): p. 870-9.
24. Tabibian, J.H., et al., *Physiology of cholangiocytes.* Compr Physiol, 2013. **3**(1): p. 541-65.
25. Weiskirchen, R. and F. Tacke, *Cellular and molecular functions of hepatic stellate cells in inflammatory responses and liver immunology.* Hepatobiliary Surg Nutr, 2014. **3**(6): p. 344-63.
26. Kawada, N., et al., *Effect of antioxidants, resveratrol, quercetin, and N-acetylcysteine, on the functions of cultured rat hepatic stellate cells and Kupffer cells.* Hepatology, 1998. **27**(5): p. 1265-74.
27. Elferink, M.G., et al., *Gene expression analysis of precision-cut human liver slices indicates stable expression of ADME-Tox related genes.* Toxicol Appl Pharmacol, 2011. **253**(1): p. 57-69.
28. Martin, H., et al., *Morphological and biochemical integrity of human liver slices in long-term culture: effects of oxygen tension.* Cell Biol Toxicol, 2002. **18**(2): p. 73-85.

29. Schaefer, O., et al., *Absolute quantification and differential expression of drug transporters, cytochrome P450 enzymes, and UDP-glucuronosyltransferases in cultured primary human hepatocytes.* Drug Metab Dispos, 2012. **40**(1): p. 93-103.
30. Swift, B., N.D. Pfeifer, and K.L. Brouwer, *Sandwich-cultured hepatocytes: an in vitro model to evaluate hepatobiliary transporter-based drug interactions and hepatotoxicity.* Drug Metab Rev, 2010. **42**(3): p. 446-71.
31. Keppler, D., *Uptake and efflux transporters for conjugates in human hepatocytes.* Methods Enzymol, 2005. **400**: p. 531-42.
32. Esch, E.W., A. Bahinski, and D. Huh, *Organs-on-chips at the frontiers of drug discovery.* Nat Rev Drug Discov, 2015. **14**(4): p. 248-60.
33. LeCluyse, E.L., et al., *Organotypic liver culture models: meeting current challenges in toxicity testing.* Crit Rev Toxicol, 2012. **42**(6): p. 501-48.
34. Wikswo, J.P., *The relevance and potential roles of microphysiological systems in biology and medicine.* Exp Biol Med (Maywood), 2014. **239**(9): p. 1061-72.
35. Khetani, S.R., et al., *Use of micropatterned cocultures to detect compounds that cause drug-induced liver injury in humans.* Toxicol Sci, 2013. **132**(1): p. 107-17.
36. Bale, S.S., et al., *In vitro platforms for evaluating liver toxicity.* Exp Biol Med (Maywood), 2014. **239**(9): p. 1180-91.
37. Ramsden, D., et al., *Bridging in vitro and in vivo metabolism and transport of faldaprevir in human using a novel cocultured human hepatocyte system, HepatoPac.* Drug Metab Dispos, 2014. **42**(3): p. 394-406.
38. Kostadinova, R., et al., *A long-term three dimensional liver co-culture system for improved prediction of clinically relevant drug-induced hepatotoxicity.* Toxicol Appl Pharmacol, 2013. **268**(1): p. 1-16.
39. Messner, S., et al., *Multi-cell type human liver microtissues for hepatotoxicity testing.* Arch Toxicol, 2013. **87**(1): p. 209-13.
40. Nguyen, D.G., et al., *Bioprinted 3D Primary Liver Tissues Allow Assessment of Organ-Level Response to Clinical Drug Induced Toxicity In Vitro.* PLoS One, 2016. **11**(7): p. e0158674.
41. Norona, L.M., et al., *Modeling compound-induced fibrogenesis in vitro using three-dimensional bioprinted human liver tissues.* Toxicol Sci, 2016.
42. Zeilinger, K., et al., *Scaling down of a clinical three-dimensional perfusion multicompartment hollow fiber liver bioreactor developed for extracorporeal liver support to an analytical scale device useful for hepatic pharmacological in vitro studies.* Tissue Eng Part C Methods, 2011. **17**(5): p. 549-56.
43. Novik, E., et al., *A microfluidic hepatic coculture platform for cell-based drug metabolism studies.* Biochem Pharmacol, 2010. **79**(7): p. 1036-44.

44. Vivares, A., et al., *Morphological behaviour and metabolic capacity of cryopreserved human primary hepatocytes cultivated in a perfused multiwell device.* Xenobiotica, 2015. **45**(1): p. 29-44.
45. Domansky, K., et al., *Perfused multiwell plate for 3D liver tissue engineering.* Lab Chip, 2010. **10**(1): p. 51-8.
46. Sarkar, U., et al., *Metabolite profiling and pharmacokinetic evaluation of hydrocortisone in a perfused three-dimensional human liver bioreactor.* Drug Metab Dispos, 2015. **43**(7): p. 1091-9.
47. Lee, P.J., P.J. Hung, and L.P. Lee, *An artificial liver sinusoid with a microfluidic endothelial-like barrier for primary hepatocyte culture.* Biotechnol Bioeng, 2007. **97**(5): p. 1340-6.
48. Vernetti, L.A., et al., *A human liver microphysiology platform for investigating physiology, drug safety, and disease models.* Exp Biol Med (Maywood), 2016. **241**(1): p. 101-14.
49. Allen, J.W. and S.N. Bhatia, *Formation of steady-state oxygen gradients in vitro: application to liver zonation.* Biotechnol Bioeng, 2003. **82**(3): p. 253-62.
50. Kelly, E.J., et al., *Innovations in preclinical biology: ex vivo engineering of a human kidney tissue microperfusion system.* Stem Cell Res Ther, 2013. **4 Suppl 1**: p. S17.
51. Andersen, M.E., et al., *Developing microphysiological systems for use as regulatory tools--challenges and opportunities.* ALTEX, 2014. **31**(3): p. 364-7.
52. Sutherland, M.L., K.M. Fabre, and D.A. Tagle, *The National Institutes of Health Microphysiological Systems Program focuses on a critical challenge in the drug discovery pipeline.* Stem Cell Res Ther, 2013. **4 Suppl 1**: p. I1.
53. *The Body-on-a-Chip.*
54. Giles, J., *Animal experiments under fire for poor design.* Nature, 2006. **444**(7122): p. 981.
55. Moja, L., et al., *Flaws in animal studies exploring statins and impact on meta-analysis.* Eur J Clin Invest, 2014. **44**(6): p. 597-612.
56. Scott, S., et al., *Design, power, and interpretation of studies in the standard murine model of ALS.* Amyotroph Lateral Scler, 2008. **9**(1): p. 4-15.
57. Ioannidis, J.P., *Extrapolating from animals to humans.* Sci Transl Med, 2012. **4**(151): p. 151ps15.
58. Huh, D., G.A. Hamilton, and D.E. Ingber, *From 3D cell culture to organs-on-chips.* Trends Cell Biol, 2011. **21**(12): p. 745-54.
59. Griffith, L.G., A. Wells, and D.B. Stolz, *Engineering liver.* Hepatology, 2014. **60**(4): p. 1426-34.
60. Huh, D., et al., *Reconstituting organ-level lung functions on a chip.* Science, 2010. **328**(5986): p. 1662-8.

61. Schuetz, E.G., et al., *Regulation of gene expression in adult rat hepatocytes cultured on a basement membrane matrix.* J Cell Physiol, 1988. **134**(3): p. 309-23.
62. Rodriguez-Antona, C., et al., *Cytochrome P450 expression in human hepatocytes and hepatoma cell lines: molecular mechanisms that determine lower expression in cultured cells.* Xenobiotica, 2002. **32**(6): p. 505-20.
63. Odom, D.T., et al., *Control of pancreas and liver gene expression by HNF transcription factors.* Science, 2004. **303**(5662): p. 1378-81.
64. Shulman, M. and Y. Nahmias, *Long-term culture and coculture of primary rat and human hepatocytes.* Methods Mol Biol, 2013. **945**: p. 287-302.
65. Burke, M.D., et al., *Cytochrome P450 specificities of alkoxyresorufin O-dealkylation in human and rat liver.* Biochem Pharmacol, 1994. **48**(5): p. 923-36.
66. Lehmann, J.M., et al., *The human orphan nuclear receptor PXR is activated by compounds that regulate CYP3A4 gene expression and cause drug interactions.* J Clin Invest, 1998. **102**(5): p. 1016-23.
67. Choi, K., et al., *Development of 3D dynamic flow model of human liver and its application to prediction of metabolic clearance of 7-ethoxycoumarin.* Tissue Eng Part C Methods, 2014. **20**(8): p. 641-51.
68. Paine, M.F., et al., *First-pass metabolism of midazolam by the human intestine.* Clin Pharmacol Ther, 1996. **60**(1): p. 14-24.
69. Borlak, J., A. Chougule, and P.K. Singh, *How useful are clinical liver function tests in in vitro human hepatotoxicity assays?* Toxicol In Vitro, 2014. **28**(5): p. 784-95.
70. Werk, A.N. and I. Cascorbi, *Functional gene variants of CYP3A4.* Clin Pharmacol Ther, 2014. **96**(3): p. 340-8.
71. Reif, R., et al., *Bile canalicular dynamics in hepatocyte sandwich cultures.* Arch Toxicol, 2015.
72. Vernetti, L.A., et al., *A human liver microphysiology platform for investigating physiology, drug safety, and disease models.* Exp Biol Med (Maywood), 2015.
73. You, J., et al., *Impact of Nanotopography, Heparin Hydrogel Microstructures, and Encapsulated Fibroblasts on Phenotype of Primary Hepatocytes.* ACS Appl Mater Interfaces, 2015. **7**(23): p. 12299-308.
74. Berger, D.R., et al., *Enhancing the functional maturity of induced pluripotent stem cell-derived human hepatocytes by controlled presentation of cell-cell interactions in vitro.* Hepatology, 2015. **61**(4): p. 1370-81.
75. Trask, O.J., Jr., A. Moore, and E.L. LeCluyse, *A micropatterned hepatocyte coculture model for assessment of liver toxicity using high-content imaging analysis.* Assay Drug Dev Technol, 2014. **12**(1): p. 16-27.

76. Kim, H.J., et al., *Human gut-on-a-chip inhabited by microbial flora that experiences intestinal peristalsis-like motions and flow.* Lab Chip, 2012. **12**(12): p. 2165-74.
77. Trietsch, S.J., et al., *Microfluidic titer plate for stratified 3D cell culture.* Lab Chip, 2013. **13**(18): p. 3548-54.
78. Kim, H.J. and D.E. Ingber, *Gut-on-a-Chip microenvironment induces human intestinal cells to undergo villus differentiation.* Integr Biol (Camb), 2013. **5**(9): p. 1130-40.
79. Kleinman, H.K., D. Philp, and M.P. Hoffman, *Role of the extracellular matrix in morphogenesis.* Curr Opin Biotechnol, 2003. **14**(5): p. 526-32.
80. Lutolf, M.P. and J.A. Hubbell, *Synthetic biomaterials as instructive extracellular microenvironments for morphogenesis in tissue engineering.* Nat Biotechnol, 2005. **23**(1): p. 47-55.
81. Jeon, J.S., et al., *Generation of 3D functional microvascular networks with human mesenchymal stem cells in microfluidic systems.* Integr Biol (Camb), 2014. **6**(5): p. 555-63.
82. van der Meer, A.D., et al., *Three-dimensional co-cultures of human endothelial cells and embryonic stem cell-derived pericytes inside a microfluidic device.* Lab Chip, 2013. **13**(18): p. 3562-8.
83. Sung, J.H. and M.L. Shuler, *A micro cell culture analog (microCCA) with 3-D hydrogel culture of multiple cell lines to assess metabolism-dependent cytotoxicity of anti-cancer drugs.* Lab Chip, 2009. **9**(10): p. 1385-94.
84. Berthier, E., E.W. Young, and D. Beebe, *Engineers are from PDMS-land, Biologists are from Polystyrenia.* Lab Chip, 2012. **12**(7): p. 1224-37.
85. Wang, J.D., et al., *Quantitative analysis of molecular absorption into PDMS microfluidic channels.* Ann Biomed Eng, 2012. **40**(9): p. 1862-73.
86. Wong, I. and C.M. Ho, *Surface molecular property modifications for poly(dimethylsiloxane) (PDMS) based microfluidic devices.* Microfluid Nanofluidics, 2009. **7**(3): p. 291-306.
87. Domansky, K., et al., *Clear castable polyurethane elastomer for fabrication of microfluidic devices.* Lab Chip, 2013. **13**(19): p. 3956-64.
88. Andersen, M.E., et al., *Developing Microphysiological Systems for Use as Regulatory Tools - Challenges and Opportunities.* Altex-Alternatives to Animal Experimentation, 2014. **31**(3): p. 364-367.
89. Elijah J. Weber, A.C., Brian D. Chapron, Jenna L. Voellinger, Kevin A. Lidberg, Catherine K. Yeung, Zhican Wang, Yoshiyuki Yamaura, Dale W. Hailey, Thomas Neumann, Danny D. Shen, Kenneth E. Thummel, Kimberly A. Muczynski, Jonathan Himmelfarb, Edward J. Kelly, *Development of a*

microphysiological model of human kidney proximal tubule function. Kidney International, 2016. **90**(3): p. 627–637.
90. Nortier, J.L., et al., *Urothelial carcinoma associated with the use of a Chinese herb (Aristolochia fangchi).* N Engl J Med, 2000. **342**(23): p. 1686-92.
91. Stiborova, M., et al., *Mechanisms of enzyme-catalyzed reduction of two carcinogenic nitro-aromatics, 3-nitrobenzanthrone and aristolochic acid I: Experimental and theoretical approaches.* Int J Mol Sci, 2014. **15**(6): p. 10271-95.
92. Debelle, F.D., J.L. Vanherweghem, and J.L. Nortier, *Aristolochic acid nephropathy: a worldwide problem.* Kidney Int, 2008. **74**(2): p. 158-69.
93. Grollman, A.P., et al., *Aristolochic acid and the etiology of endemic (Balkan) nephropathy.* Proc Natl Acad Sci U S A, 2007. **104**(29): p. 12129-34.
94. IARC, *IARC Monographs on the Evaluation of Carcinogeneic Risks to Humans: Some Traditional Herbal Medicines, Some Mycotoxins, Naphthalene and Styrene.* 2002. **82**.
95. Sato, N., et al., *Acute nephrotoxicity of aristolochic acids in mice.* J Pharm Pharmacol, 2004. **56**(2): p. 221-9.
96. Shibutani, S., et al., *Selective toxicity of aristolochic acids I and II.* Drug Metab Dispos, 2007. **35**(7): p. 1217-22.
97. Mengs, U., W. Lang, and J.A. Poch, *The Carcinogenic Action of Aristolochic Acid in Rats.* Archives of Toxicology, 1982. **51**(2): p. 107-119.
98. Mengs, U., *On the histopathogenesis of rat forestomach carcinoma caused by aristolochic acid.* Arch Toxicol, 1983. **52**(3): p. 209-20.
99. Schmeiser, H.H., et al., *Aristolochic Acid Activates Ras Genes in Rat-Tumors at Deoxyadenosine Residues.* Cancer Research, 1990. **50**(17): p. 5464-5469.
100. Zeng, Y., et al., *Aristolochic acid I induced autophagy extenuates cell apoptosis via ERK 1/2 pathway in renal tubular epithelial cells.* PLoS One, 2012. **7**(1): p. e30312.
101. Li, B., et al., *[Cellular mechanism of renal proximal tubular epithelial cell injury induced by aristolochic acid I and aristololactam I].* Beijing Da Xue Xue Bao, 2004. **36**(1): p. 36-40.
102. Balachandran, P., et al., *Structure activity relationships of aristolochic acid analogues: toxicity in cultured renal epithelial cells.* Kidney Int, 2005. **67**(5): p. 1797-805.
103. Zhou, L., et al., *Activation of p53 promotes renal injury in acute aristolochic acid nephropathy.* J Am Soc Nephrol, 2010. **21**(1): p. 31-41.
104. Hsin, Y.H., et al., *Effect of aristolochic acid on intracellular calcium concentration and its links with apoptosis in renal tubular cells.* Apoptosis, 2006. **11**(12): p. 2167-77.

105. Liu, Q., et al., *Differential cytotoxic effects of denitroaristolochic acid II and aristolochic acids on renal epithelial cells.* Toxicol Lett, 2009. **184**(1): p. 5-12.
106. Bieler, C.A., et al., *32P-post-labelling analysis of DNA adducts formed by aristolochic acid in tissues from patients with Chinese herbs nephropathy.* Carcinogenesis, 1997. **18**(5): p. 1063-7.
107. Stiborova, M., et al., *Metabolic activation of carcinogenic aristolochic acid, a risk factor for Balkan endemic nephropathy.* Mutat Res, 2008. **658**(1-2): p. 55-67.
108. Stiborova, M., et al., *Bioactivation versus detoxication of the urothelial carcinogen aristolochic acid I by human cytochrome P450 1A1 and 1A2.* Toxicol Sci, 2012. **125**(2): p. 345-58.
109. Stiborova, M., et al., *Human hepatic and renal microsomes, cytochromes P450 1A1/2, NADPH:cytochrome P450 reductase and prostaglandin H synthase mediate the formation of aristolochic acid-DNA adducts found in patients with urothelial cancer.* Int J Cancer, 2005. **113**(2): p. 189-97.
110. Sidorenko, V.S., et al., *Bioactivation of the human carcinogen aristolochic acid.* Carcinogenesis, 2014. **35**(8): p. 1814-22.
111. Peck, E., et al., *Activation of aristolochic acid to mutagenic metabolites by human CYPs 1A1, 1A2 and 3A4.* Toxicological Sciences 2008. **102(1): #6760**.
112. Stiborova, M., et al., *The role of biotransformation enzymes in the development of renal injury and urothelial cancer caused by aristolochic acid: urgent questions and difficult answers.* Biomed Pap Med Fac Univ Palacky Olomouc Czech Repub, 2009. **153**(1): p. 5-11.
113. Yun, B.H., et al., *New Approaches for Biomonitoring Exposure to the Human Carcinogen Aristolochic Acid.* Toxicol Res (Camb), 2015. **4**(4): p. 763-776.
114. Stiborova, M., et al., *Knockout and humanized mice as suitable tools to identify enzymes metabolizing the human carcinogen aristolochic acid.* Xenobiotica, 2014. **44**(2): p. 135-45.
115. Stiborova, M., et al., *Dicoumarol inhibits rat NAD(P)H:quinone oxidoreductase in vitro and induces its expression in vivo.* Neuro Endocrinol Lett, 2014. **35 Suppl 2**: p. 123-32.
116. Chen, M., et al., *Inhibition of renal NQO1 activity by dicoumarol suppresses nitroreduction of aristolochic acid I and attenuates its nephrotoxicity.* Toxicol Sci, 2011. **122**(2): p. 288-96.
117. Barta, F., et al., *The effect of aristolochic acid I on expression of NAD(P)H:quinone oxidoreductase in mice and rats--a comparative study.* Mutat Res Genet Toxicol Environ Mutagen, 2014. **768**: p. 1-7.
118. Han, W.K., et al., *Kidney Injury Molecule-1 (KIM-1): a novel biomarker for human renal proximal tubule injury.* Kidney Int, 2002. **62**(1): p. 237-44.

119. Ozer, J., et al., *The current state of serum biomarkers of hepatotoxicity.* Toxicology, 2008. **245**(3): p. 194-205.
120. Shao, X., et al., *Diagnostic value of urinary kidney injury molecule 1 for acute kidney injury: a meta-analysis.* PLoS One, 2014. **9**(1): p. e84131.
121. Guollo, F., et al., *Significance of alanine aminotransferase levels in patients admitted for cocaine intoxication.* J Clin Gastroenterol, 2015. **49**(3): p. 250-5.
122. Liu, M., et al., *Acute kidney injury leads to inflammation and functional changes in the brain.* J Am Soc Nephrol, 2008. **19**(7): p. 1360-70.
123. Ichimura, T., et al., *Kidney injury molecule-1 is a phosphatidylserine receptor that confers a phagocytic phenotype on epithelial cells.* J Clin Invest, 2008. **118**(5): p. 1657-68.
124. Tourovskaia, A., et al., *Tissue-engineered microenvironment systems for modeling human vasculature.* Exp Biol Med (Maywood), 2014. **239**(9): p. 1264-71.
125. Stiborova, M., et al., *Enzymes metabolizing aristolochic acid and their contribution to the development of aristolochic acid nephropathy and urothelial cancer.* Curr Drug Metab, 2013. **14**(6): p. 695-705.
126. Robertson, N., et al., *Factors affecting sensitivity to EO9 in rodent and human tumour cells in vitro: DT-diaphorase activity and hypoxia.* Eur J Cancer, 1994. **30A**(7): p. 1013-9.
127. Plumb, J.A., M. Gerritsen, and P. Workman, *DT-diaphorase protects cells from the hypoxic cytotoxicity of indoloquinone EO9.* Br J Cancer, 1994. **70**(6): p. 1136-43.
128. Scott, K.A., et al., *Inhibitors of NQO1: identification of compounds more potent than dicoumarol without associated off-target effects.* Biochem Pharmacol, 2011. **81**(3): p. 355-63.
129. Martinek, V., et al., *Comparison of activation of aristolochic acid I and II with NADPH:quinone oxidoreductase, sulphotransferases and N-acetyltranferases.* Neuro Endocrinol Lett, 2011. **32 Suppl 1**: p. 57-70.
130. Stiborova, M., et al., *The human carcinogen aristolochic acid i is activated to form DNA adducts by human NAD(P)H:quinone oxidoreductase without the contribution of acetyltransferases or sulfotransferases.* Environ Mol Mutagen, 2011. **52**(6): p. 448-59.
131. Arlt, V.M., et al., *Role of P450 1A1 and P450 1A2 in bioactivation versus detoxication of the renal carcinogen aristolochic acid I: studies in Cyp1a1-/-, Cyp1a2-/-, and Cyp1a1/1a2-/- mice.* Chem Res Toxicol, 2011. **24**(10): p. 1710-9.

132. Hashimoto, K., et al., *Sulfotransferase-1A1-dependent bioactivation of aristolochic acid I and N-hydroxyaristolactam I in human cells.* Carcinogenesis, 2016. **37**(7): p. 647-55.
133. Gustafson, D.L. and C.A. Pritsos, *Enhancement of xanthine dehydrogenase mediated mitomycin C metabolism by dicumarol.* Cancer Res, 1992. **52**(24): p. 6936-9.
134. Sung, J.H., C. Kam, and M.L. Shuler, *A microfluidic device for a pharmacokinetic-pharmacodynamic (PK-PD) model on a chip.* Lab Chip, 2010. **10**(4): p. 446-55.
135. Miller, P.G. and M.L. Shuler, *Design and demonstration of a pumpless 14 compartment microphysiological system.* Biotechnol Bioeng, 2016.
136. Esch, M.B., et al., *Body-on-a-chip simulation with gastrointestinal tract and liver tissues suggests that ingested nanoparticles have the potential to cause liver injury.* Lab Chip, 2014. **14**(16): p. 3081-92.
137. Tatosian, D.A. and M.L. Shuler, *A novel system for evaluation of drug mixtures for potential efficacy in treating multidrug resistant cancers.* Biotechnol Bioeng, 2009. **103**(1): p. 187-98.
138. Viravaidya, K., A. Sin, and M.L. Shuler, *Development of a microscale cell culture analog to probe naphthalene toxicity.* Biotechnol Prog, 2004. **20**(1): p. 316-23.
139. Li, A.P., *Evaluation of Adverse Drug Properties with Cryopreserved Human Hepatocytes and the Integrated Discrete Multiple Organ Co-culture (IdMOC(TM)) System.* Toxicol Res, 2015. **31**(2): p. 137-49.
140. Schmeiser, H.H., M. Stiborova, and V.M. Arlt, *Chemical and molecular basis of the carcinogenicity of Aristolochia plants.* Curr Opin Drug Discov Devel, 2009. **12**(1): p. 141-8.
141. Arlt, V.M., et al., *Aristolochic acid mutagenesis: molecular clues to the aetiology of Balkan endemic nephropathy-associated urothelial cancer.* Carcinogenesis, 2007. **28**(11): p. 2253-61.
142. Schmeiser, H.H., et al., *Detection of DNA adducts formed by aristolochic acid in renal tissue from patients with Chinese herbs nephropathy.* Cancer Res, 1996. **56**(9): p. 2025-8.
143. Yun, B.H., et al., *Biomonitoring of aristolactam-DNA adducts in human tissues using ultra-performance liquid chromatography/ion-trap mass spectrometry.* Chem Res Toxicol, 2012. **25**(5): p. 1119-31.
144. Attaluri, S., et al., *DNA adducts of aristolochic acid II: total synthesis and site-specific mutagenesis studies in mammalian cells.* Nucleic Acids Res, 2010. **38**(1): p. 339-52.

145. Jelakovic, B., et al., *Aristolactam-DNA adducts are a biomarker of environmental exposure to aristolochic acid.* Kidney Int, 2012. **81**(6): p. 559-67.
146. Chen, C.H., et al., *Aristolochic acid-associated urothelial cancer in Taiwan.* Proc Natl Acad Sci U S A, 2012. **109**(21): p. 8241-6.
147. Shibutani, S., et al., *Detoxification of aristolochic acid I by O-demethylation: less nephrotoxicity and genotoxicity of aristolochic acid Ia in rodents.* Int J Cancer, 2010. **127**(5): p. 1021-7.
148. Chan, W., et al., *Study of the phase I and phase II metabolism of nephrotoxin aristolochic acid by liquid chromatography/tandem mass spectrometry.* Rapid Commun Mass Spectrom, 2006. **20**(11): p. 1755-60.
149. Rosenquist, T.A., et al., *Cytochrome P450 1A2 detoxicates aristolochic acid in the mouse.* Drug Metab Dispos, 2010. **38**(5): p. 761-8.
150. Pfau, W., H.H. Schmeiser, and M. Wiessler, *Aristolochic acid binds covalently to the exocyclic amino group of purine nucleotides in DNA.* Carcinogenesis, 1990. **11**(2): p. 313-9.
151. Boelsterli, U.A., et al., *Bioactivation and hepatotoxicity of nitroaromatic drugs.* Curr Drug Metab, 2006. **7**(7): p. 715-27.
152. Zeng, Y., et al., *Organic anion transporter 1 (OAT1) involved in renal cell transport of aristolochic acid I.* Hum Exp Toxicol, 2012. **31**(8): p. 759-70.
153. Dickman, K.G., et al., *Physiological and molecular characterization of aristolochic acid transport by the kidney.* J Pharmacol Exp Ther, 2011. **338**(2): p. 588-97.
154. Riedmaier, A.E., et al., *Organic Anion Transporters and Their Implications in Pharmacotherapy.* Pharmacological Reviews, 2012. **64**(3): p. 421-449.
155. Ekaratanawong, S., et al., *Human organic anion transporter 4 is a renal apical organic anion/dicarboxylate exchanger in the proximal tubules.* J Pharmacol Sci, 2004. **94**(3): p. 297-304.
156. Aleksunes, L.M., M. Goedken, and J.E. Manautou, *Up-regulation of NAD(P)H quinone oxidoreductase 1 during human liver injury.* World J Gastroenterol, 2006. **12**(12): p. 1937-40.
157. Hagos, Y. and N.A. Wolff, *Assessment of the role of renal organic anion transporters in drug-induced nephrotoxicity.* Toxins (Basel), 2010. **2**(8): p. 2055-82.
158. Xue, X., et al., *Critical role of organic anion transporters 1 and 3 in kidney accumulation and toxicity of aristolochic acid I.* Mol Pharm, 2011. **8**(6): p. 2183-92.
159. Glatt, H., *Sulfation and sulfotransferases 4: bioactivation of mutagens via sulfation.* FASEB J, 1997. **11**(5): p. 314-21.

160. Gamage, N., et al., *Human sulfotransferases and their role in chemical metabolism.* Toxicol Sci, 2006. **90**(1): p. 5-22.
161. Riches, Z., et al., *Quantitative evaluation of the expression and activity of five major sulfotransferases (SULTs) in human tissues: the SULT "pie"*. Drug Metab Dispos, 2009. **37**(11): p. 2255-61.